THE UNIVERSITY OF ASTON IN BIRMINGHAM

"A study of fatigue failure in vulcanized rubber."

Thesis submitted for the degree of

Doctor of Philosophy

by

Anthony Gordon James

Physics Department.

September, 1970.

ACKNOWLEDGEMENTS

I would like to thank my Supervisor Dr. D.G. Marshall and Mr. T. Mulvey, the Project Advisor for their advice and encouragement during the course of this project. My thanks are also due to Mr. D. Bulgin and Mr. G.D. Hubbard of the Physical Research Department of the Dunlop Central Research and Development Division, whose help has been invaluable and to the Dunlop Company for supporting this work. Finally I would like to thank Mrs. G.A. Taylor for her patience with the typing.

SUMMARY

Some aspects of fatigue failure in rubbers have been examined. Scanning electron micrographs of the surface exposed by the failure confirm the incremental, crack-propagation nature, of the fatigue process. Many other features of the failure surface have been identified and related to this process. The complicating effect of a reinforcing filler has also been investigated.

The fatigue resistance of rubber test-pieces deformed in simple tension was measured as a function of frequency and temperature. This showed that an increase in frequency was equivalent to a decrease in temperature; for an amorphous unfilled rubber the time and temperature effects obeyed a well known transformation. The effect of crystallisation and fillers on the validity of this transformation is considered. This transformation indicates that hysteresis plays an important part in the fatigue process. Torsional pendulum measurements were used to demonstrate the dependence of the fatigue life on the mechanical damping.

An apparatus was developed to measure the hysteresial energy loss directly at deformations, rates of deformation and temperatures consistent with a typical fatigue test. Measurements made with this apparatus are compared with fatigue values and a quantitative relationship is suggested describing fatigue, in terms of the energy lost per unit energy input in a cycle of a fatigue test.

CONTENTS

APPENDICES

I. FATIGUE AND FATIGUE TESTING IN RUBBERS.

I. 1. Introduction

It has been known for a long time that certain metal machine components, subjected to loads which vary or are repeated a number of times, break abruptly without any permanent deformation to herald the fracture, although these same components will withstand greater loads if the load is applied steadily and then maintained constant. As early as 1829, Albert, a German mining engineer, was subjecting mine-hoist chains to repeated proof-loadings (sometimes as many as 100,000) before they were put into service. The cause of this type of failure to which any metal may be prone if subjected to varying loads was given the name "fatigue".

The word "fatigue" was applied to the process causing failure and not to the failure itself. It implies that, as time elapses, changes take place that render a structure or a material unsuitable for its intended use and thus has an analogy with the idea of fatigue in the human body.

With the increased use of high polymers in engineering it was recognised that fatigue in these materials was, in many cases, an even greater problem than in metals. This is particularly true of rubbers, which because of their high reversible extensibility are ideally suited to many of the applications associated with dynamic loading.

1.2. Definition of Fatigue

The dictionary definition of fatigue, e.g. Webster's International, is "the action that takes place in a material, especially a metal, which causes deterioration and failure after a repetition of stress". In the field of high polymers this definition has been extended by some authors to cover the time dependent failure which occurs under a statically applied stress. Dillon [1] even introduced the idea of time dependent failure due to chemical action as a facet of fatigue, and included, in a list of tests to assess fatigue, the following effects :-

(1) Dynamic Cycling Tests

(2) Static Ageing Tests

(3) Creep and Stress Relaxation Tests

(4) Swelling and Solubility in Solvents

(5) Impact and Single Cycle Rupture Tests

(6) Measurement of complex phenomena involving tearing, cutting and abrasion, etc.

However, in order to limit this investigation to a reasonable scope, the concept of failure being due to repetition of stress is retained and fatigue is defined as "That action which causes, after the repeated application of a finite stress, a failure defined as rupture of the material, or as the change in some

relevant property of the material which renders it unsuitable for use".

The number of applications of the stress necessary to cause failure is variously known as the fatigue life, the fatigue strength and the fatigue resistance. For the purposes of this investigation the convention of using "fatigue resistance" to describe the number of repetitions of stress, and "fatigue life" to describe the total time of the experiment, has been standardised.

1.3. Fatigue in Rubber

At the molecular level vulcanized rubber consists of a three dimensional network of long chain molecules bound together by random inter-molecular crosslinks. These long chain molecules may occur naturally as in natural rubber or may be created synthetically by joining smaller molecules together, the process being called polymerisation. The backbone of these chains is usally made up of carbon atoms although there is a commonly used rubber based upon another Group Four element, Silicon. Table I shows the structural formulae of some common rubbers.

TABLE I

STRUCTURE OF SOME TYPICAL RUBBER MOLECULAR CHAINS

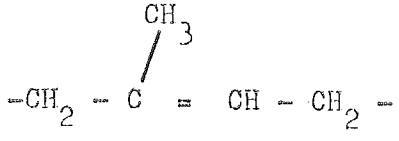

Poly-isoprene (Natural Rubber and gutta percha)

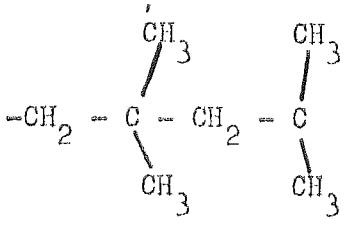

Poly-isobutylene (butyl rubber)

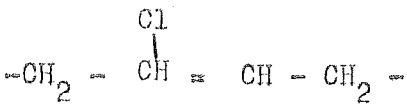

Poly-chloroprene (Neoprene)

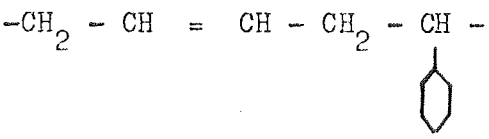

Butadiene-Styrene (SBR)

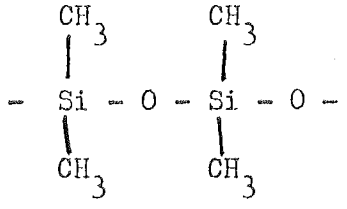

Silicone Rubber

It is the characteristics of this network that lead to the phenomenon known as rubber-like elasticity. In metals the elasticity arises from the distortion of atomic bonds, but in rubber, the elastic properties arise because of the uncoiling of the molecular chains. This uncoiling is made possible by the rotation of individual elements of the chain about carbon-carbon or carbon-oxygen backbone single bonds.

The ability of rubber to behave elastically at large deformations has resulted in its widespread use in engineering to transmit forces and to isolate vibrations. In such uses as motor mountings, torsion, shear and compression springs, tyres, flexible couplings and many others it is subjected to repeated loadings often in unsympathetic ambient atmospheres and is thus susceptible to fatigue.

In practice the catastrophic failure of rubber components due to fatigue can often be predicted from the appearance of cracks in the surface of the material. For this reason it is widely believed that the process leading to fatigue failure is a process which causes the formation and growth of cracks in the material. In 1954 A. Angioletti[2], produced cracks in solid tyres and truck shock absorbers by the application of dynamic stresses. He observed the growth of these cracks by a photo-elastic technique

and showed that they led to eventual failure of the product. This work was also important in showing that the directions and magnitude of local rather than general deformation in the material led to the formation and growth of cracks causing fatigue failure. This has been substantiated by many authors [3], [4], [5], [6], [7], [8], [9]. After the repeated application of mechanical stress, cracks were seen to appear, usually in regions of stress concentration, and then grow with time until complete failure occurred. In tyres such regions of stress concentration are in the grooves in the tyre tread, in between the layers of material or "plies" making up the carcass of the tyre and also in the sidewall of the tyre (especially in "radial ply" tyres where the deformation of the sidewall is larger than in "cross-ply" tyres). These cracks were also seen to appear in torsion springs, shear springs, motor mounts, containers and diaphragms especially where any angle or groove provided a local increase in the stress in the rubber.

Other authors [10], [11], [12] have shown that there is a correlation in theory and practice between the ability of a rubber to resist dynamic fatigue failure and the amount of material which is worn from the surface of a rubber component under given conditions of abrasion. Under these conditions, which are a function of the abrading surface, increased fatigue resistance correlates with increased wear resistance which is an important

consideration in determining the "life-span" of e.g. tyre treads and conveyor belts.

1.4. Classification of Fatigue Resistance Measurements

In assessing the ability of a rubber to resist fatigue failure, two distinct failure mechanisms have been recognized and have led to two main classifications of fatigue test.

Some of the energy expanded in deforming a rubber is stored elastically and is returned when the deformation is removed. The remainder however, is not recoverable and is given to the production of heat. This loss of energy is a consequence of the visco-elastic nature of high polymers and arises from the internal friction of the molecular chains moving over one another when the polymer is deformed. It is manifested as a difference in phase between the stress and strain, so that if the stress and strain in cyclic deformation are plotted against each other they produce a loop ("hysteresis loop") the area of which is a measure of the energy loss. The heat generation caused by this mechanical hysteresis mechanism results in a rise in temperature of the rubber, the magnitude of which depends on the thermal conductivity of the rubber, its dimensions, and the rate of cooling at the surface. In a dynamically strained rubber there is always a rise in temperature in the initial period of cycling [1]. The

temperature eventually reaches an equilibrium distribution where the heat lost is equal to the heat generated. If this temperature is then maintained constant until fatigue failure occurs we have one broad classification of fatigue failure. On the other hand in rubber components which have been repeatedly stressed at high temperatures structural changes such as chain scission may occur which cause a further rise in temperature and lead to a type of failure which has been called "blow-out" and is the second broad classification of fatigue. It is characterised by a further rise in temperature before failure occurs.

1.5. Fatigue Tests with a Temperature Rise

Many tests of this type are described in the literature [13], [14], [15], [16]. R.S. Havenhill's machine known as the "St. Joe Flexometer" is still used in assessing the resistance of rubber stocks to "blow-out". The machine vibrates samples in shear to a constant shear load or shear deflection. Two other machines still in use are the Goodrich Flexometer of E.T. Lessig and the Dunlop Fatigue Tester of Gough and Parkinson.

The Gough and Parkinson machine which carried out compressional fatigue of rubber blocks to a constant load, deflection or work-input was used in an investigation which led to

the formulation of empirical relationships describing the phenomenon of fatigue failure.

These machines have proved useful in the practical assessment of fatigue resistance of rubbers. They were designed to operate at known loads and deflections rather than stresses or strains and the results obtained from them did not lead to any theory of the basic mechanism of the fatigue process.

1.6. Fatigue Tests at Constant Temperature

Tests in this classification of fatigue fall into two main groups. The first group [17], [18], [19] of tests utilises flat or cylindrical dumbell test-pieces which are usually deformed sinusoidally, in simple tension. The temperature remains constant after a short initial period since the test-piece is small and heat transfer to the surroundings is rapid. The fatigue resistance in this test is defined as the number of cycles of deformation necessary to cause the samples to break into two pieces.

The second group [20], [21], [22], [23], [24], [25] is based on the measurement of the rate of growth of a cut in a rectangular sample which if flexed through a range of predetermined angles thus giving a range of stress situations at the point of

flexure. The sample is grooved at the point of bending and a cut introduced into the groove with a pin or a razor blade, the rate of growth of this cut being measured. The flexing can be achieved with a variety of mechanical devices. Torrance and Peterson [20] held the samples in a rotating disc so that they were bent at right angles on striking a stationary pin. Carlton and Reinbold [23] bonded the samples to a belt which passed over rotating pulleys and there were also many reciprocating devices to achieve the required flexure.

The temperature of the rubber in these tests is also constant due to heat transfer with the surroundings. However, since the test-pieces are bulkier than the dumbell type the operating temperature is generally higher. Torrance and Peterson controlled the temperature in their tests by mounting the machine in a water bath.

The above are examples of a large number of fatigue tests many of which are still used to measure the resistance of rubber to "fatigue-failure", "crack-growth" and "flex-cracking". These tests led to the observation of many of the more important facets of fatigue failure, for example, many of the authors mentioned, observed the important property that the fatigue resistance drops as the minimum of deformation approaches zero strain and these observations are helpful to the designer of rubber engineering

components. From the results of these tests empirical equations have been derived which enable the rubber technologist to calculate the number of oscillations necessary to cause failure of the test-piece. Unfortunately the various test machines do not always rate the performance of different rubbers in the same order.

Rainer and Gerke [22] measured the amount of crack-growth in a sample by the change in bending moment of the flexed sample. N, the number of cycles of oscillation to give a 1% reduction in bending moment was found to be related to strain by the equation:-

$$N = k/S^n \qquad \ldots \qquad \ldots \qquad \ldots \qquad 1.1.$$

where S is the strain at the sample surface and k and n are constants.

Cassie et al [18] related the number of cycles to failure to the observed drop in the tensile strength (U) of the material. The empirical equation derived by them also recognised the importance of loss mechanisms in determining the fatigue resistance, given by the equation :-

$$N = (k/(U_o - U)) - \alpha h \qquad \ldots \qquad 1.2.$$

where h is the internal friction loss (hysteresis) and k and α are constants.

Springer [26], [27] emphasized the role of chemical reactions in fatigue. He proposed that fatigue resistance under dynamic conditions ought to be inversely proportional to the net rate of reaction. Thus the cycles of failure N and the absolute temperature T ought to be related by a law of the form :-

$$N = C \exp (E/RT) \quad \ldots \quad \ldots \quad 1.3.$$

where 'E is an activation energy.

Equations analogous to the Rainer and Gerke equation appear later in the work of Bartenev and Gail-Ogly, the background to these being summarized by Bartenev and Zuyev [28]. They are equivalent equations relating the maximum deformation S and the maximum stress σ to the cycles to failure N in a dynamic experiment :-

$$N = C/S^m \quad \ldots \quad \ldots \quad 1.4.$$

$$N = C_1/\sigma^m \quad \ldots \quad \ldots \quad 1.5.$$

where C and C_1 are constants.

These are useful empirical equations but do not relate to any basic property of the material; they allow fatigue results to be predicted for a particular test but are not very helpful in determining the basic nature of fatigue or in predicting fatigue resistance for other types of strain cycle.

In 1953 Rivlin and Thomas [29] proposed a mechanism of crack-propagation in elastomers based on a concept of "Tearing Energy". They argued that the energy necessary to cause crack-propagation was a basic property of the elastomer and did not depend upon the type of test employed. Subsequent work led to the development of a theory of fatigue based on the growth of cracks through the material. This work which is summarized in the following pages has been useful in understanding the nature of fatigue failure and should, lead to a generalized theory of design.

1.7. Tearing Energy Considerations

In 1920 A.A. Griffith [30] postulated a criterion for the fracture of brittle materials based on the potential energy associated with the surfaces formed by the fracture. Rivlin and Thomas generalised this criterion to cover the case of highly elastic materials by considering the total reduction in stored elastic energy per unit area of surface formed during the fracture propagation. They called this the tearing energy of the material. It was defined as the strain energy dissipated per unit area of crack growth. Thus :-

$$T = -(\partial E/\partial A)_\theta \quad \ldots \quad \ldots \quad \ldots \quad 1.6.$$

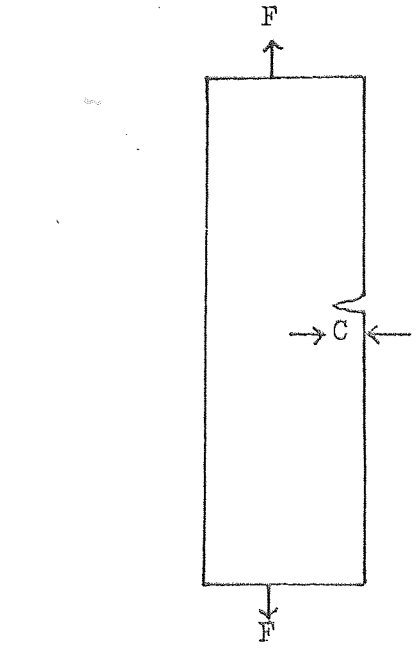

Tensile Strip

Tearing Energy $\mathcal{T}$ = 2KWc

W = Strain Energy per unit vol.

K = fn of strain.

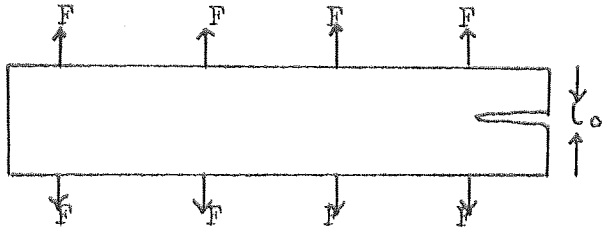

Pure Shear

Tearing Energy $\mathcal{T}$ = Wt_o

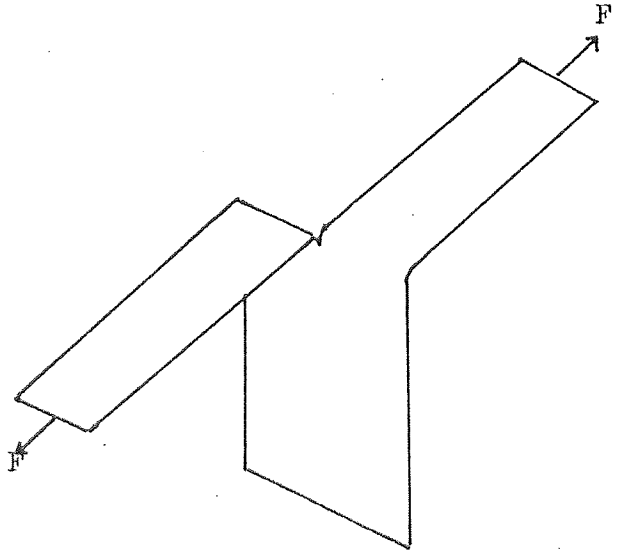

Simple Extension

"Trousers" Test-piece

Tearing Energy $\mathcal{T}$ = 2F/h

F = Force

h = Thickness

Figure 1.1. Tearing Energy Associated with Three Sample Shapes.

where E is the total strain energy of the specimen and A is the area of the crack referred to the unstrained state; ∂ denotes that the differentiation is carried out at constant deformation.

Rivlin and Thomas derived simple approximations for tear energies of test-pieces which, by virtue of their shape, had a well defined mode of deformation. Sample shapes and the tearing energy associated with them are illustrated in Figure 1.1.

Later, Thomas [31] observed the growth of cuts in natural rubber test-pieces in simple tension and pure shear. Tearing of the rubber was seen to take place when the deformation of the rubber was increasing and to stop when deformation stopped. This tearing was called smooth cut-growth from the nature of the torn-surface. Smooth cut-growth continues until there is a rapid increase in cut length signifying the onset of a catastrophic tearing mechanism. The amount of smooth growth taking place (ΔC) was found to obey the empirical relation

$$\Delta C = \mathcal{T}^2/G_s \quad \ldots \quad \ldots \quad \ldots \quad 1.7.$$

where the constant G_s is termed the smooth cut-growth constant of the material and $\mathcal{T}$ is the tearing energy.

When the test-piece was repeatedly deformed to a value of $\mathcal{T}$ less than the critical level of tearing energy necessary for

catastrophic failure the cut was seen to grow by a small amount each cycle. If the cut was made with a razor blade the initial growth was given by equation 1.7. but after a few hundred cycles the growth rate decreased to a nearly constant amount per cycle which again obeyed an equation of the form

$$dc/dn = \mathcal{J}^2/G \qquad \ldots \qquad \ldots \qquad \ldots \qquad 1.8.$$

In this case G was called the rough-growth constant, because the decrease in cut-growth rate was seen to be accompanied by a visible roughening of the tip of the crack.

Rivlin and Thomas came to the conclusion that by expressing both tearing and cut-growth in rubber in terms of the Tearing Energy it is possible to obtain results that are independent of the size and shape of the test-piece, indicating that the Tearing Energy is a fundemental property of the material.

By assuming that fatigue is due to the growth of a flaw present in the sample, the growth becoming catastrophic when the flaw has reached some critical size or configuration, a theory of fatigue may be developed in terms of cut-growth theory [32].

If a tensile strip with a cut of length c in one edge is repeatedly extended from the unstrained state then from equation 1.8. the rate of growth of the cut is

$$dc/dn = (2kW)^2 c^2/G \quad \ldots \quad \ldots \quad \ldots \quad 1.9.$$

where $2kWc$ is the tearing energy T of a tensile strip, k being a constant which changes slightly with strain [33].

If this equation is integrated to give the number of cycles in which the cut grows from its original length, C_o, to a length, c, we get

$$N = G/(2kW)^2 \ (1/c_o - 1/c) \quad \ldots \quad \ldots \quad 1.10.$$

If the fatigue resistance is defined as the instant when c becomes very much greater than c_o or, when $1/c$ becomes negligible compared with $1/c_o$ then

$$N = G/(2kW)^2 \ c_o \quad \ldots \quad \ldots \quad \ldots \quad 1.11.$$

Equation 1.11. was examined by counting the number of deformations necessary to cause a tensile strip of natural rubber to break into two halves at a number of different strains (and hence strain energies W). Good agreement was obtained between theory and experiment.

Lake and Lindley [34] extended the work of Thomas to the case of fatigue in a non-crystallising rubber on the same basis as that used for the crystallising natural rubber.

In a non-crystallising styrene-butadiene, unlike natural rubber, tearing occurs in test-pieces held at constant deformation.

This was termed "static" cut-growth. If the same deformation is applied and removed a large number of times, the rate of growth is greatly increased. Both forms of cut-growth are markedly dependent on the amount of deformation. Cut-growth experiments were performed with both tensile and pure-shear specimens. As with natural rubber "smooth" and "rough" growth was observed during the transition from the initial razor cut to the cut-growing at a slower rate of propagation. The equations relating cut-growth to tearing energy obtained were similar to those obtained with natural rubber but the Tearing Energy is raised to the fourth power.

Statically $dc/dt = \mathcal{J}^4/G_o$ ... ... 1.12.

where G_o is the static cut-growth constant.

and dynamically $dc/dn = \mathcal{J}^4/G$ ... ... 1.13.

In this latter case G was called the cut-growth characteristic.

As in equations 1.9. and 1.10. the expression 1.13. can be integrated to give a relationship between the fatigue resistance and the stored elastic energy. In the amorphous case this equation becomes

$$N = G/3(2kW)^4 \ c_o^3 \quad \ldots \quad \ldots \quad \ldots \quad 1.14.$$

Thus the generalised expression for fatigue resistance is

$$N = G/(2kW)^n . a C_o^{n-1} \quad \ldots \quad \ldots \quad 1.15.$$

where the significance of the index n is not yet fully understood. If a reinforcing filler such as carbon black is added to styrene-butadiene rubber then the index n is reduced from 4 to somewhere in the range 2 - 4 [35].

Equation 1.15. provides the basis for an increasing number of practical measurements of the resistance of vulcanised rubbers to failure by fatigue. A test based on this principle has the advantages :-

a) The mode of deformation is well defined e.g. simple tension or pure shear and mathematical treatments are easier.

b) The test-piece is thin and quickly takes up and maintains a temperature close to ambient.

c) The test-piece, which is small enough to be deformed easily, does not require powerful and expensive apparatus.

and the disadvantages :-

a) There is not yet sufficient evidence that results from such a small scale test are easily applicable to complicated forms

of deformation and to hysteresial heating situations which are experienced in large engineering components.

b) Fatigue life is dependent upon three quantities, W-elastic energy of deformation, G cut growth constant and c_o the 'inherent' flaw size. C_o is not an easily determinable quantity for a particular compound and to find G it is necessary to measure the fatigue life or cut-growth rate over a wide range of stored energies which is a time consuming operation.

Typically the test can be used to evaluate the effect on compounded rubbers of adding antiozonants and fillers, and of prolonged exposure to high temperatures and various liquids.

The fatigue resistance of a compound is measured over a range of strain energies and fatigue resistance (N) is plotted against 2kW on a logarithmic scale as in Figure 1.2.

The effect of changing compounding ingredients is to move the line of the graphs to a parallel position, in a positive or negative direction with respect to the log N axis, indicating an increase or decrease in the fatigue resistance of the rubber over a range of strain energies. Encouraging results have been obtained when laboratory results were compared with service data.

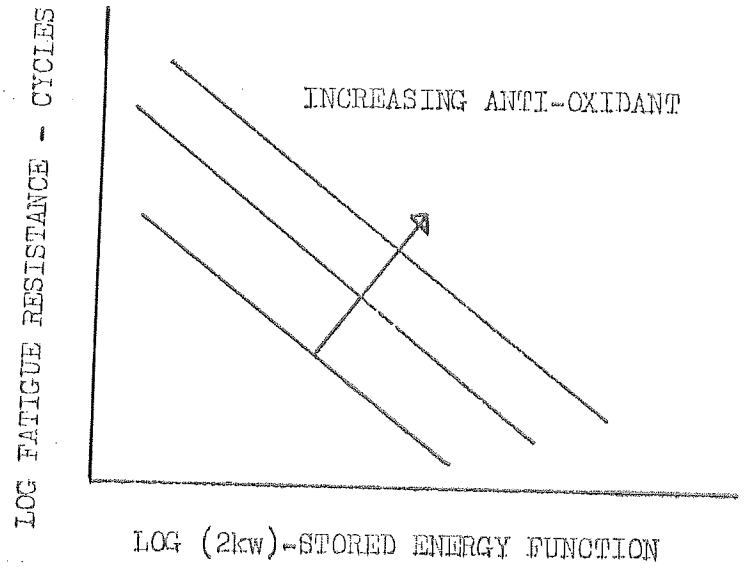

Figure 1.2. The effect of anti-oxidant on fatigue resistance (4).

2. FACTORS AFFECTING FATIGUE

2.1. The Deformation Cycle

When a tyre tread strikes the road it is subjected to rapid rates of stressing (of the order of 100 cycles per second [36]), but in most of the period of rotation of the wheel it is under a steady stress. A vehicle shock absorber is subjected to a randomly applied damped harmonic stress imposed upon a steady stress. In both of these cases the variation of stress with time is in general complex. However, the factors in the deformation cycle which have been identified as having a significant effect on the fatigue life of the component are the rate at which the rubber is deformed and the maximum and minimum values of the deformation in the cycle. Although the wave-form affects the rate of deformation of the rubber, most fatigue measurements have been based either on sinusoidal motion or on an interrupted type of sine-wave motion. The effects of the frequency of deformation are discussed later in the section.

(a) The Maximum Deformation

The maximum deformation decides the maximum values of stress, strain and strain energy to which the rubber is subjected.

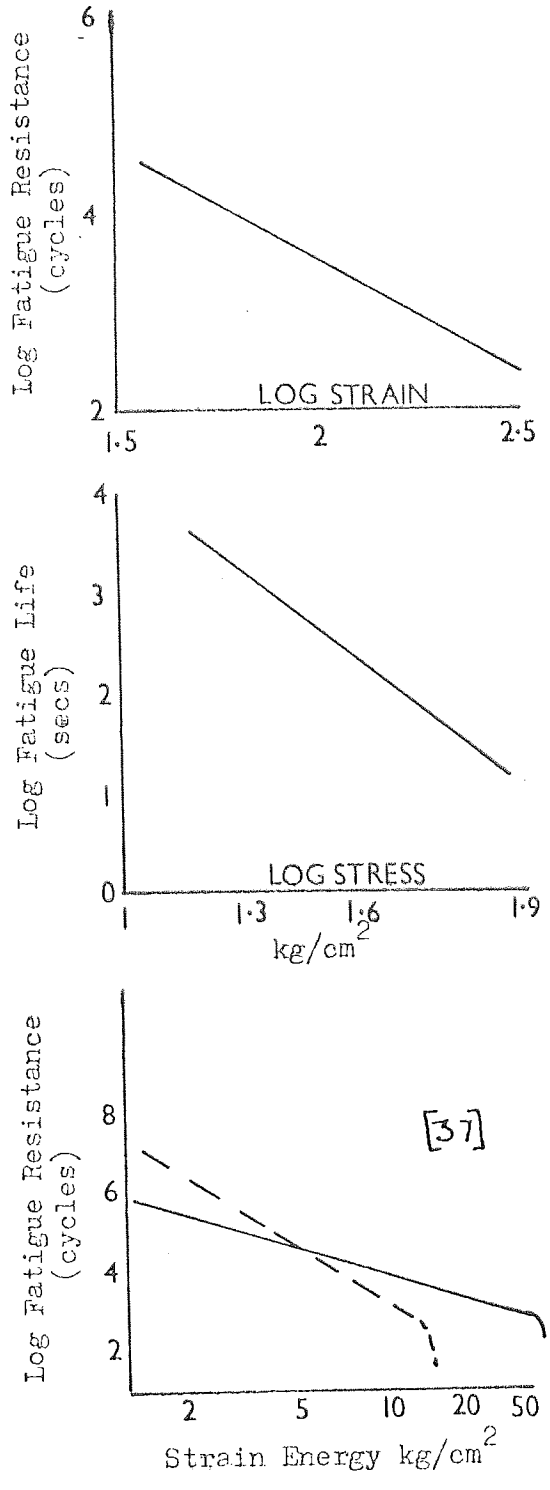

Figure 2.1. The Effect of Deformation Cycle on Fatigue.

Consideration of equations 1.4., 1.5., and 1.15. illustrate the empirically observed decrease in fatigue resistance as the maximum deformation increases. Figure 2.1. shows the effect of increasing the maximum deformation as the minimum is held constant.

(b) The Minimum Deformation

Busse [38] was among the first to realize the importance of the minimun of the strain cycle in determining the fatigue resistance of rubber. Busse's early results on natural rubber are given in Table 2.1.

TABLE 2.1.

EFFECT OF STRAIN CYCLE

Strain Cycle		Fatigue Life (minutes)
Minimum	Maximum	
5%	60% extension	10
10%	60% extension	25
15	60% extension	90
17	60% extension	150 +
20	60% extension	∞

Even though the energy input decreases slightly as the minimum strain increases, there is clearly a marked effect of the minimum imposed strain upon the fatigue life of the test-piece. Cadwell et al [19] produced a more definitive study of the effect in natural rubber extending the investigation to both shear and compression. Gurney and Cheetham [39] further extended the work to cover other elastomers and came to the conclusion that cut-growth rate and hence fatigue resistance is critically dependent on the minimum strain.

2.2. The Effects of Compounding

(a) The Elastomer

Beatty [5] in discussing the effects of the elastomer produced results (shown here as Table 2.2.) to illustrate that the fatigue resistance of an elastomer depends upon its chemical constitution.

He also pointed out that the comparison of elastomers is radically modified by the strain cycle over which testing is carried out. (Table 2.3.).

TABLE 2.2.

THE EFFECT OF ELASTOMERS ON FATIGUE RESISTANCE

Elastomer	Fatigue Life - cycles
Natural Rubber	4.0×10^6
Styrene-Butadiene	0.6×10^6
Neoprene	0.3×10^6
Butyl	4.0×10^6
Nitrile	2.0×10^6

TABLE 2.3.

EFFECT OF STRAIN CYCLE ON ELASTOMERIC VARIATION IN FATIGUE RESISTANCE

Elastomer	Fatigue Life x 10^6 cycles	
	strain -75 to 0%	+50 to 125%
Natural Rubber	4.0	30.0
Styrene-Butadiene	22.0	0.2
Ethylene Propylene Terpolymer (EPT)	30.00	23.0

(b) Fillers

In general the literature suggests that the addition of fillers to a rubber affects its fatigue resistance in two ways. Sites are provided for crack-initiation [37] and the modulus of the rubber is increased so that, for a given deformation, the strain energy is higher. Both of these effects are detrimental to the fatigue resistance of the rubber. It is suggested later in this work, however, that fillers can have an additional beneficial effect on fatigue resistance.

(c) Degree of Vulcanisation and the Vulcanising System

The degree to which a rubber is vulcanised can profoundly affect its fatigue resistance, particularly in synthetic rubbers.

Unreacted vulcanising agents result in subsequent breakdown of the structure of the rubber due to oxidation; over-vulcanisation produces a high modulus which, as in the case of fillers, leads to higher strain energy and hence reduced fatigue resistance. The effect of the vulcanising system used has not been widely investigated but there is some agreement [4], [40], [41] that, for natural rubber vulcanised by sulphur, systems giving a high number of polysulphidic cross-links result in better fatigue resistance than systems giving largely mono-sulphidic cross-links. However, the effect of an

increase in temperature may alter this conclusion as the research was carried out at room-temperature and monosulphidic systems have improved oxidation resistance at elevated temperatures [41].

2.3. Initiators of Fatigue Failures

Angiolletti [42] discussed the effect of inhomogeneities in causing rubber to crack. He placed small discs of metal in samples of transparent vulcanised rubber and followed the effect of these discs on the stress distribution in the rubber by a photo-elastic technique. He found that a stress concentration occurred at the discs which was more severe when there was no adhesion between the metal and the rubber. It is possible that this conclusion applies to inhomogeneities of all kinds. The inhomogeneity acts as a stress-raiser and if the stress at this inhomogeneity exceeds the breaking stress of the material then rupture takes place and a crack if formed which propagates to give the fatigue failure.

Inhomogeneities may take the form of voids due to trapped air, particles of foreign material or pigment, polymer gel, areas of unequal vulcanisation and the phenomenon reported by Hess and Burgess [43] and Smith and Black [44] on the reagglomeration of materials normally dispersed in the rubber which the former authors have associated with groove cracking in tyre treads.

2.4. The Ambient Atmosphere

The most important way in which the atmosphere surrounding a rubber test-piece which is being repeatedly deformed affects the fatigue process, is by the reaction which takes place between the rubber and the ozone or oxygen in the air. This is illustrated by the results given in Table 2.4.

TABLE 2.4.

EFFECT OF THE SURROUNDING ATMOSPHERE ON THE FATIGUE RESISTANCE

Compound	Atmosphere	Fatigue Resistance - Cycles
Natural Rubber (NR)	Nitrogen	8.5×10^6 - no failure
Natural Rubber (NR)	Air, ozone free	3.5×10^6
Natural Rubber (NR)	Air	2.2×10^6
Natural Rubber (NR)	Oxygen	2.5×10^6
Natural Rubber (NR)	Ozone 10 pphm	1.6×10^6
(NR) + antiozonant	Ozone 10 pphm	2.2×10^6

Many workers [21] [35] [45] [46] [47] have established the role of oxidisation and ozonisation in fatigue failure. The general conclusions are that above a critical tearing energy a flaw grows because molecular chains are ruptured in part mechanically and in part by scission of the chains due to oxidation. Below this energy cut-growth is solely attributable to ozone attack.

Chemical additives (anti-oxidents and antiozonants) have been developed to limit the effect of oxygen attack on the rubber and Table 2.4. shows that the addition of an antiozonant, N,N'-bis (1 - methyl heptyl) - p - phenylene diamine, gives the compound the same fatigue resistance in ozone as it has in air without the additive.

2.5. Temperature

Lake and Lindley [34] measured the fatigue life of styrene-butadiene rubber and natural rubber at one frequency over a range of temperatures from 0°C. to 100°C. the results being shown in Figure 2.2. They point out that the large reduction in fatigue life of the styrene-butadiene rubber correlates well with the increase in static cut-growth rate measured over the same temperature range by Greensmith and Thomas [48].

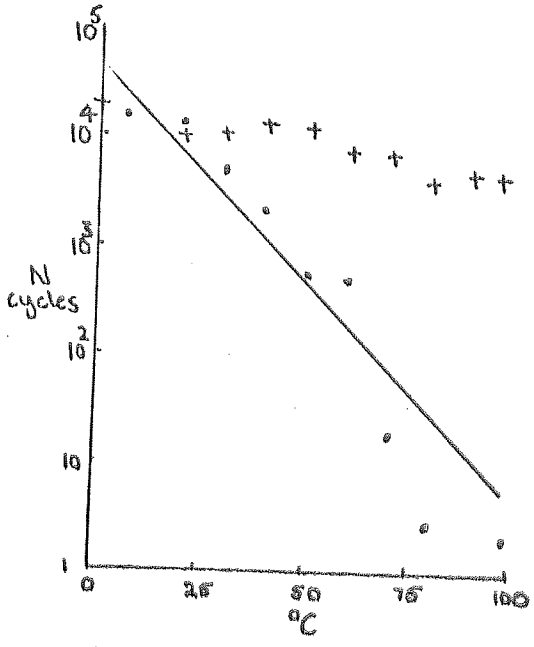

Figure 2.2. Effect of Temperature on the Dynamic Fatigue life of dumbell test-piece at 100 cycles/min. (•) SBR at 175% maximum strain (+) Natural Rubber at 250% maximum strain.

2.6. Frequency

Although the effect of the frequency of deformation of the rubber upon its fatigue resistance has not been widely studied, it has been shown to be an important factor in cut-growth measurements. In this latter case it can be shown, Appendix 1, that the rate of growth in the dynamic case is not just a summation of the individual elements of static-growth during each cycle but

that there is an additional purely dynamic contribution to cut-growth which is frequency dependent.

Lake and Lindley [34] measured the cut-growth constant G from plots of log dc/dn vs Log $\mathcal{J}$ at different test frequencies for a styrene-butadiene co-polymer. A predicted dynamic cut-growth calculated from static cut-growth measurements is compared with the experimentally determined G values in Figure 2.3. (a). The purely dynamic contribution, which is the difference between these two curves, is plotted separately against frequency in Figure 2.3. (b).

The total cut-growth constant, G, is seen to change by two decades in four decades of frequency and from the form of the equation for fatigue life $N = G/(2kW)^4 co^3$, N might be expected to show the same sort of frequency dependence as G if W was independent of frequency. Gd changes by less than half a decade over the same range of frequencies.

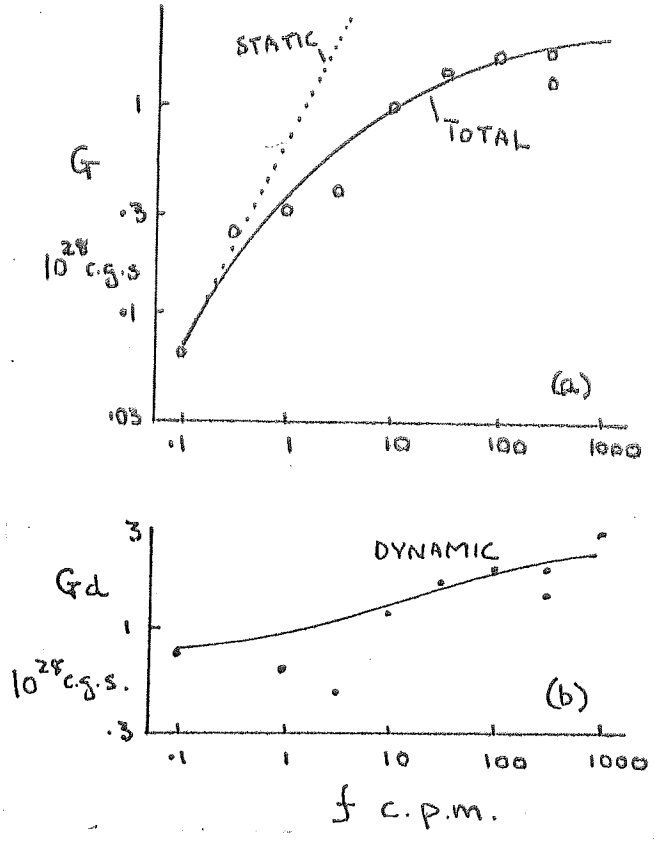

Figure 2.3. Variation of cut-growth constants G and Gd with frequency f. After Lake and Lindley.

3. THE IMPORTANCE OF TEMPERATURE AND FREQUENCY.

3.1. The Effect of Temperature and Frequency on Mechanical Properties.

The effect of test temperature and test time on the ultimate tensile properties of elastomers was the subject of an investigation by T.L. Smith [49], [50]. He measured the tensile strength of styrene-butadiene rubber and found that measurements at a particular temperature over a range of rates of extension could be "shifted" to form a composite curve with results measured at another temperature. When this process was repeated for results obtained over a range of temperatures a "master" curve was obtained describing the tensile properties over a wide range of temperature and extension rate.

The temperature/rate dependence was essentially the same as the temperature/frequency dependence observed when dynamic stress-strain data obtained at different temperatures and frequencies was superposed. The empirical equation obeyed in both of these cases is known as the Williams, Landel and Ferry (W-L-F) equation. This equation has been successfully applied to the temperature/rate interdependence of a number of mechanical and electrical properties of amorphous polymers. The transform was first described by

Williams, Landel and Ferry [51] and the W-L-F equation is a mathematical relationship between the rate and temperature at which a property is measured and the glass transition temperature of the polymer. When physical properties can be transformed in this way, the implication is that the chemical composition of the polymer is important only in the way it affects the glass transition temperature.

3.2. The Glass Transition Temperature

The degree of uncoiling of the molecular chains in a polymer is determined by the restrictions imposed by neighbouring groups of atoms from other chains. These restrictions are called inter-molecular or steric hindrances and they present an energy barrier to the rotating molecular element. The probability of these barriers-to-rotation being surmounted increases rapidly with increase in temperature. The height of the potential barrier is only slightly temperature dependent. Thus at low temperatures rotation becomes difficult and the polymer is no longer flexible but rigid and glass-like, while at high temperatures rotation is easy and the polymer is soft and rubber-like.

At intermediate temperatures the material goes through a transition region which is associated with a marked change in mechanical properties. Figure 3.1. shows the change in mechanical

damping and shear modulus measured on a low amplitude torsional pendulum, as the temperature is raised through the glass transition temperature.

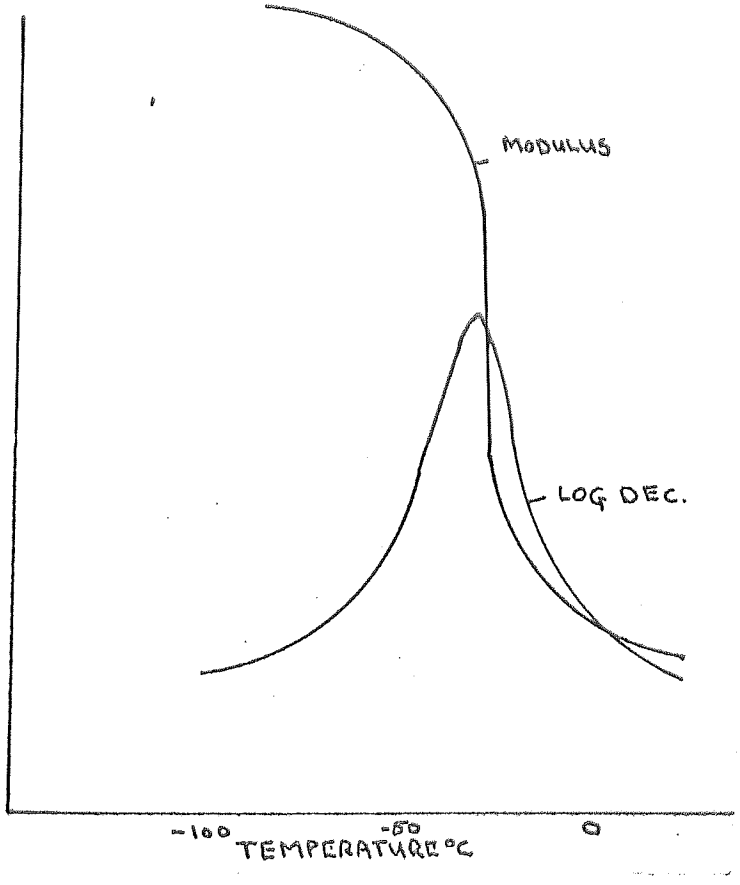

Figure 3.1.
Modulus and Logarithmic Decrement versus Temperature.

The temperature at which the transition takes place depends upon the chemical structure of the molecule. The harder

it is for molecular rotation to take place, the higher will be the glass transition temperature. For example, the work reported in the present investigation is mainly concerned with a group of styrene-butadiene copolymers, of varying styrene content, the molecular structure of which is :-

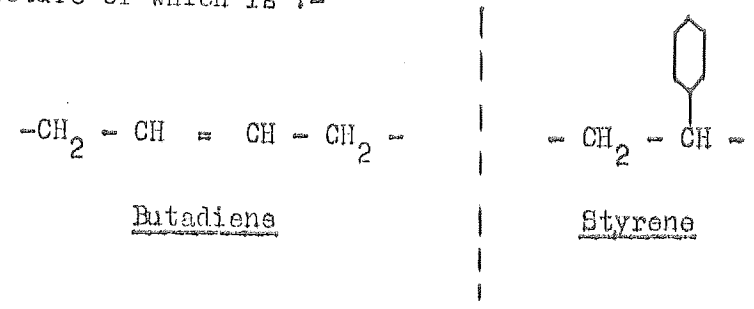

The benzene ring side group which is introduced with the styrene is an obvious hindrance to rotation and, as the percentage of the styrene in the butadiene is increased so the temperature of transition from the glassy state increases.

The alternative way of considering the glass transition is in terms of free volume [52], that is, the amount by which the volume occupied by unit mass of the material is greater than the minimum necessary to contain the atoms of the structure. Figure 3.2. is a graph of specific volume against temperature for an amorphous polymer. The graph (a) consists of two linear portions joined together by a short curve. Extrapolating the linear regions gives an intersection which depends on the rate of heating or cooling. The temperature at the intersection is the (apparent) transition temperature.

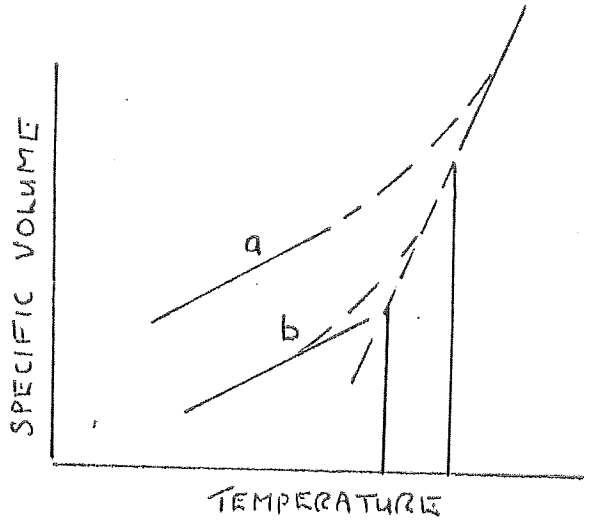

Figure 3.2.

Specific volume versus temperature.

Curve a)-high heating rate

Curve b)-low heating rate

The true or static transition temperature occurs when the changes in temperature are made infinitely slowly, that is they are reversible; line (b) shows that decreasing the rate of temperature change lowers the transition towards a limiting value. The discontinuity in the curves (a) and (b) is associated with a discontinuity in the change in free volume. Many of the properties of liquids and "soft-solids" reflect the presence of free-volume, which may be thought of as holes of molecular dimensions or voids associated with packing irregularities. The thermal expansion of liquids is increased by the creation of extra free volume as the temperature is increased. This, and the discontinuity

of the co-efficient of expansion at the transition point is illustrated in Figure 3.3.

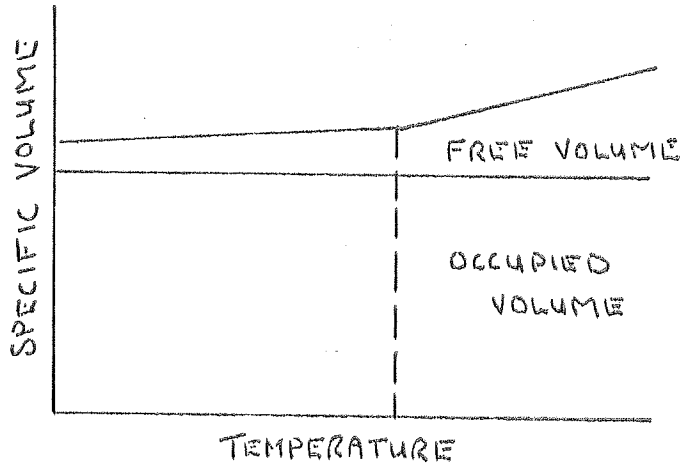

Figure 3.3. Specific Volume against Temperature [52].

Physically the free volume arises because as Tg is reached and passed the "Brownian" motion of the molecules increases appreciably and this motion creates temporary holes in the material.

3.3. The Williams-Landel-Ferry (W-L-F) Equation

Considerations of molecular mobility and "free volume" make possible a theoretical deviation of the equation found

empirically by Williams, Landel and Ferry [51]. This empirical equation is :-

$$\text{Log } A_T = -8.86\ (T - T_s)/(101.6 + T - T_s) \quad \ldots \quad 3.1.$$

where T is the experimental temperature, T_s is a reference temperature, and A_T is the ratio of the change in rate or frequency of test from T to T_s necessary to attain equivalence of the physical property under consideration at the two temperatures.

This equivalence of time (as rate, or frequency) and temperature has been predicted theoretically by Andrews [53] who assumed that the function expressing the probability of molecular rotation taking place can be given in terms of "free-volume" rather than temperature.

He arrived at the equation :-

$$P = \exp\ (-B/V_f) \quad \ldots \quad \ldots \quad 3.2.$$

where P is the probability of a chain segment being able to rotate, V_f is the free volume, and B is the height of the barrier to rotation.

If N molecular segments rotate in a time t then the probability of rotation in unit time is N/t.

It a constant elastic property is proportional to a constant number of segmentary rotations then -

$$\text{property } N = tP = \text{a constant}$$

$$\text{so} \qquad tP = t.\exp(-B/V_f) = \text{a constant} \quad \ldots \quad 3.3.$$

$$\text{therefore} \quad \log t - B/f = \text{a constant}$$

For a change in time,

$$\therefore \quad \Delta(\log t) = B\,\Delta(1/V_f)$$

$$\log(t/t_o) = B(1/V_f - 1/V_{fo}) \quad \ldots \quad \ldots \quad 3.4.$$

Thus a change in time scale is equivalent to a change in free volume, but by normal laws of thermal expansion

$$V_f = V_{fo} + \alpha_f (T - T_o)$$

$$\text{thus } \log(t/t_o) = \left[-B/V_{fo}.(T - T_o)\right] / \left[(V_{fo}/\alpha_f) + (T - T_o)\right]$$

$$\ldots \quad \ldots \quad 3.5.$$

It is seen that this equation is of the same form as the

experimentally observed equation 3.1. Thus, for any mechanical property depending on molecular segmentary rotation, a shift in the time scale will produce the same change in the property as a shift in the temperature according to this equation.

If a property is found to follow this pattern then the above theory is a good basis on which to found a description of the molecular processes which govern the property. When a polymer is extended at high rates or low temperatures work must be done against viscous forces (barriers to rotation) which impede the rearrangement of the network chains. These viscous forces are responsible for the delay between the stress and strain in a material subjected to cyclic deformation and hence can be measured from the hysteresis loop area.

3.4. The Role of Hysteresis in Fracture

A process which is common to all forms of fracture is that of crack-propagation. E.H. Andrews [54] simulated the stress distribution at the tip of a propagating crack. He compared the results with the stress distribution around a crack which was not propagating. Andrews came to the conclusion that in a perfectly elastic material the stress distributions were similar, but in a

material showing mechanical hysteresis the stress at the tip of the propagating crack was less than at the stationary crack. The magnitude of the effect was shown to be dependent on strain as well as on hysteresis, and led to the conclusion that stress concentration at a propagating crack was dependent upon the deformed rather than the undeformed geometry of the crack. Thus, if a crack exists in a hysteresial material the application of external stresses brings about the static situation of high stress concentration at the tip of the crack and therefore propagation of the crack. However, as soon as the dynamic situation is encountered the stress concentration is reduced and the crack is stabilized and no further growth occurs until the stress is increased or removed and reapplied. The tensile rupture and tearing of a polymer also involve crack propagation from a pre-existing crack in the material and Andrews came to the conclusion that a unified theory of rupture in elastomers "may eventually be based upon their hysteresial properties".

3.5. The Investigations of Smith, Mullins and Harwood.

The work of T.L. Smith has been previously mentioned. Smith showed [55] that the ultimate stresses and strains in a material depended on the conditions of rate and temperature under

which rupture occured. The dependence of these two quantities was found to obey the W-L-F equation and hence information regarding tensile strength was unified over a wide range of temperature and frequency.

Greensmith & Thomas [48] measured the tearing energy of a propagating cut for an imposed rate of cut propagation. Mullins [56] applied the principles of time-temperature superposition discussed previously to the results of Greensmith and Thomas and found that the characteristic tearing energy of a range of butadiene-styrene and butadiene-acrilonitrile polymers which were not reinforced by inorganic fillers could be described in a simple unifying way over a wide range of temperature and frequencies. An important feature of this work was that the rate-temperature transform found necessary to describe the tearing data differed from the W-L-F equation for viscous processes. The success of that type of transform did, however, establish the importance of visco-elastic processes in the smooth tearing of rubber. This was further demonstrated when a simple proportionality between values of tearing energy and hysteresial damping measured on a torsional pendulum was found to exist.(Figure 3.4.) The different symbols refer to different polymers or co-polymers and the two lines represent two different rates of tearing.

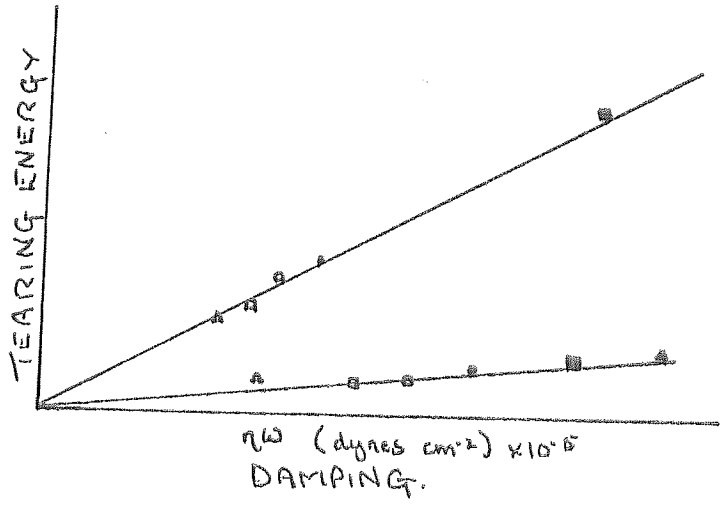

Figure 3.4. Dependence of Tearing Energy on Damping.

Harwood [57] measured the hysteresial energy loss of a number of polymers by comparing the areas under the extension and retraction curves during a tensile test. He derived an empirical relationship between the energy to break and the energy loss up to the same extension. The results showed that increased hysteresis gave increased strength or increased resistance to crack propagation and added weight to much of the theory described in the preceeding pages. Harwood further showed that other dissipative

mechanisms such as the hysteresis energy loss caused by reinforcing fillers can contribute to strength.

Measurement of temperature and frequency effects on the ultimate properties of polymers have led to a better understanding of the mechanisms involved as is outlined above. These measurements have also led to the observation of the technologically important "master-curves" which unify data obtained under different test conditions.

3.6. Objects of This Work

In spite of the importance of the effects of temperature and frequency on many mechanical properties, the subject of the change in fatigue resistance with changes in these parameters has not been thoroughly investigated. The effect of temperature and frequency are not only technologically important to fatigue, but, as explained earlier, the interrelation of the parameters can indicate the molecular mechanisms which affect the process. Hence it was decided to investigate the effects of temperature and frequency of deformation on the fatigue resistance of rubber. The work involved the development and evaluation of a method of fatigue resistance measurement.

Some attention was also paid to another neglected area of the subject of rubber fatigue, that of the morphology of fracture surfaces. A study of fracture surfaces has proved useful in understanding fatigue mechanisms in the metallurgical field [58] but in rubber polymers this study has been restricted to observations of the torn surface as an artificially induced cut grows through a rubber test-piece.

Finally in view of the importance of hysteresial energy loss in determining the resistance of rubber to other modes of failure it was also decided to investigate the relationship between fatigue resistance and hysteresial energy loss in the rubber.

4. MORPHOLOGY OF FRACTURE SURFACES

Equations such as 1.15. which describe the fatigue resistance of a rubber test-piece deformed in simple tension depend upon quantitative observations of the "rough" cut-growth process, and the fatigue process is thought of as the incremental growth of one or more cracks through the material until one crack reaches a critical size, when the sample fails catastrophically. This type of crack propagation process has been called, "stable" crack propagation [53] and the mechanisms involved may well form the basis of a coherent theory of fatigue failure.

4.1. Stable Crack Propagation

In a material which shows marked energy loss due to mechanical hysteresis, the stress at the tip of a propagating crack is much less than that at the same crack under conditions of non-propagation. Thus when a crack begins to propagate in a hysteretic material, the stress redistributes so as to oppose this propagation. Two possible explanations have been given for this phenomenon.

The first explanation assumes that the stress distribution around the tip of a crack can be frozen in position because of

hysteresis. If the stress distribution does not move as the crack propagates then the crack will follow the locus of maximum stress, which deviates from the axis of propagation, and it will also move into regions of lower and lower stress and will eventually stop unless the stress is increased again. The second possible explanation derives from the time dependence of the energy necessary for tearing. The faster the propagation the more the energy needed and hence there is a tendency to deceleration.

In the case of crack-growth at constant deformation the crack propagates and some mechanism (possibly one of those described above) opposes this propagation and finally stops it. For the crack to grow again, the stresses in the components of the molecular network must reorganise themselves until the critical condition for propagation is again achieved. Under dynamic conditions, that is, conditions of repeated deformation, the critical condition is restored by removing and reapplying the deformation. The conclusion may be drawn that fatigue failure, that is, accelerated failure arising out of repeated deformation, only occurs when the time for relaxation or redeformation is shorter than for the time of the natural redistribution of stress.

Implicit in this description of the fatigue process are the assumptions :-

(a) Fatigue is the growth of a flaw which is present in the material.

(b) The same rules govern the growth of small flaws as those which govern the growth of large scale "model" cracks.

During crack-propagation studies on a strain crystallising elastomer, natural rubber, [59] conditions of "rough" and "smooth" cut-growth were observed at the tip of a cut in a "pure shear" cut-growth test-piece (see Figure 1.1.). From the cut surfaces micrographs were obtained showing the incremental nature of the growth under both conditions. The increments of growth take the form of bands running perpendicular to the direction of crack-propagation between the major surfaces of the test-piece (Figure 4.1.). The number of bands appearing in a given time is equal to the number of cycles of deformation applied to the test-piece.

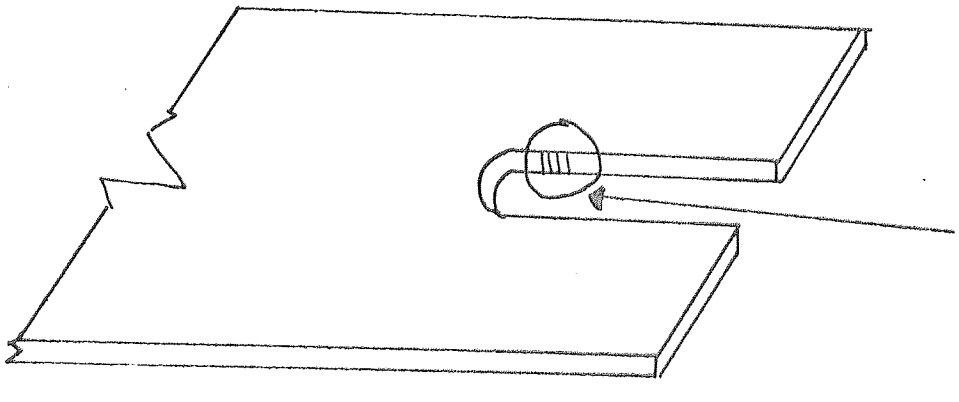

Figure 4.1. Striations seen in the surface of a growing crack in a "Pure Shear" cut-growth test-piece
After Andrews

Under conditions of "smooth" growth the bands are parallel and of equal width, under "rough" growth conditions they are not parallel and of varying widths. Interferograms reveal the surface of the banded region to be "cusped" and this fact led to the conclusion that the bands arise because of the deviation of the growing tip of the crack from the straight ahead direction. It was further shown that the crack follows the locus of maximum stress which deviates off-axis. None of these effects were observed in amorphous rubbers.

In the present investigation the fatigue-failure surfaces of an amorphous and a crystallising rubber were examined for evidence of the crack-growth phenomena described above and for any other information on the process leading to failure by fatigue.

4.2. Experimental

The failure surfaces of fatigue test-pieces of the dumbell type described in Chapter I were viewed as shown in Figure 4.2.

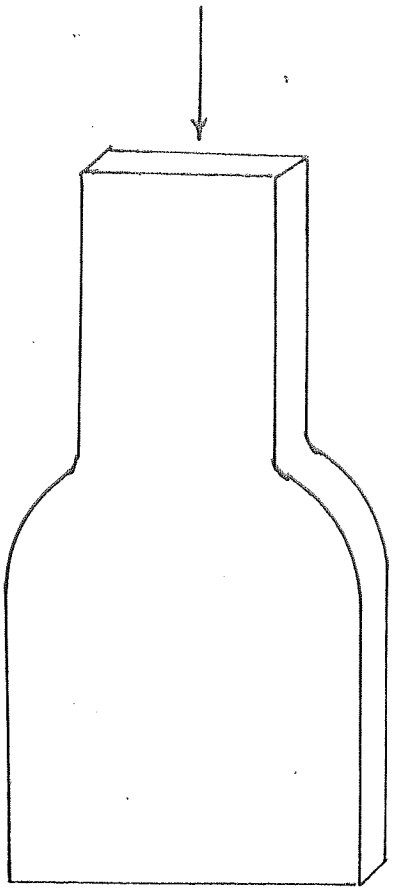

Figure 4.2.

Samples are viewed as indicated in the diagram.

The surface was examined at a number of magnifications ranging from 10x to 20,000x using a light miscroscope at lower magnification and a "Stereoscan" electron miscroscope at higher magnifications. The cut-growth nature of the failure surfaces was evident when they were viewed at about 100x magnification. Montages of the whole of the failure surface were constructed

for a number of different test-pieces to investigate the effect of such things as strain, filler content and crystallisation. The best montages were obtained with photographs taken from the screen of a scanning electron microscope.

4.3. The Scanning Electron Microscope

The scanning electron microscope (SEM) uses electrons and electron lenses but other than that is entirely different in principle to the transmission electron microscope (TEM). The SEM is shown schematically in Figure 4.3.

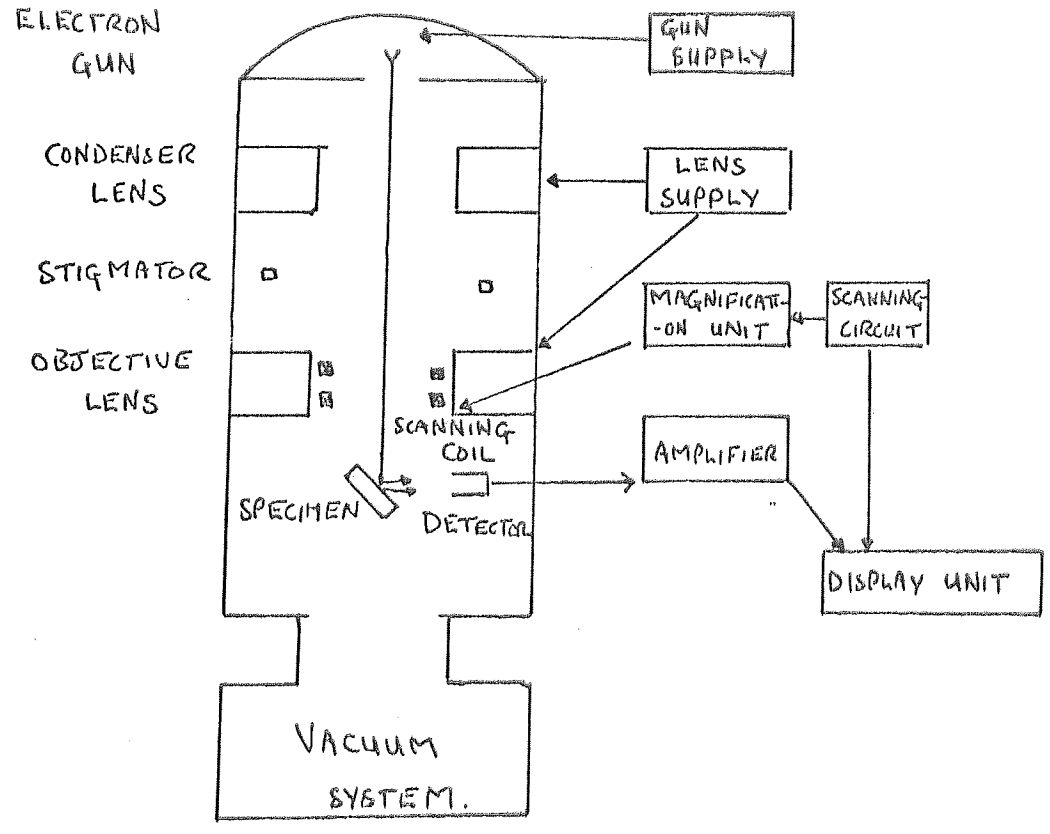

Figure 4.3. Block diagram of the scanning electron microscope.

The electron gun produces a stream of electrons which is formed into a fine beam ($\bar{}$ 100A^{o} diameter). This beam on striking the sample generates signals due to secondary electron emission, a reflected electron current, cathodoluminescence and X-rays. These signals are detected and amplified and used to control the brightness of a display of cathode ray tubes and the position of the spot with respect to these tubes depends upon the position of the incident beam which can be scanned across the sample to build up a picture of a surface.

Figure 4.4. shows how the incident beam spreads as it hits the specimen.

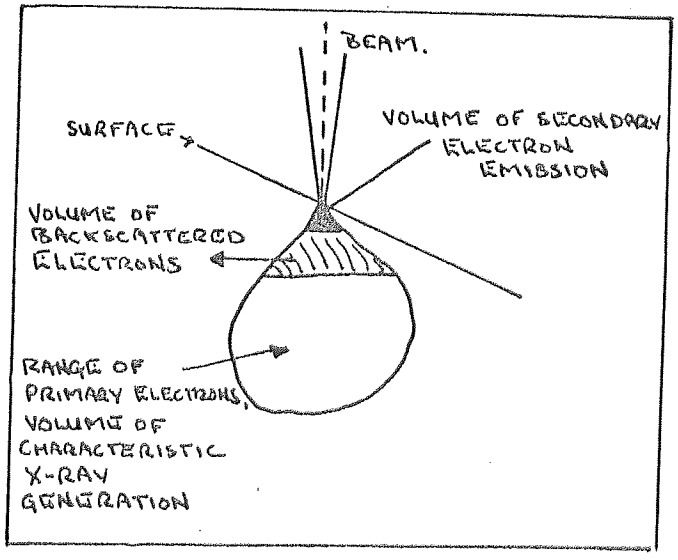

Figure 4.4. Penetration of Electrons in the test-piece.

Secondary electrons from deep in the sample are absorbed because of their low energy (30 eV) only those generated near the surface are detected and as Figure 4.4. shows these come from a small area and, therefore, give the best resolution. Changes in the angle of the emitting area cause changes in contrast in the image, so that edges expose more surface area and appear bright. This variation in brightness with surface angle produces an image much the same as in the visual world. The angle of the incident beam at the cross-over is very small (2.10^{-3}) so that, if the sample surface is close to the cross-over point the area emitting secondary electrons varies little in size over quite a wide range. This gives a good depth of field (1,000μm at 100X) and 10μm at 10,000X). The resolution and depth of focus which can be obtained make the SEM an excellent instrument for surface studies. Added advantages are that no replication of the surface is necessary and focussing is independent of manigication so that an area can be examined in detail at any magnification without continually refocussing.

The SEM was convenient for the montages constructed for this investigation for the following reasons. The raster size on the viewing tube is constant, so that the raster size on the

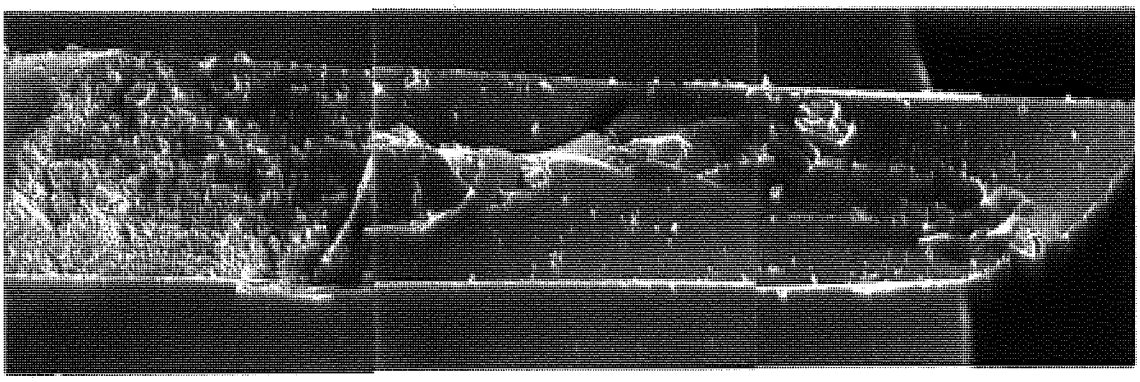

Fig. 4.5. Failure surface of Natural Rubber Test-piece. Montage of stereoscan electron-micrographs. Magnification 80 X. 60^{o} incidence gives foreshortening from top to bottom of picture

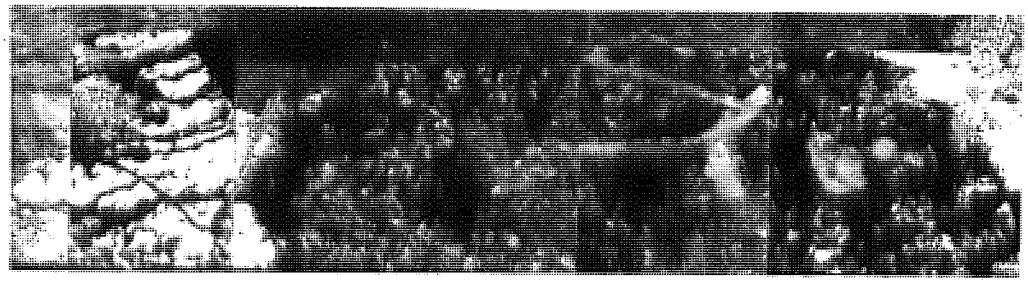

Fig. 4.6. Failure surface of Natural Rubber Test-piece. Montage of light microscope photographs. Magnification 80 X. Normal incidence. Compare with Fig. 4.5. above, noting rough area developing into smooth striated region.

sample depends on the magnification. At a magnification of 100X there is an effective field of view of 1mm x 1mm. The surface to be viewed at this magnification or less was 1mm x 3mm and a montage could be conveniently constructed from three or four pictures. For example Figure 4.5. shows a montage of the failure surface of a natural rubber fatigue test-piece obtained from photographs of the screen of a SEM.

'The light microsceope available has a field of view of only $\frac{1}{2}$mm x 1mm and so a montage of the failure surface contained more pictures and was consequently much more difficult to prepare, because of the problems of constancy of illumination and magnification, when changing from one area to another. Photographs of neighbouring areas are much more difficult to "match" and constructing a uniform montage under these conditions is time consuming. Figure 4.6. shows the failure surface of a natural rubber test-piece as seen with a light microscope. The advantages derived from the SEM are conclusively demonstrated when Figures 4.5. and 4.6. are compared.

4.4. Failure-Surface Morphology

Test-pieces of styrene-butadiene rubber and natural rubber were repeatedly deformed at room temperature to a maximum

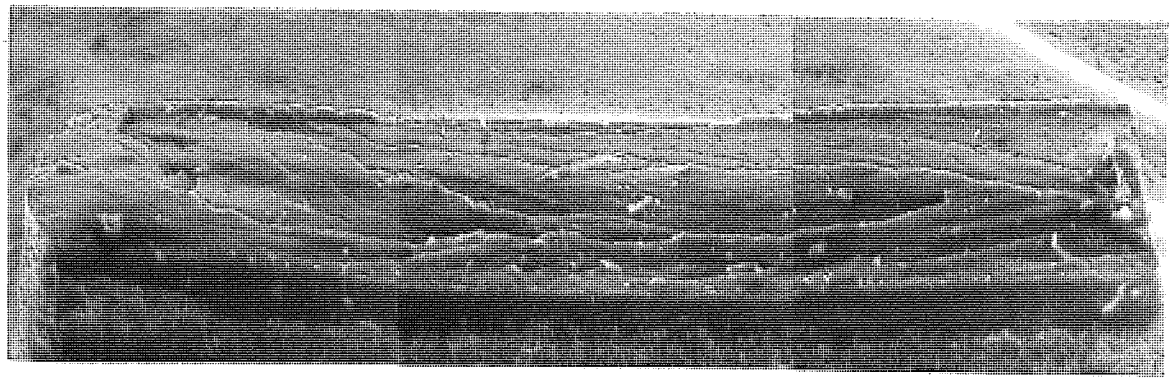

Fig. 4.7. Failure surface of Styrene-Butadiene Test-piece. Magnification 60 X.

Montage of stereoscan micrographs. Foreshortened from top to bottom of picture by 60° incidence. Note smooth surface except for V-shaped markings.

extension of 200%. the choice of test conditions being purely arbitrary. The surface revealed by the ensuing fracture was viewed as described previously and a composite picture of each surface was constructed.

4.4.1. Styrene-Butadiene Rubber

The failure surface obtained in this case is shown in Figure 4.7. The characteristic of this surface is the shallow ridge pattern which forms a V-shape pointing in the direction of crack propagation. Andrews [59] noted that there is no evidence in the crack-growth surface of a non-crystallising polymer of deviation of the crack from the axis of propagation, and a relatively smooth surface is obtained when compared with the crystallising case. This is confirmed in the fatigue-failure-surface shown here.

4.4.2. Conic Markings

The V-shaped markings in the surface are probably due to a similar mechanism to the so-called "conic markings" which have been identified in the failure surface of polymethylmethacrylate (PMMA) and filled elastomers at low temperatures [53]. These

"brittle" fractures leave a "conic-shaped" ridge pattern on the fracture surface which is explained as follows.

The stress concentrations at inhomogeneities in the material, when superimposed on the stress concentration surrounding the approaching crack-tip, cause the breaking stress of the material to be exceeded in a number of regions to the side of and to the front of the main fracture. These fractures spread in a circular manner in a plane parallel to the main fracture plane and if the planes are sufficiently close the fractures become joined at a small step in the surface. The main fracture being diverted into the secondary fracture plane [60].

If the main fracture advances in the x - y plane at velocity v, then :-

$$x = vt$$

If the secondary fracture expands circularly at radial velocity u, so that the "fronts" meet at time t then at this time

$$y = u^2t^2 - (x_o - x)^2 \quad \tfrac{1}{2}$$

where x_o is the distance between the main fracture front and the inhomogenerty at time $t = 0$. Eliminating t an equation of the form

$$x^2 (u^2/v^2 - 1) - y^2 = x_o(x_o - 2x)$$

is obtained which is "conic" in form, e.g. parabolic when $u = v$. This suggests that the majority of the failure surface in a styrene-butadiene fatigue sample is associated with a single fracture step, and that the process taking place in the fifty thousand or so cycles making up the fatigue test was confined to a small area, which is not easily identified in the fracture surface.

4.4.3. Natural Rubber

Figure 4.5. is the fatigue-failure surface of a natural rubber test-piece. There are two distinct regions in the surface. There is an extremely rough surface which becomes gradually smoother, and there is a region which is generally characterised by a ridge running in the direction of the propagating crack with striations running between the ridge and

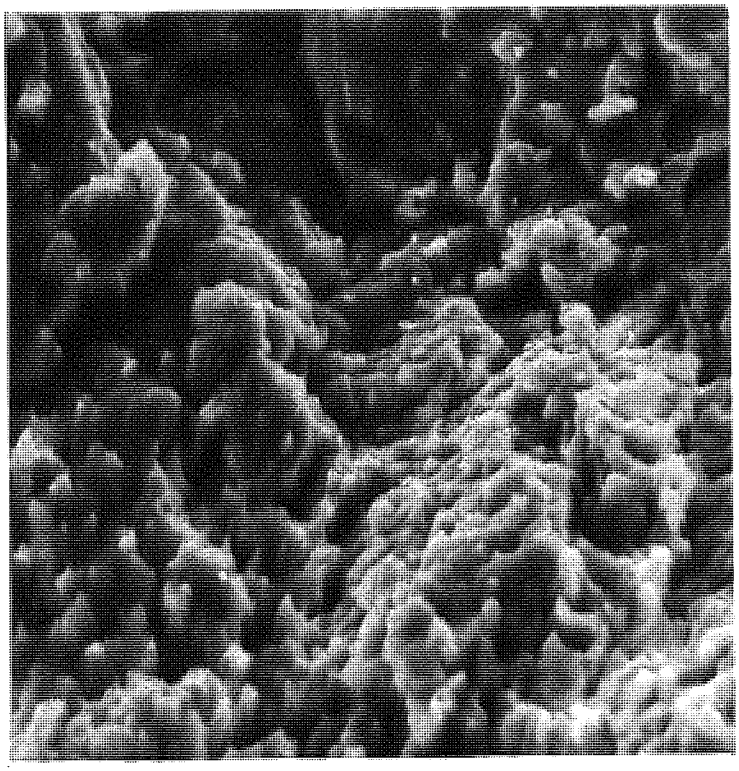

Fig. 4.8. Stereoscan Micrograph.

Magnification 1,000 X.

Area of rough growth in Natural Rubber Failure Surface.

Fig. 4.9.

Stereoscan Micrograph
Magnification 1,000 X.

Incremental smooth growth in natural rubber failure surface.

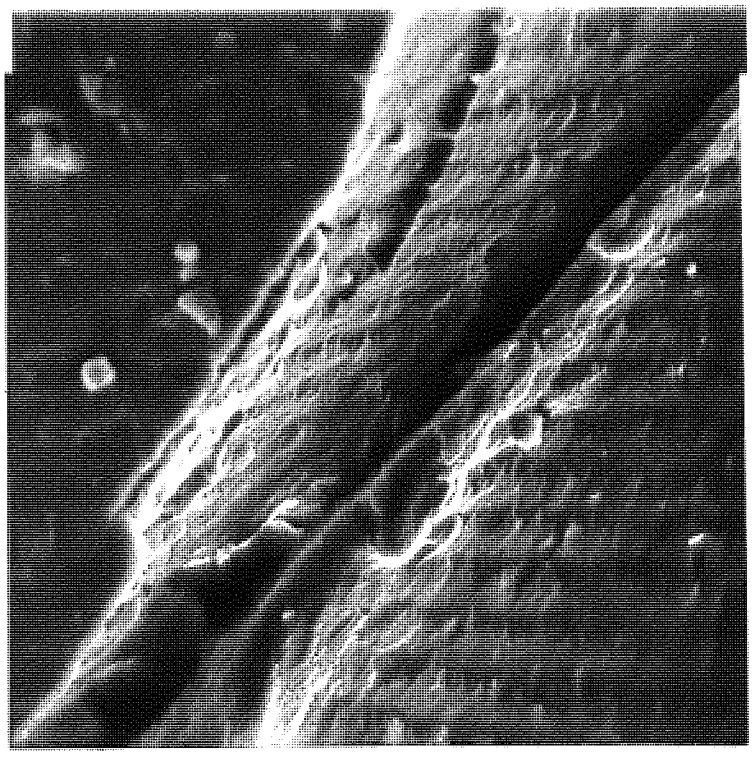

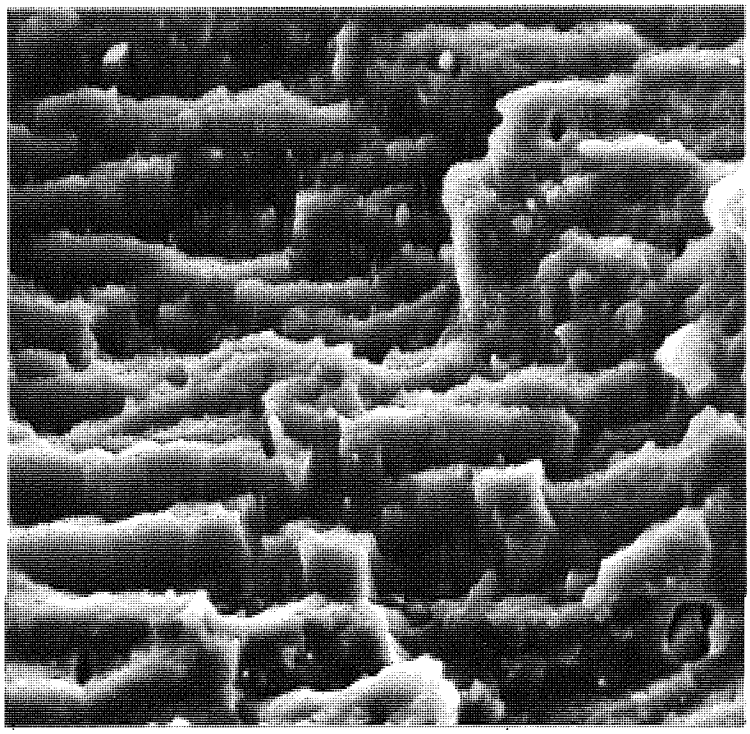

Fig. 4.10. Stereoscan Micrograph.
Magnification 1,000 X.

Rough growth area of a filled Natural Rubber Test-piece. Note the ridged appearance of the surface.

Figure 4.9. is a magnified picture of the "smooth" region of the fatigue-failure-surface. The striations are clearly visible as a "cusped" wave pattern on the surface of the sample. The striations are parallel sided and are similar to the pictures of "smooth" growth at the tip of a propagating crack [59].

4.4.4. Crack-"Forking"

There is ample evidence of cut-growth in the fatigue-failure-surface of a crystallising rubber. This evidence arises because of the tendency of the crack to deviate from its axial direction. Under the conditions giving rise to the "rough" surface this deviation is random in size and direction but under the conditions of "smooth" growth the deviation is more ordered and forms a pattern on the failure surface.

The deviation from the axis has been explained [53] in terms of a "frozen" stress distribution at the tip of a propagating crack. A crack usually propagates so that the locus of maximum stress moves with the crack. Thus a crack in a uniform field of force propagates in a straight line. If the stress distribution does not move with the crack or if it does not move at a speed approaching the velocity of propagation then the

locus of maximum stress does not coincide with the axis and the crack deviates. (Figure 4.11.)

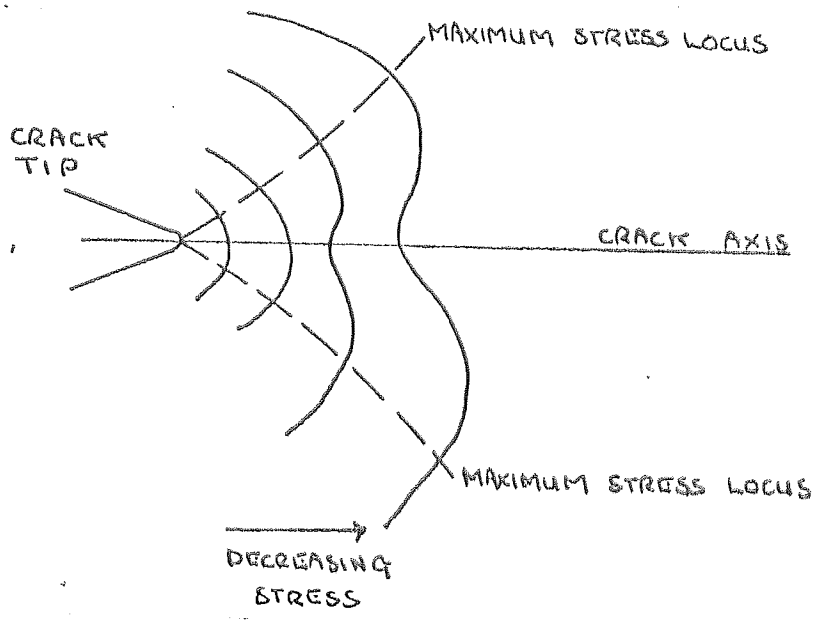

Figure 4.11. The Maximum Stress Loci in the Distribution at a Crack Tip.

In materials where the stress is proportional to the strain this occurs when the velocity of crack propagation approaches the speed of sound. In rubbers this occurs at much lower velocities and is probably due to the visco-elastic nature of the material or to losses in energy by some other mechanism.

"Forking" can result in a series of undercut mounds on the surface of the rubber. (Figure 4.12.)

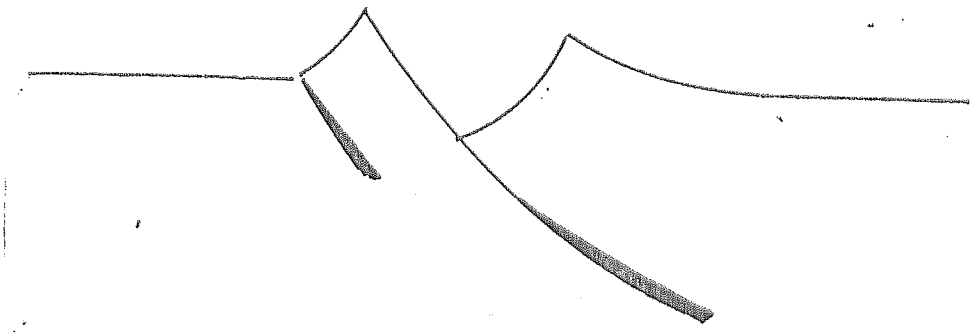

Figure 4.12. Undercutting of a Fracture Surface due to crack "forking" (after Andrews)

This type of surface is well known to occur in styrene-butadiene rubber under conditions of so-called "stick-slip" tearing [53]. Its appearance in the fatigue-failure-surface of natural rubber indicates that "forking" can take place oven when the crack is growing in a number of discrete steps. The "forking" makes the crack grow along two parallel planes at the same time.

4.4.5. Rough and Smooth Crack-Growth

The following observations were made to determine the relative contributions of the "rough" and "smooth" regions to the fatigue failure. The major surfaces of a fatigue test-piece were viewed (at intervals throughout the fatigue test), as shown in Figure 4.13.

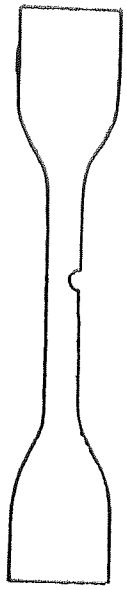

Figure 4.13. Crack developing in the edge of a test-piece during a fatigue test.

The plane in which final failure occurs becomes evident after the test has progressed for a large proportion of the total lifetime. A crack opens-up in the edge of the sample or occasionally in the centre of the sample. This crack increases in size until at some stage it begins to propagate quickly through the sample. It was seen that, depending on the maximum strain, the crack grows different distances across the sample before catastrophic failure occurs. This is consistent with the assumption that crack growth is a function of the tearing energy of the material. The energy necessary to cause "catastrophic" tearing in a test-piece in simple extension (T_o) is related to the strain and the crack length by the expression.

$$T_c = 2kWc \quad \ldots \quad \ldots \quad \ldots \quad 4.1.$$

Hence at higher strains i.e. higher values of the stored energy (W) the length of crack c which will satisfy the expression 4.1. is smaller.

At 200% maximum extension of a natural rubber test-piece at room temperature the crack grows to a length equal to about 1/5th of the sample width before the final stage of failure begins.

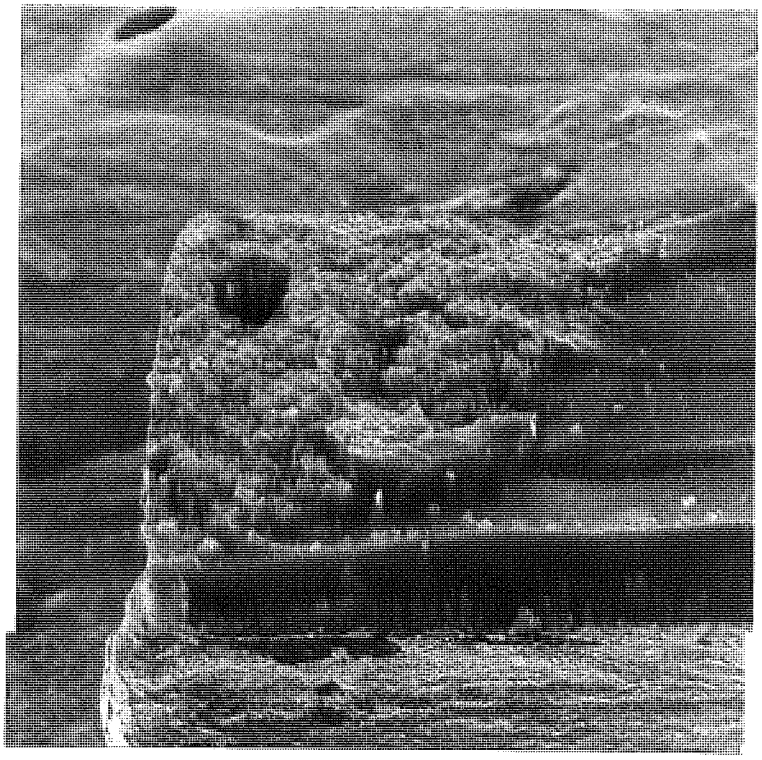

Fig. 4.14. Stereoscan Micrograph
Magnification 60 X.

Test-piece torn across prior to the
onset of 'Smooth' growth.

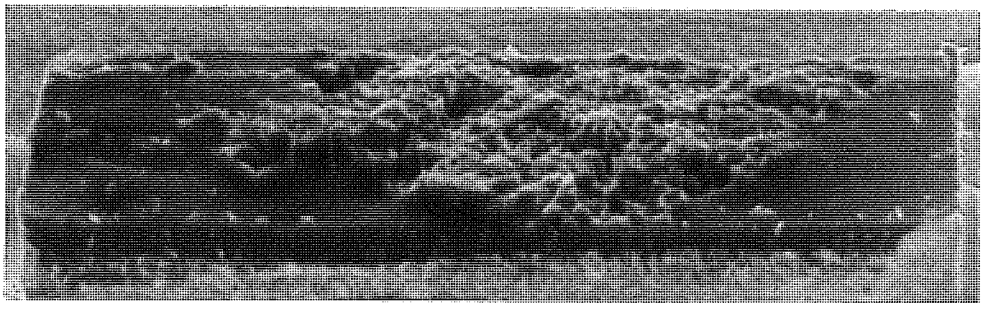

Strain Cycle 0 - 150%

Strain Cycle 0 - 200%

Strain Cycle 0 - 250%

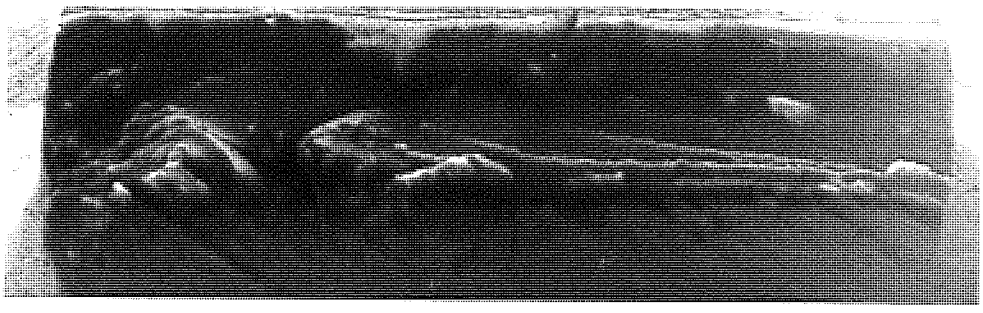

Strain Cycle 0 - 300%

Fig. 4.15. Stereoscan Micrographs. Magnification 40 X.

The effect of strain on the failure surface of Natural Rubber. Note the decrease in the visible area of 'Rough' growth with increased strain.

In this final stage the crack begins to grow rapidly across the sample. The initial stage corresponds to about 50,000 cycles of deformation and the final stage to about 300 cycles of deformation.

A natural rubber sample was tested under these conditions until a crack appeared and grew to about 1/5th of the sample width. The test was then stopped and the surface "torn" across from this crack. The resulting surface is shown in Figure 4.14. The rough region of the fatigue surface is evident but there is then a typical "tear" surface with no evidence of "smooth" cut-growth striations. If the crack is allowed to propagate across the whole of the sample the striations in the "smooth" region are seen to agree in number with the number of cycles making up the final stage of failure. This is only a small percentage of the total lifetime except at severe strains. It is still less than 1% at 300% extension and so the fatigue process is identified with the "rough" growth region.

At lower strains one would therefore expect to see a larger "rough" region and at higher strains a smaller "rough" region. This is confirmed in Figure 4.15. which shows montages of the fatigue-failure-surfaces of natural rubber test-pieces, failure being brought about at four different levels of maximum

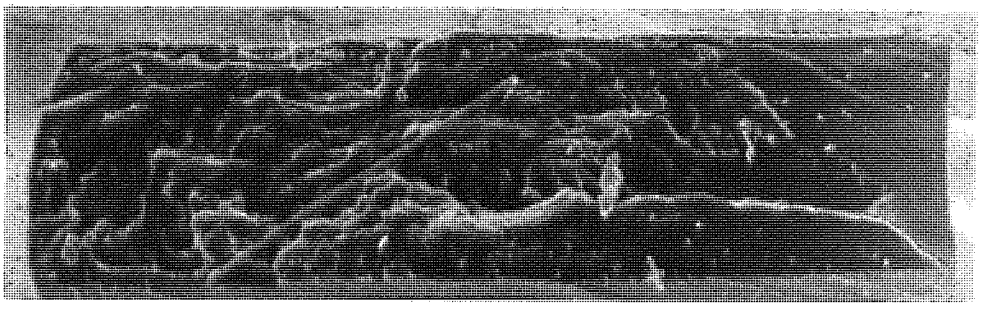

Strain Cycle 0 - 100%

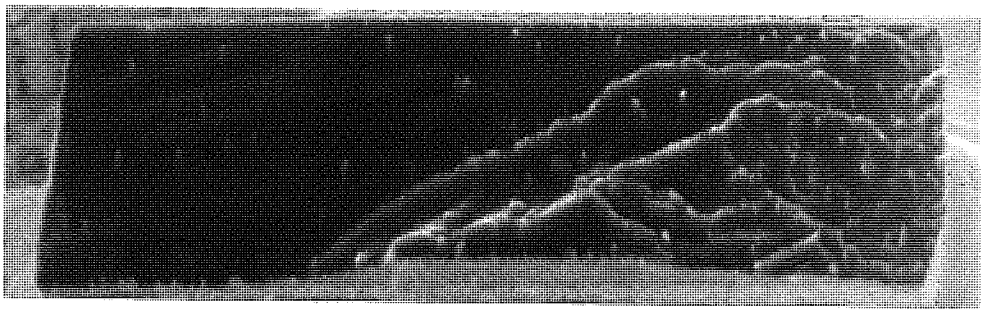

Strain Cycle 0 - 150%

Strain Cycle 0 - 200%

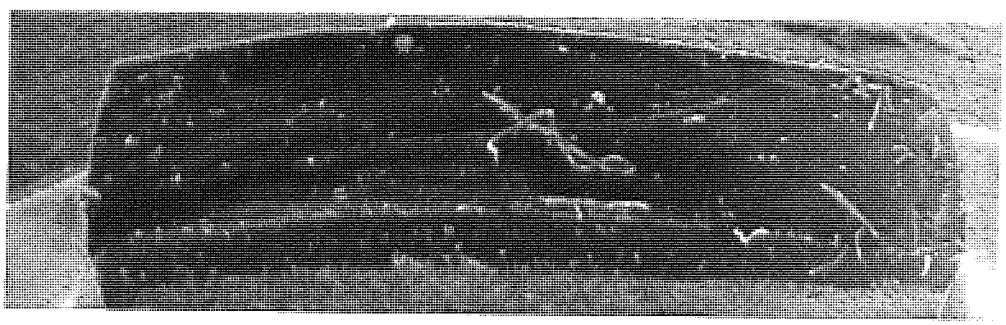

Strain Cycle 0 - 250%

Fig. 4.16. Stereoscan Micrographs. Magnification 40 X.

The effect of strain on the failure surface of Styrene-Butadiene Test-pieces: Note the appearance of 'Rougher' sufface at lower strain.

deformation. The visible "rough" region is diminished as the strain is increased until at high strain (300%) there is almost no "rough" region to be seen and the failure surface is very much like that observed in the amorphous case.

If styrene-butadiene test-pieces are observed as in Figure 4.12. during the fatigue test. At 200% maximum extension and room temperature the plane of failure is evident for a much shorter time than with natural rubber. If however, the strain is reduced then as with natural rubber the crack is seen to open up and grow across the sample as might be expected from the above theory. At 100% extension the test-piece supports a crack which extends across more than half of the test-piece, before the final stage of failure occurs. In this case the final stage of failure is "catastrophic", the crack progressing across the sample in a very short time during a single cycle of deformation.

Montages of the fatigue-failure-surface of SBR samples were constructed for tests carried out at different maximum deformations. As is seen in Figure 4.16. regions of "rough" growth become apparent at lower strains. Though this rough growth is less "coarse" than in the crystallising case the same pattern of failure is now established in both the amorphous and the crystallising cases.

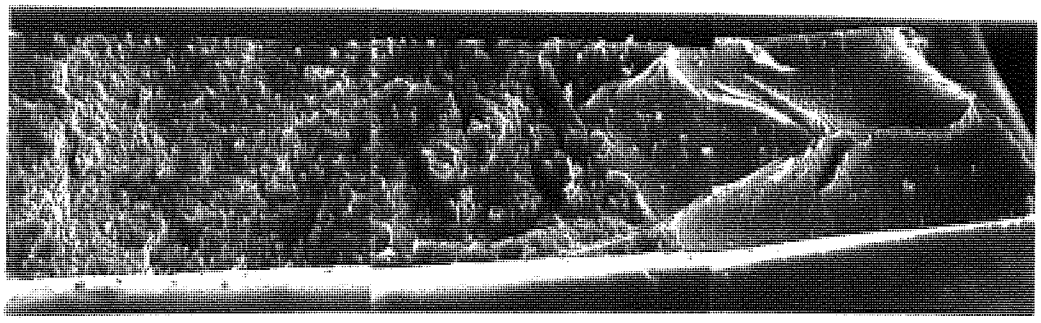

+10 Parts of Filler.

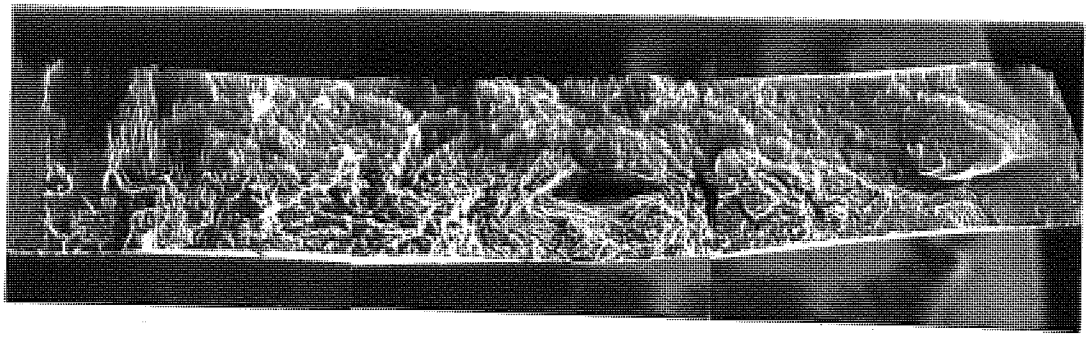

+50 Parts of Filler.

Fig. 4.17. Stereoscan Micrographs. Magnification 40 X.

Failure surface of Natural Rubber as the amount of filler in the Rubber is increased. Compare with Fig. 4.5. i.e. 0 parts of filler.

4.4.6. The Effect of Fillers

The addition of carbon-black as a filler to the rubber gives results which support the conclusions obtained from the investigations on unfilled rubbers. In the natural rubber test-pieces the length of the cut which can be supported before failure occurs is increased as the amount of filler in the rubber is increased. (Figure 4.17.) The addition of carbon black is known to increase the tear strength (T_c) of the rubber [62]. This does not necessarily imply an increased fatigue resistance as increasing the filler also increases the energy of deformation and hence the rate of cut-growth in the rubber. (see Chapter I). At comparable energies of deformation the crack-length which can be supported is increased with filler content up to some maximum value. This explains the observed increase in fatigue resistance (N) when plotted against the energy of deformation W (see Chapter I) for different filler contents. (Figure 4.18.)

The gradient is seen to change slightly with increased filler indicating a decreased cut-growth rate. This change in growth rate is not sufficient to account for the changes in the fatigue resistance. However, tear strength may be increased by a decade or so [62] and could easily account for this increase.

25 Parts of filler.

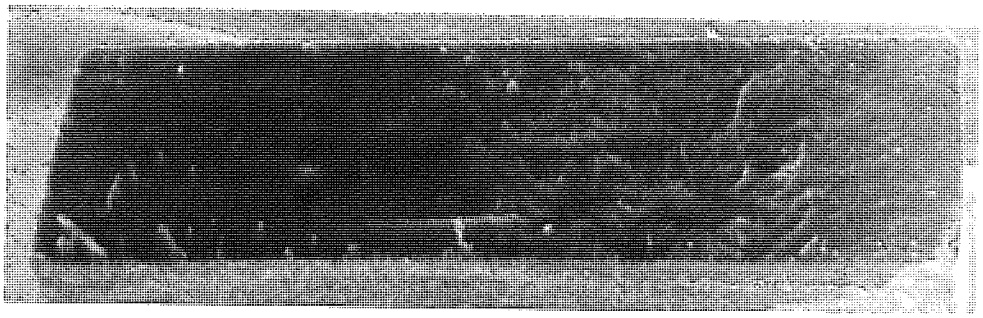

50 Parts of filler.

75 Parts of filler.

Fig. 4.19. Stereoscan Micrographs. Magnification 40 X.

The effect of filler on the failure surface of Styrene-Butadiene Test-pieces. Compare with Fig. 4.7. i.e. 0 Parts of filler.

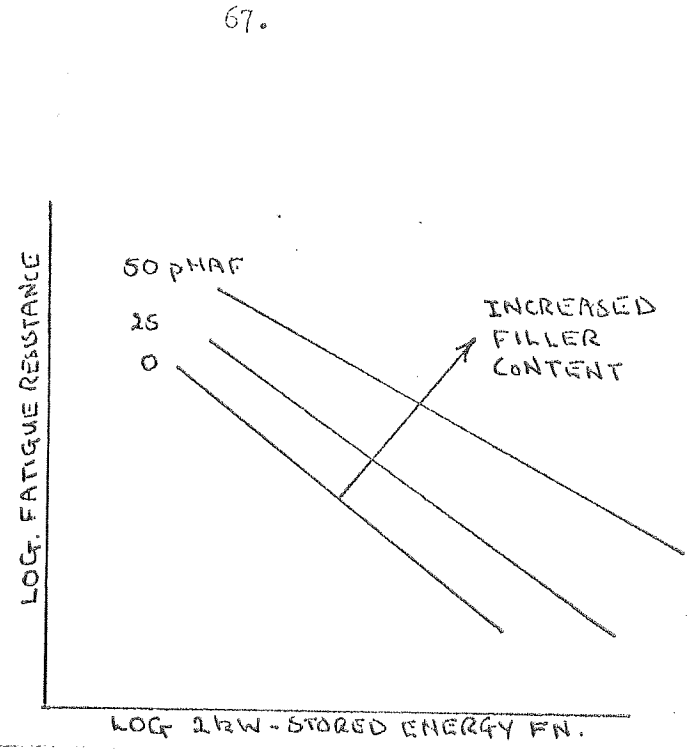

Figure 4.18. The Effect of Filler Content on the Fatigue Resistance of Styrene-Butadiene Rubber.

In the amorphous rubber the addition of filler caused a fatigue-failure-surface much closer in appearance to the rough surface seen in natural rubber. Figure 4.19. shows the effect of increasing the amount of filler in the rubber on the fatigue-failure-surface at the same maximum deformation. The visible rough region is decreased as the strain energy of the rubber is increased. The lowest filler content shows a Natural Rubber-

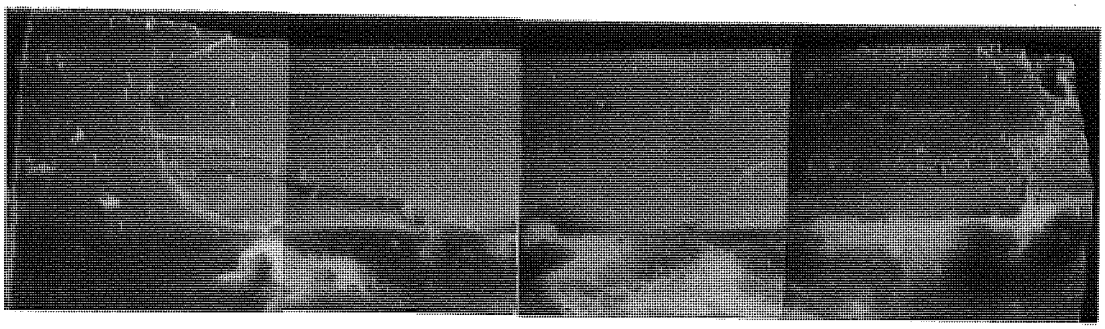

Natural Rubber Tear from razor cut at left-hand end.

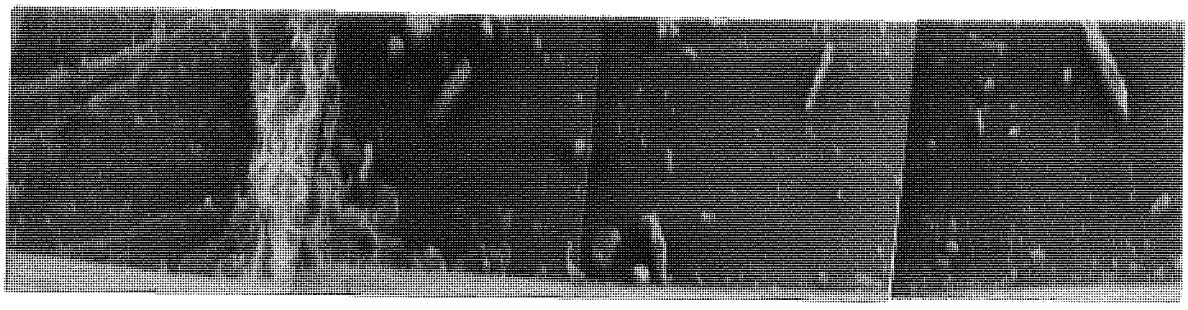

Natural Rubber Tensile.

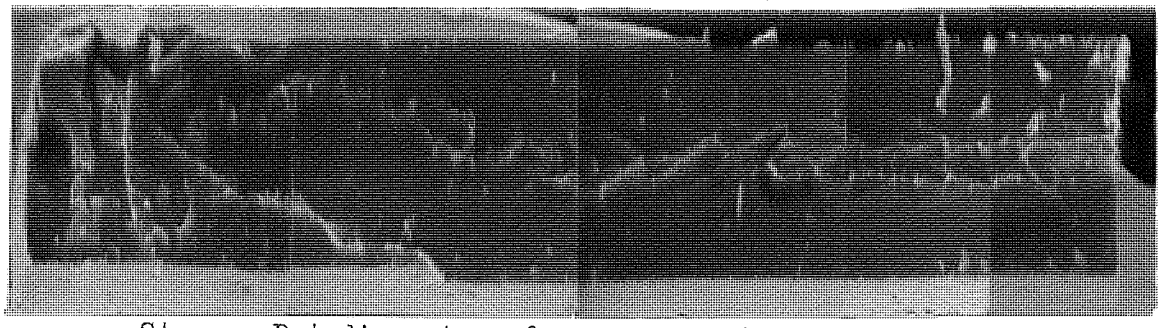

Styrene-Butadiene tear from razor cut at left-hand end.

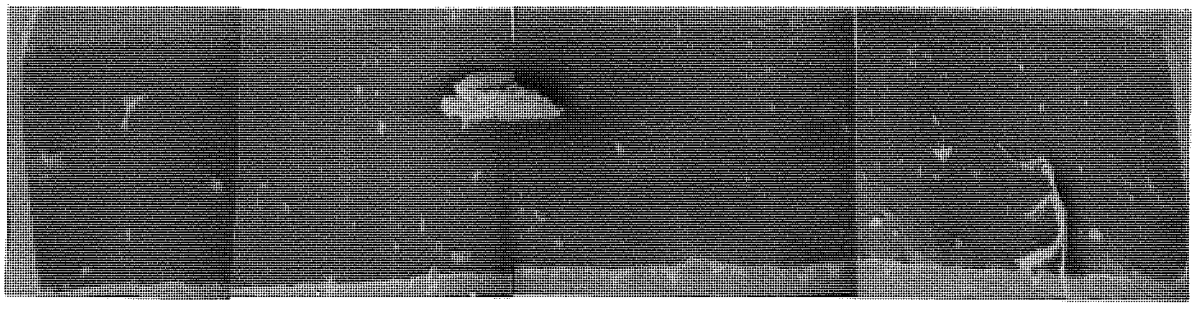

Styrene-Butadiene tensile.

Fig. 4.20. Stereoscan Micrographs. Magnification 40 X.

Tear and tensile failure surfaces of amorphous and crystallising rubbers.

like roughness which extends across most of the failure surface. Also with amorphous rubbers the addition of filler is seen to increase the tearing energy [62] and hence the length of crack which can be supported before the onset of the final stages of failure.

4.4.7. "Tensile" and "Tear" Failure Surfaces

Figure 4.20. is included in order that a comparison may be made with the fatigue-failure-surface and the surfaces revealed by these other modes of fracture. It is seen that the "rough" region is unique to the fatigue surface. However, some of the features of crack propagation observed in the fatigue samples are observed in these "one-cycle" failure surfaces. "Conic markings" and "undercutting" are visible in the styrene-butadiene tear sample.

4.4.8. Dimple Rupture

During the investigation some test-pieces were broken at low temperatures by bending them under liquid nitrogen. The purpose of this was to see whether the surface revealed was changed

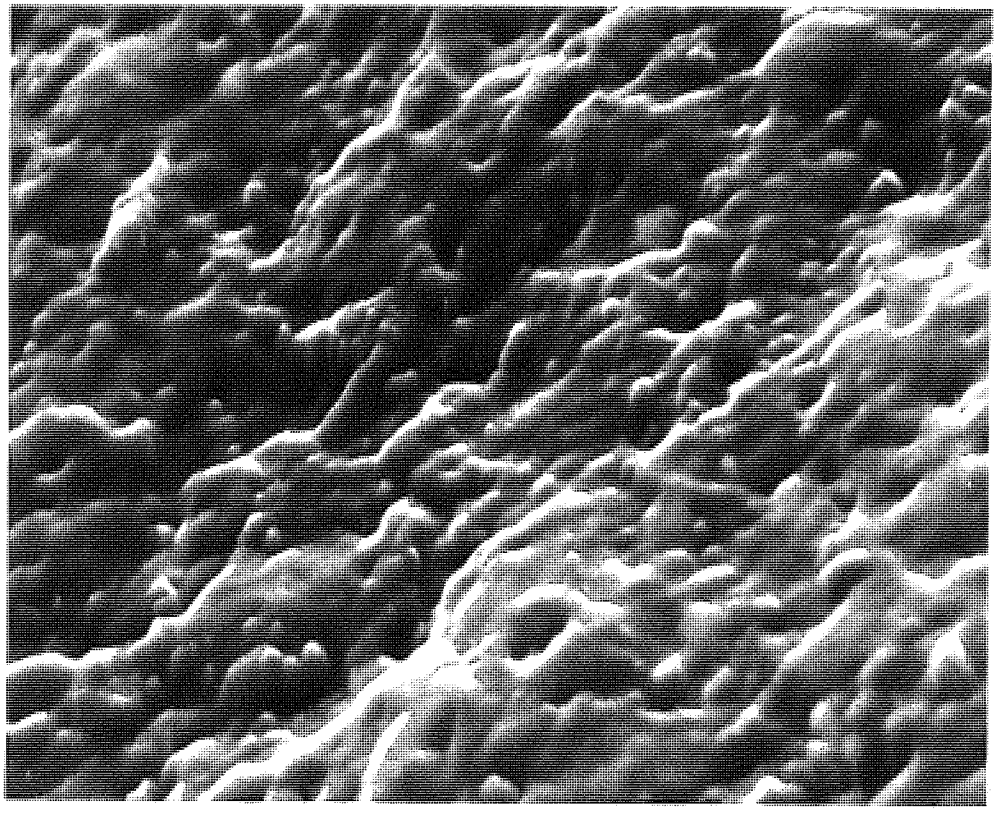

Fig. 4.21. Stereoscan Micrograph. Magnification 11,000 X.

Uncycled Natural Rubber Test-piece surface revealed by fracturing after freezing. 'Dimple' nature of the surface is clearly visible.

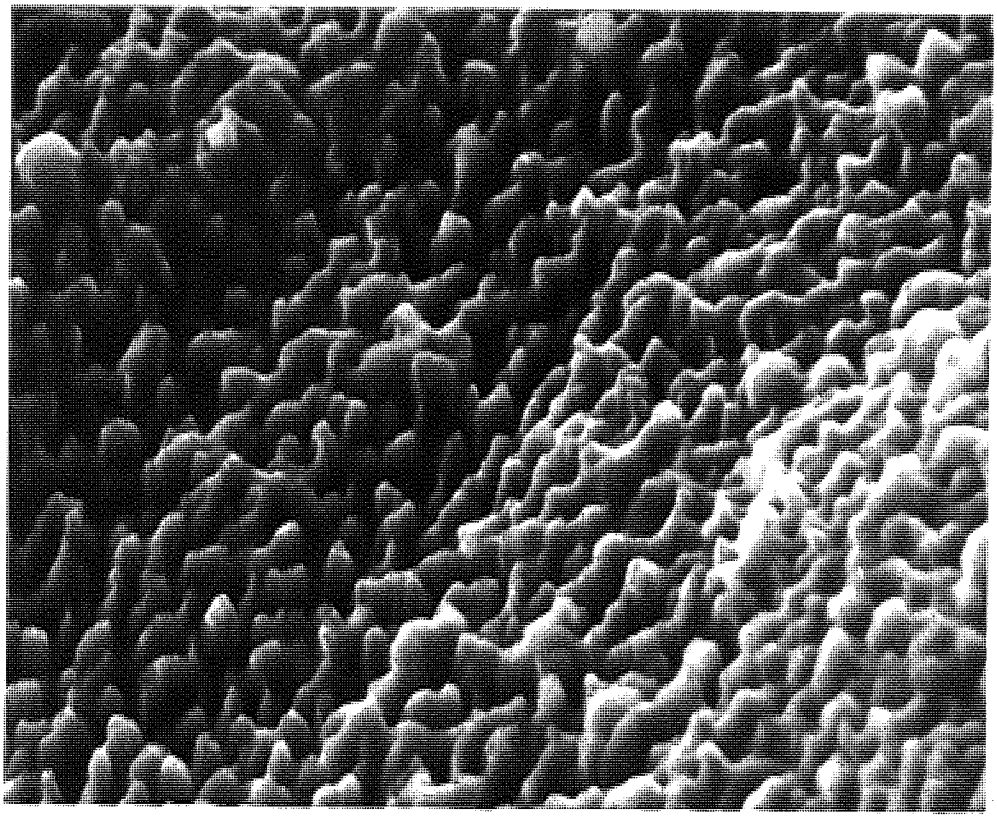

Fig. 4.22. Stereoscan Micrograph. Magnification 11,000 X.

Natural Rubber Test-piece failed afted 80,000 cycles. Surface is not the failure surface but one exposed by fracturing after freezing. High magnification of micro-roughness very similar in appearance to 'Dimple' fracture in metals.

by giving the test-piece a fixed number of deformations. An interesting result of these experiments was the observation of a type of fracture, well known in metals, and called "Dimple" fracture. In metals this type of fracture is associated with ductile failures and fractures which absorb large amounts of energy. The fracture surface consists of cavities "Dimples", which are concave and often contain a small particle of material at the bottom. The mechanism of fracture proposed is that voids in the material grow when the sample is deformed and join together to form the fracture surface.

Figure 4.21. shows the fracture surface of a natural rubber test-piece which has been fractured in a brittle fashion by first freezing the rubber under liquid nitrogen and then bending it. Many "dimples" are observed in the surface. When the sample has been subjected to a fatigue test and a surface (not the fracture surface) is exposed by freezing and bending, then large "rough" areas of this surface (Figure 4.22.) are remarkably similar in appearance to the "dimple" fracture seen in metallographic surfaces (e.g. stainless steel [63]).

The fact that his sort of surface was only observed in samples which had been repeatedly deformed suggests that voids may

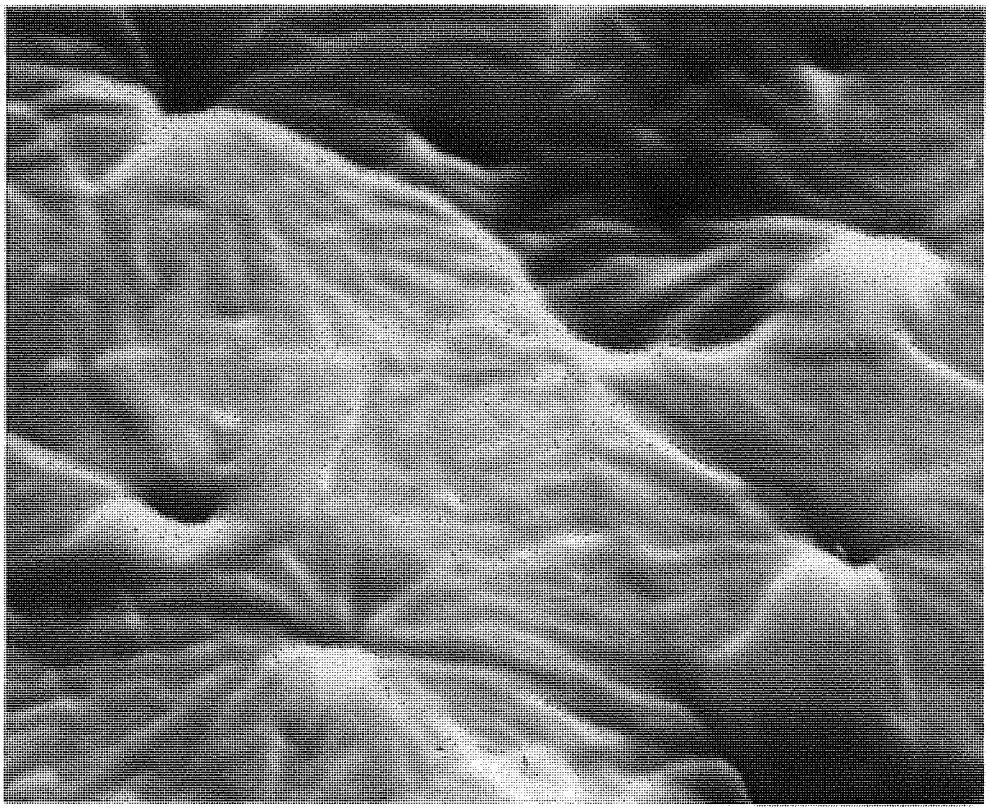

Fig. 4.23. Stereoscan Micrograph. Magnification 10,000 X.

Styrene-Butadiene Rubber surface exposed by freezing and fracturing to show 'Dimple' type rupture.

be formed during the fatigue process at a microscopic level in addition to the macroscopic crack growth and indeed may contribute to a mechanism by which macroscopic growth proceeds.

Figure 4.23. shows the surface of a styrene-butadiene test-piece fractured by freezing as above. Again the "dimple" type of fracture is observed as failure takes place by the joining together of voids and inclusions. There appears to be little difference however, between the cycled and uncycled surfaces as revealed in this material. However, it may be a question of density of "dimples" and this in turn may depend on the conditions of the experiment and further investigation is warranted.

In the metallurgical field much analytical work has been done on this type of fracture [64], [65], [66], [67], [68]. Dimple size has been related to ductility and fracture strength and it may be possible to derive knowledge of polymer fracture strength from similar considerations.

4.5. Discussion

Fatigue-failure-surfaces appear to have a morphology which is unique to this mode of fracture. Two regions can be identified in the surface. The first is "rough" and is closely

associated with the fatigue process. The second region is "smooth" and corresponds to the final stage of "catastrophic" failure. This is consistent with the findings of A.G. Thomas [31] who derived expression for fatigue resistance based on observations of crack-growth when the crack tip was rough in appearance.

This work suggests that the fatigue resistance (N) is related to the critical energy for tearing (tear-strength) T_o in that at higher values of T_c a test-piece can support a greater amount of growth without the onset of catastrophic rupture. This suggests that G in the expression derived by Thomas (see Section II) :-

$$N = G/(2kW)^n c_o^{n-1}$$

is some function of T_c and that changes in N at constant energy of deformation (W) such as those measured with changes in temperature and frequency are associated with changes in the tear strength T_c of the material. Greensmith and Thomas [44] measured the change in T_c with frequency and temperature and these changes are of the same order as the changes observed in fatigue

resistance (N) during this investigation. The picture in filled rubbers is more complicated but in general increases in fatigue resistance (N) caused by increased filler content are matched by increases in tear strength T_c.

The degree of "roughness" in the surface seems to be influenced by such things as crystallisation and carbon-black filler. Deviation of a propagating crack "off-axis" has been explained in terms of hysteresial energy loss and both crystallisation and fillers are associated with increased "lossiness" especially at the high level of strain which would be expected to occur at the tip of a propagating crack.

The observations of fatigue-failure-surfaces carried out in connection with this investigation are, therefore, consistent with quantitative and qualitative observations of the tip of a growing crack and the crack-growth hypothesis of fatigue failure appears to be well founded.

5. MEASUREMENT OF ISOTHERMAL FATIGUE RESISTANCE

5.1. Introduction

In Chapter I fatigue resistance was defined as the number of deformations necessary to bring about a predefined condition in the rubber known as failure. In designing a fatigue test the following variables were considered :-

a) The limit of the deformation :- is the test to be carried out under conditions of constant machine throw, constant sample strain amplitude, constant sample stress amplitude, or constant strain energy amplitude.

b) The type of wave-form :- sinusoidal, square wave or rectangular wave and is the deformation to be repeated regularly or irregularly.

c) The mode of deformation :- tension or shear.

d) The form of the test-piece.

e) What constitutes failure.

Many existing fatigue tests use a fixed strain cycle, sinusoidal motion and deform in simple tension. This type of test has the following advantages :-

a) Sinusoidal Motion is easily achieved. N.B. Eccentric Motion is only approximately harmonic, the error involved being related to the relative lengths of the cam and the connecting rod arm.

b) Tensile fatigue has been well described theoretically.

The simple tension test-piece can be made thin enough to give good heat transfer with the surroundings thereby limiting the heat built up in the test-piece due to hysteresial energy loss. The following measurements were made on the test-piece of an existing fatigue testing machine to estimate the order of magnitude of temperature rise that might be experienced because of these effects.

5.2. Temperature Rise in a Rubber Test-piece

Although the energy loss causing the heat build up may be

easily determined, the actual running temperature depends on the rate of cooling at the surface of the test-piece which is complex and therefore the running temperature cannot be calculated simply. Also the thicker the test-piece the more important is the thermal conductivity of the rubber in determining the heat build-up.

To avoid this heat build-up many fatigue tests use thin samples. One such test is in use in the Dunlop Research Centre.' This test extends a sample 1mm thick (Figure 5.1.) sinusoidally.

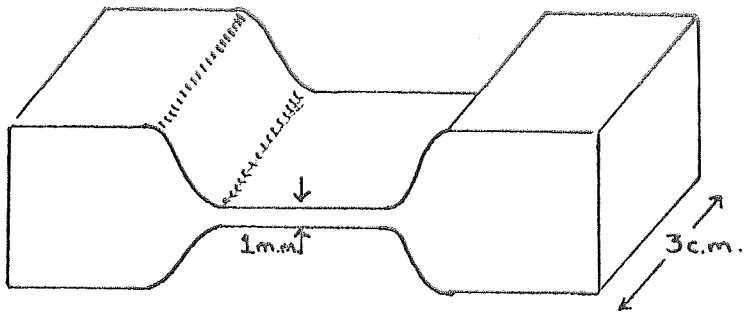

Figure 5.1. Fatigue Sample.

Test-pieces of this form were constructed from a number of different rubber compounds (Appendix II). The temperature

during a fatigue test was measured by introducing a fine thermocouple into a hole made with the tip of a needle in the centre of the sample and setting it in position with rubber solution. (Figure 5.2.)

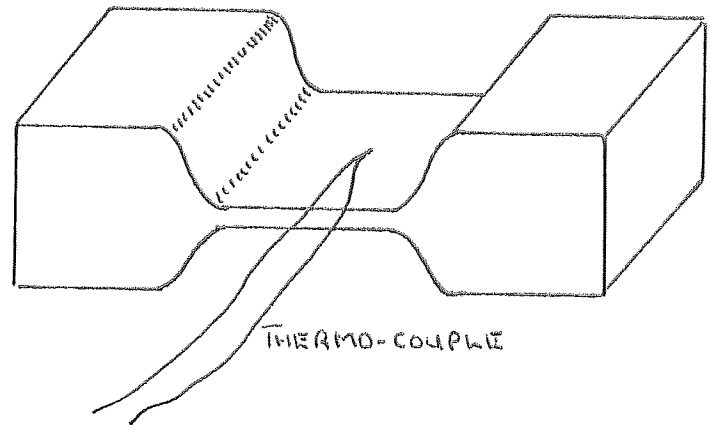

Figure 5.2. Thermo-couple in Fatigue Sample.

The temperature at the tip of the thermo-couple was displayed on a chart recorder. Each test-piece was subjected to a fatigue test at 500 cycles per minute and 250% maximum extension. The ambient temperature was 22°C. The frequency and strain chosen were the severest conditions likely to be encountered in the investigation from the point of view of

hysteretic temperature rise.

The sample temperature was seen to rise slightly at the beginning of the test and then remain constant throughout the test. The temperature difference between running and ambient temperature for each compound is shown in Table 5.1.

Rubber	Temperature Difference
Natural	1°C
Natural & filler	2.5°C
SBR (Intol)	2.0°C
SBR & filler	3.0°C
88/12 SBR	1°C
71/24 SBR	2°C
64/36 SBR	2°C
52/48 SBR	2.5°C

Table 5.1. Temperature Rise above Ambient in Rubber Test-pieces.

The rise in temperature is quite small, on average about $2^{o}C$. The fatigue testing described in this investigation is in general at lower frequencies and lower maximum deformations and the temperature rise would be even less. Thus in most cases the temperature of the sample was judged to be that of the surroundings. When testing was carried out at high frequencies an allowance was made for this slight increase.

5.3. Constant Maximum Deformation Testing

If a fatigue test is carried out by simply moving one end of the test-piece through a fixed distance each cycle then problems are introduced in the interpretation of the results because of a phenomenon known as "set". The effect of "set" is that a rubber which has been stretched does not return immediately to its original length because of alterations to the molecular network on elongation. These alterations may take the form of molecular chain entanglements or rupture of certain molecular chains either mechanically or because of oxidation. This effect is more pronounced in dynamic experiments because of a temporary "set" which is caused by the delay in the recovery of the sample, an effect which is more important at high frequencies.

The effect of this "set" is that the "gauge length" of the test-piece increases during the experiment and the strain in the sample therefore decreases. The following experiment was carried out to observe the effects of "set" on the stress, strain and strain energy in a fatigue sample which is being taken through a fixed deformation cycle.

The apparatus used to deform the test-piece described in Section 5.2. was modified so that the fixed end of the test-piece was attached to a stiff leaf-spring. When the sample was extended the force in the sample caused a small deflection of the leaf-spring which was measured by a displacement transducer (Figure 5.3.) the output from which was relayed through a meter to a chart recorder.

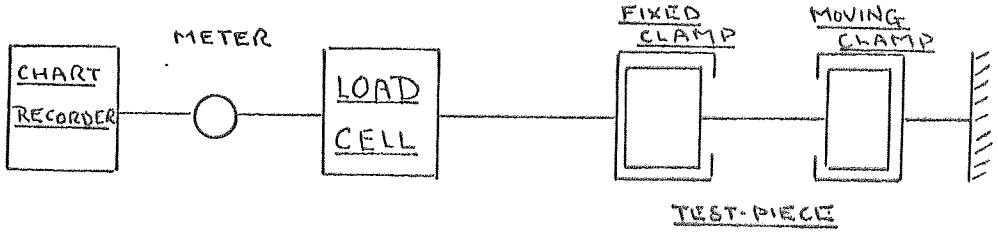

Figure 5.3. Apparatus for Measuring the Effects of "Set".

A high pass filter prevents the meter from following the motion of the test machine so that only the average motion is recorded. The movement of the spring is proportional to the force in the sample, thus the force to achieve maximum deformation is displayed on the chart recorder and this can be measured throughout the test. The rubbers which were used for the test described in 5.2. were also used in this test. Each test-piece was subjected to a fixed displacement-extension cycle. The apparatus described above was used to obtain a plot of the force required to achieve maximum extension as a function of time ; the strain in the sample at maximum extension was also measured at intervals throughout the test. The following observations were made :-

a) The gauge length of the sample increases over the first few cycles of testing and hence the strain decreases, a constant strain being achieved after a few hundred cycles.

b) This is matched by a decrease in stress, until a constant level of stress is achieved.

Thus in testing we have two choices either to adjust the stress or strain continually during the test or to allow this "set" to develop in which case the operating stress or strain will be different from the initial conditions and must be allowed for.

5.4. The Measurement of Fatigue Resistance

The results of 5.1. and 5.2. suggested that a constant strain-amplitude fatigue test on a thin test-piece would be suitable for this investigation and could be achieved without a great deal of technical difficulty. Sinusoidal motion was chosen because it is relatively simple to achieve and because in a regular, known deformation the frequency of deformation can be taken as equivalent to the rate of deformation [69]. The mode of deformation chosen was simple tension, as a simple tension test-piece is easy to produce in a thin form and failure is conveniently defined as the point at which the test-piece breaks into two pieces. The fatigue test was designed with facilities to alter the ambient temperature and the frequency of deformation in order that the objects of the experiment outlined in 3.6. could be achieved.

5.5. The Test-piece

Test-pieces were cut from moulded slabs of rubber. They were stamped from a sheet of rubber using a pneumatic die stamp. The sheet of rubber had rectangular bars moulded along its length, 5cms. apart. The test-piece was cut from the slab in the shape of a dumb-bell (Figure 5.4.) in such a way that the rectangular bar coincided with the broad end of the dumb-bell giving a raised "lip" which facilitates gripping of the sample.

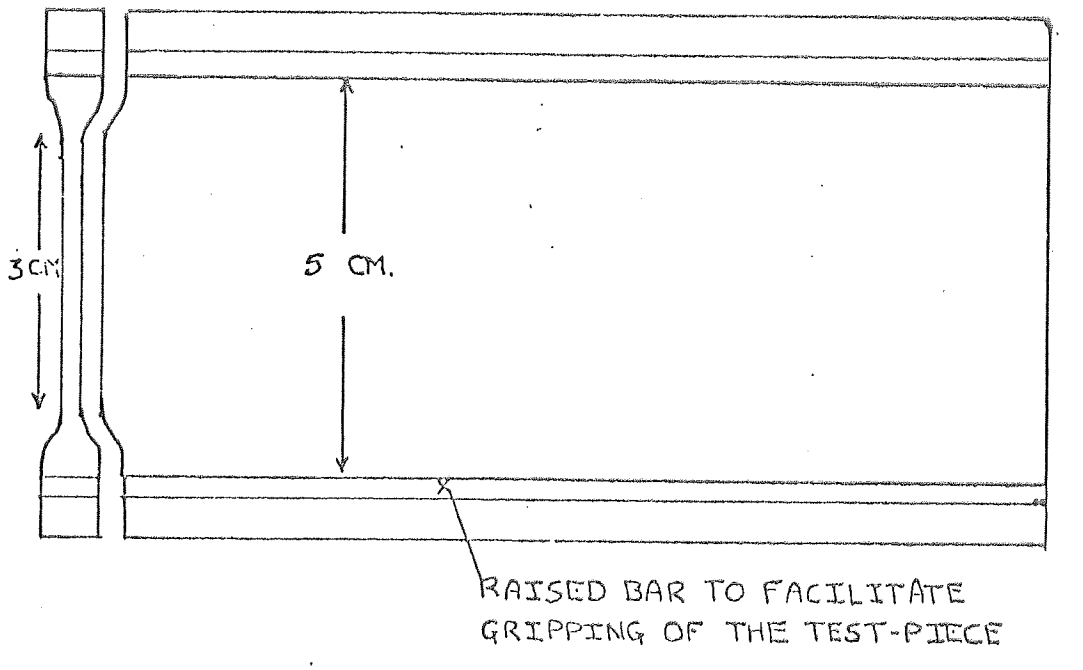

Figure 5.4. Fatigue Test-piece Die-stamped from Moulded Sheet.

The dumb-bell shape has the additional advantage that the broad end of the sample serves to reduce stresses at the grips thereby preventing failure from occuring in this region. The central portion of the sample is about ten times as long as it is wide, ensuring that the sample is in simple tension. The moulded slabs were approximately 1mm thick.

5.6. The Apparatus

It was found inconvenient to produce a frequency range wide enough for the purposes of the investigation in a single machine. To withstand frequencies of the order of 500 cycles per minute at the extension necessary to deform the above sample, robust machinery is required to avoid excessive vibration and eventual machine breakdown. As will be explained later it is in the nature of fatigue failure that it is necessary to test a number of samples simultaneously under any one set of conditions to evaluate fatigue resistance and the more samples tested the larger and more expensive the machinery becomes. The combination of high frequencies and large sample batches is therefore doubly difficult (expensive) to obtain. In this

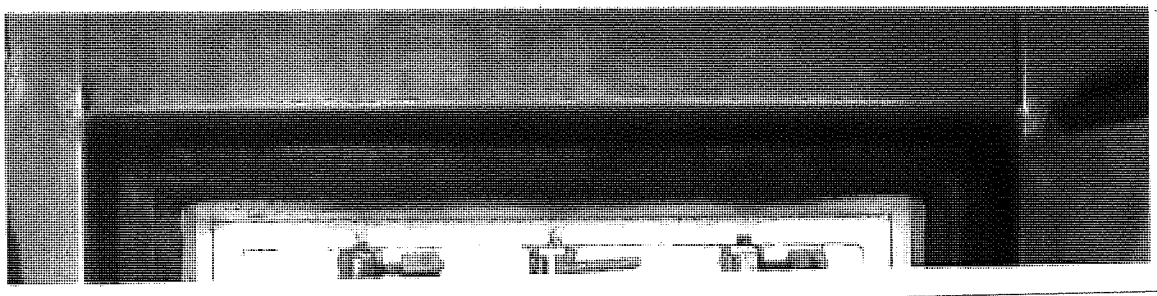

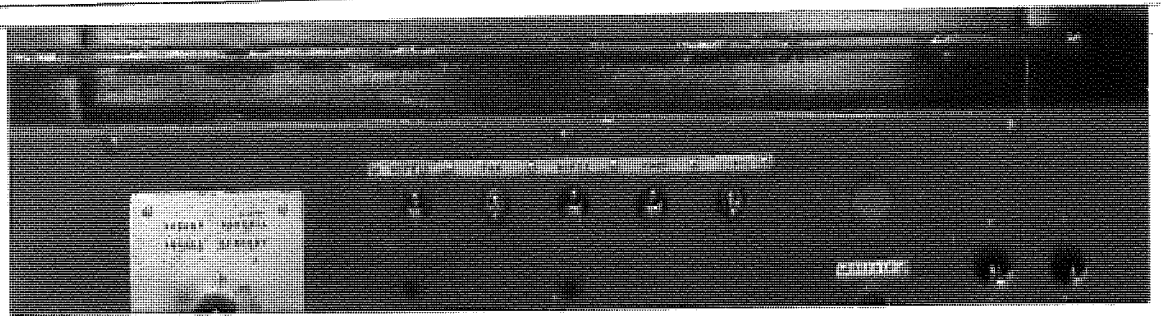

Fig. 5.5. Fatigue test seen through the door of the Temperature cabinet. A and B are the upper and lower sample clamps. C are the microswitches which activate the counters. The bolts around the edge of the opening are for securing a glass inspection panel.

investigation use was made of the fact that at high frequencies tests are shorter and can be repeated. Thus two machines were constructed, one to test a single test-piece at three high frequencies (300, 500, 700 RPM) and one to test twelve samples over the variable frequency range .2 to 200 revolutions per minute. These two machines will in future be referred to as the high and low frequency testers respectively.

The Low Frequency Tester

In this apparatus, which is shown in Figure 5.5., twelve test-pieces are held vertically in clamps which at the top end are attached to a fixed bar and at the bottom end to a bar which is driven to and fro sinusoidally in a vertical plane by a motor, gear-box and eccentric arrangement.

The amplitude of the displacement can be altered by adjusting the "throw" of the eccentric. The "fixed" bar can be adjusted on screw threads to give a variable minimum of deformation. The position of each clamp on the moveable bar is adjustable by means of a knurled nut and a fine screw thread in order that "set" can be allowed for.

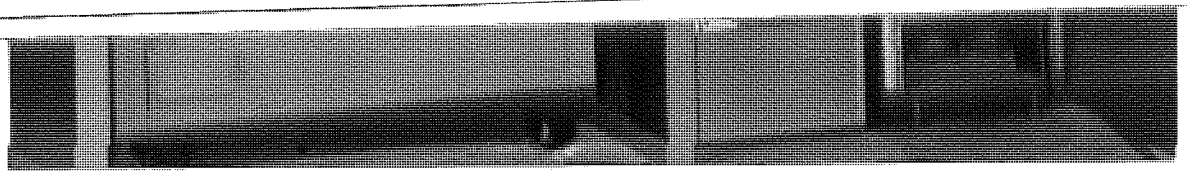

Fig. 5.6. Fatigue testing apparatus-showing from left to right temperature cabinet, counter and speed control.

The machine is driven by a 2 h.p., 2,000 R.P.M. shunt wound D.C. motor, whose speed is controlled by varying the armature current with thyratrons operated in a push-pull circuit. The speed is held constant despite variations in load. A further speed control is obtained by taking the output from the motor through a "Carter" variable gear-box. There are two further gearboxes which can be switched into the drive system to give reductions of five or seventy-five times. This lay-out gives a range of three decades of speed from 200 revolutions per minute down to .2 revolutions per minute.

The test machine is mounted inside a thermal chamber with the motor and gear box mounted on a platform above the chamber (Figure 5.6.), the drive to the machine passing through a hole in the roof of this chamber. The temperature in the chamber can be raised to a maximum of 100°C and maintained steady to within ± 2°C. The temperature can also be reduced to nominally - 80°C although the lowest temperature achieved was only -50°C, probably because of the aperture through which the drive shaft passes. The refrigeration temperature can be maintained to within ± 2°C by a thermostat operated by a constant pressure valve in the refrigerant line. The motion of the machine itself and an

electric fan cause a great deal of movement of the air within the enclosure thus ensuring an even temperature throughout the chamber. Variations of temperature between different parts of the chamber were checked and found to be small.

The number of times a sample is extended before failure occurs is counted with a microswitch-electric counter arrangement. When the sample is extended the "fixed" end of the sample is pulled down against a spring and operates a microswitch, making a circuit and causing the counter to advance by one digit. This is repeated at every extension until the sample fails.

The High Frequency Machine

This machine tests samples singly. It extends a test-piece in a horizontal plane. One end of the sample is fixed whilst the other is drive back and forth by a motor, pulley and V-belt, and crank system. The fixed end may be adjusted by means of a screw thread if any variation in the minimum of deformation is required. The "throw" of the crank is variable so that the test-piece can be strained in the range 0 - 200% strain. The "set" is removed by the same adjustment.

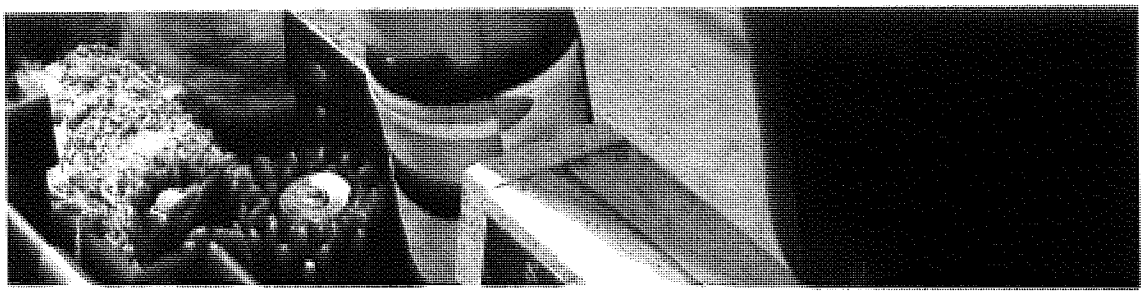

Aston University

Content has been removed for copyright reasons

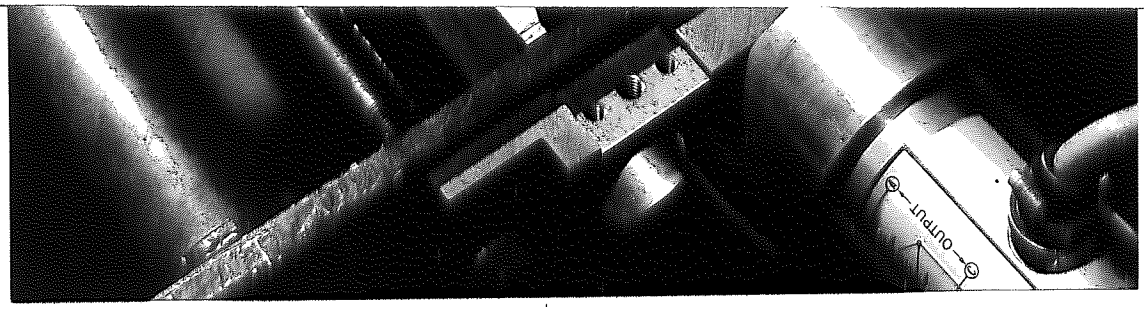

Fig. 5.7. Close-up of the high frequency test machine. In the centre is the asbestos temperature enclosure containing the Test-piece. Bottom right is the load cell in its mounting.

The frequency can be set to one of three fixed values (300, 500 and 700 rpm) by altering the pulley diameter ratios between the motor and the drive.

The sample and clamps are enclosed in a small asbestos box, as shown in Figure 5.7. Air can be passed over a heating element and introduced into the box or liquid nitrogen can be boiled from a vacuum flask and passed into the box to give a temperature range of $+100^{\circ}C$ to $-100^{\circ}C$. The temperature in the box is displayed on a "Pyromaxim" temperature recorder which also gives thermo-static control of the heating elements; the temperature can be closely controlled (to within $\pm 1^{\circ}C$). A thermo-couple can be fastened onto one end of the sample to ensure that the sample and enclosure temperatures are the same.

The clamp holding the fixed end of the sample is attached to a load cell which records the force on the sample; the output from the load cell is registered on a chart recorder. The duration of the test is calculated from the chart speed and the length of trace.

5.7. Design Problems

The mechanical difficulties of designing this apparatus

acrose mainly from the fact that the twelve-station low frequency machine was enclosed in an atmosphere which at times was at temperatures high enough to cause lubricants to run from bearings. This necessitated that as much as possible of the equipment providing the drive to the machine should be remote from the enclosure. As can be seen from photographs of the apparatus (Figure 5.6.) this was overcome by constructing a platform above the enclosure on which were mounted the motor and two variable gear boxes. The drive was transmitted to the machine via a long shaft passing through the roof of the chamber. This left only the fixed gear box inside the chamber. This was lubricated with a silicone oil and grease which was frequently replaced.

Another problem associated with the environment of the machine was that the springs activating the micro-switches which count the number of deformations, corroded at low temperatures. The strength of the springs was thereby reduced and eventually they ceased to operate. This difficulty was overcome by the use of springs made from chrome steel. At low temperatures ice formed on the micro-switches causing short circuits across the terminals; eventually ice formed inside the switch causing

complete breakdown. This was overcome to a large extent by coating the switches with an electrically insulating silicone grease.

5.8. The Assessment of Results

The fatigue resistance of a number of rubbers was measured on the low frequency apparatus, in order to determine the best way of assessing results. The elastomers included a good quality pale crepe, a natural rubber treadstock, a commercially available styrene-butadiene elastomer (Intol 1500) and a range of unfilled styrene-butadiene co-polymers containing 12, 14, 36 and 48 parts of styrene, compounding details are given in Appendix II.

Samples were cycled between 0 - 150% extension at room temperature in batches of twelve cut from the same tensile slab. The fatigue resistance was observed by noting down the number of failures in each period of fifteen minutes until the batch of samples had all failed. The results were plotted in the form of histograms with fifteen minutes as the basic interval and these histograms were then expressed as normal distribution curves.

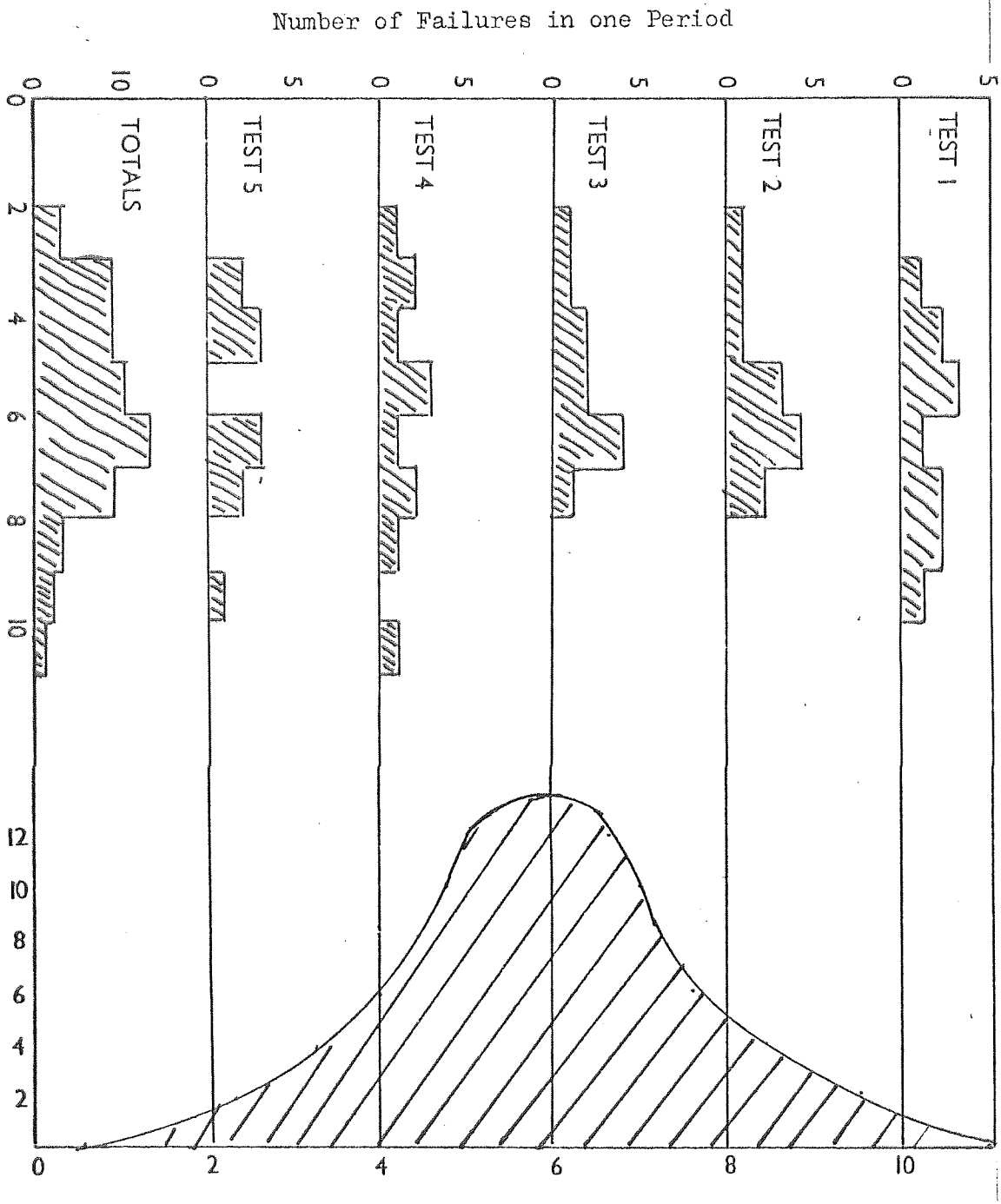

Figure 5.8. Histograms and Normal Distribution Curve for Fatigue Failures of 12/88 Styrene-butadiene Rubber.

Compound	No. of Samples Tested N	Standard Deviation σ cs.	Mean Fatigue Life $\bar{x}$ cs.	Confidence Limits 95% C.L.cs
NR Tread Stock 50pph of Black	11	6,070	42,250	± 4,200
Best Pale Crepe 50pph of Black	12	13,200	89,000	± 8,600
Intol 1500 50pph of Black	12	8,650	45,000	± 3,750
S.B.R. Gum 12 - 88	57	2,822	9,420	± 750
S.B.R. Gum 24 - 76	57	2,822	9,400	± 750
S.B.R. Gum 36 - 64	46	2,620	16,500	± 775
S.B.R. Gum	34	2,937	26,500	± 1,010

Table 5.2. A comparison of the standard deviation, mean fatigue life and 95% confidence limits for a number of rubber compounds.

A typical example of the normal distribution curve of a styrene-butadiene rubber containing 12 parts of styrene is shown in Figure 5.8. The only results ignored in the evaluation were those in which fatigue failure occurred at the clamps because of damage by the clamping screws. Different numbers of samples were tested with different compounds and the results included tests on from 12 to 57 samples for any one compound. A comparison of the mean value of fatigue resistance, the standard deviation and the 95% confidence limits is shown in Table 5.2.

The spread of results was compared in each case. For the purpose of this investigation the "spread" is defined as half the total spread expressed as a percentage of the mean, i.e. the spread either side of this average result expressed as a percentage of the average result. This assumes a normal distribution. The best value obtained was a spread of twenty per cent. Comparisons of results indicate that the spread is smaller the less severe the test, that is, the greater the fatigue resistance. The widest spread was about 66%.

The tests were not extensive enough to permit a rigorous analysis of the distribution, but it became obvious that in most cases a normal distribution was a good fit to the experimental results. More thorough investigations in this field [70],

[71] [72] have indicated a skew distribution in the case of fatigue, tear and tensile tests. The distribution in this investigation was however assumed normal and the number of samples which has to be tested to achieve a pre-determined ninety-five per cent confidence limit was examined. For example if it was required to have a ninety-five per cent confidence limit which was about ten per cent of the mean value then the number of samples which has to be tested could vary from 10 to 50 depending on the severity of the test.

To examine 50 samples per test would require increased testing facilities or it would involve longer times with the facilities available, thus other alternatives were examined.

If the means of individual groups of twelve are compared with the total means in the SBR results it can be seen that the group means are within about ten per cent of the overall means and even with batch sizes as small as four test-pieces the batch mean was still found to be within 20 per cent of the overall mean. This observation was used in arriving at a test procedure to deal with the experimental work of this investigation.

The standard deviation of a group mean is related to the standard deviation of individual results S.D. by the formula

$$S.D._{(n)} = S.D./\sqrt{n}$$

where n is the sample size.

Thus in the case of natural rubber treadstock for a sample size of four test-pieces

$$S.D._4 = 6070/2$$

$$= 3035 \text{ cycles}$$

This is within seven per cent of the mean of the distribution and approximately two thirds of the results obtained will fall within this range and ninety-five per cent of all results will fall within two standard deviations of the distribution mean, that is, within fourteen per cent of the mean.

This calculation was used in deciding how many samples to test in order to determine the fatigue resistance of a rubber. The sample size n was chosen so that S.D. the standard deviation of the mean was small compared with the changes in fatigue resistance caused by an alteration in the test conditions.

6. THE EFFECT OF TEMPERATURE AND FREQUENCY ON FATIGUE RESISTANCE

6.1. Preparation of Material and Experimental Precautions

The apparatus described in section 5 was used to measure the fatigue resistance of rubber test-pieces over a range of temperatures and frequencies. A styrene-butadiene elastomer was chosen as being typical of "rubbery" behaviour and it was also known not to crystallise on stretching [73]. The effect on the fatigue resistance of changing the elastomer was examined by changing the ratio of styrene to butadiene in the co-polymer. The effect of compounding a carbon black filler into the co-polymer also was examined. Differences due to crystallisation, were determined from experiments carried out on natural rubber test pieces which are known to partially crystallise on extension.

The compounding details of the rubbers used are given in Appendix III. The styrene-butadiene rubbers were all compounded and vulcanised to give a material which is traditionally based on a compromise between the maximum tear strength and the

maximum resilience; the addition of filler or small alterations in the styrene-butadiene ratio does not significantly change the position of these maxima with respect to cure [74]. The vulcanization process for natural rubber was again based on the tear and resilience maxima for this material, although the quantities required were different to those for the styrene-butadiene co-polymers.

The fatigue resistance was measured over the total range of frequencies available at one value of strain. This was repeated at a number of different temperatures so that the relationship between fatigue resistance and temperature and frequency could be examined. Altogether nine rubber compounds were tested at nine frequencies and seven or eight temperatures. Thus a temperature-frequency plot involved about 600 fatigue measurements the duration of which varied from a few minutes up to 30 days. Later, it will be explained from general considerations, the type of changes that might be expected with alterations in the maximum of deformation. In this investigation minimum strain was chosen to be zero; the effect of minimum strain on the temperature-frequency results will be the subject of a future investigation.

The measurements of this investigation were performed in air so that the effects of oxidation and ozonisation provide a further unknown. However, with the values of strain energies at which the tests in this investigation were conducted the effects of ozone are expected to be negligible [75], [76]. Hence the results of these measurements apply only to the mechanico-oxidative failure mechanism.

In the type of fatigue test described in the last section failure of the sample usually takes place from the growth of a flaw in the cut edge of the sample. If the knife used for cutting the samples becomes blunt or chipped then large flaws in the cut-edge can result in premature failure. For this reason a knife was kept specifically for preparing the samples used in the investigation; it was sharpened regularly and examined microscopically for blemishes in the cutting edge.

In a programme of testing such as this there is always the problem that if large batches of rubber are compounded and vulcanized at the same time, then over a period of time its properties may become altered due to the effects of oxidation. If the rubber is compounded as needed in a series of separate batches, errors in the vulcanizing and compounding processes may

cause differences in properties between batches. In this investigation all the rubber samples were compounded and vulcanized in one batch. These were then stored at $-10^{\circ}C$ to reduce atmospheric attack and control experiments were carried out at regular intervals.

When tensile fatigue is measured at temperatures other than room temperature the usual method of removing "set" at intervals throughout the test is inconvenient. A method was therefore adopted of performing all tests with the same nominal deformation cycle (0 to 175%) and then performing a separate experiment to determine the variations of strain and strain energy throughout the test. Unfilled styrene-butadiene rubbers developed amounts of "set" which under most conditions gave an experimental strain cycle from 0 to about 165 - 170%, and the strain energy of these unfilled compounds did not differ by more than ten per cent for this particular deformation cycle. The difference in strain energy in the case of the filled compounds was of course much greater due to their higher modulus.

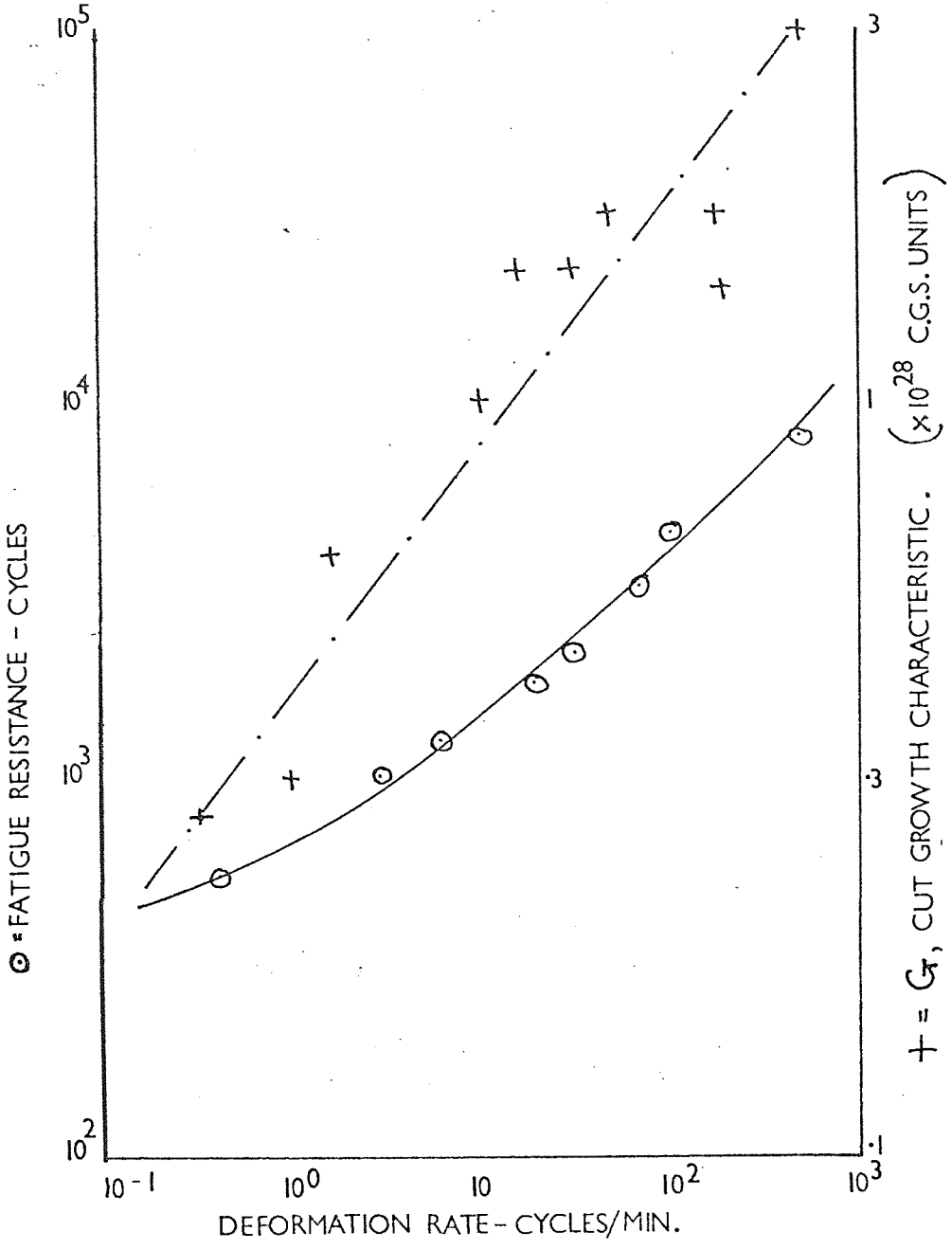

Figure 6.1. Fatigue Resistance and cut-growth characteristic vs. Deformation Rate for a styrene-butadiene gum rubber.

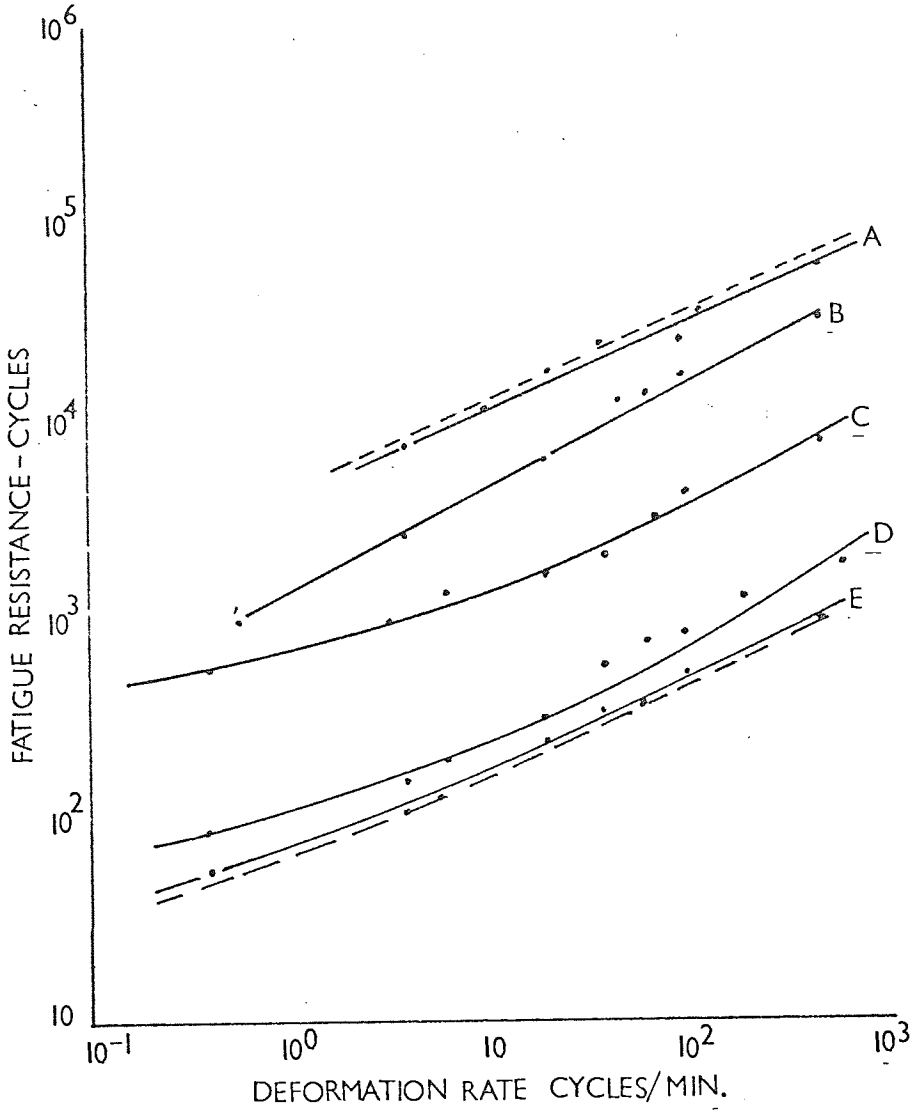

Figure 6.2. Fatigue Resistance vs. Deformation Rate for five gum styrene-butadiene rubbers with the styrene to butadiene ratio given by A - 48/52 B - 36/64 C - 24/76 D - 12/88 E - 0/100

6.2. The Frequency Dependence of Fatigue Resistance (N-f curves)

The apparatus described in Chapter 5 was used to measure the fatigue resistance of rubber over a range of frequencies. A plot of fatigue resistance (N) against the frequency (f) of deformation in cycles/min. on logarithmic scales will be referred to as an N-f curve. The rubbers will be referred to in terms of the compound number given in Appendix III. An N-f curve for compound 3 (24/76 SBR) is shown in figure 6.1. The temperature of the measurements was 20°C. The fatigue resistance is seen to change by over ten times as the frequency is changed over three decades from 0.4 to 400 cycles per minute. The broken line in the same diagram is the change in the dynamic cut-growth characteristic (G) over the same frequency as measured by Lake and Lindley [31] for a similar material. The same order of change is observed in the fatigue resistance as was observed in G.

The effect of changing the elastomer on the N-f curves was investigated by changing the styrene ratio in the styrene-butadiene co-polymers, Figure 6.2. shows the results for compounds 1 - 5 in which an increase in styrene does not greatly alter the

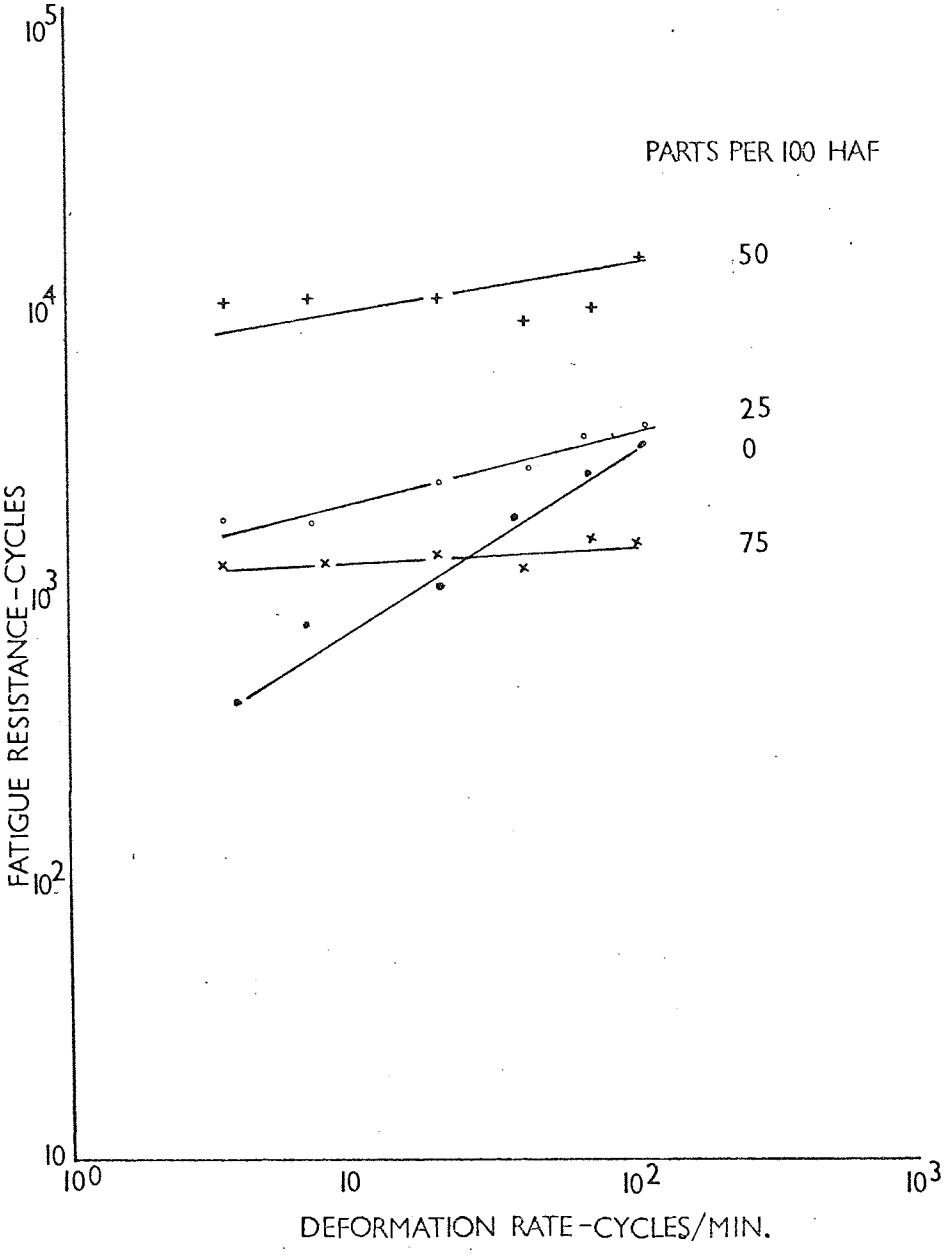

Figure 6.3. Effect of filler content on frequency dependence of fatigue resistance of styrene-butadiene rubber for a fixed deformation cycle.

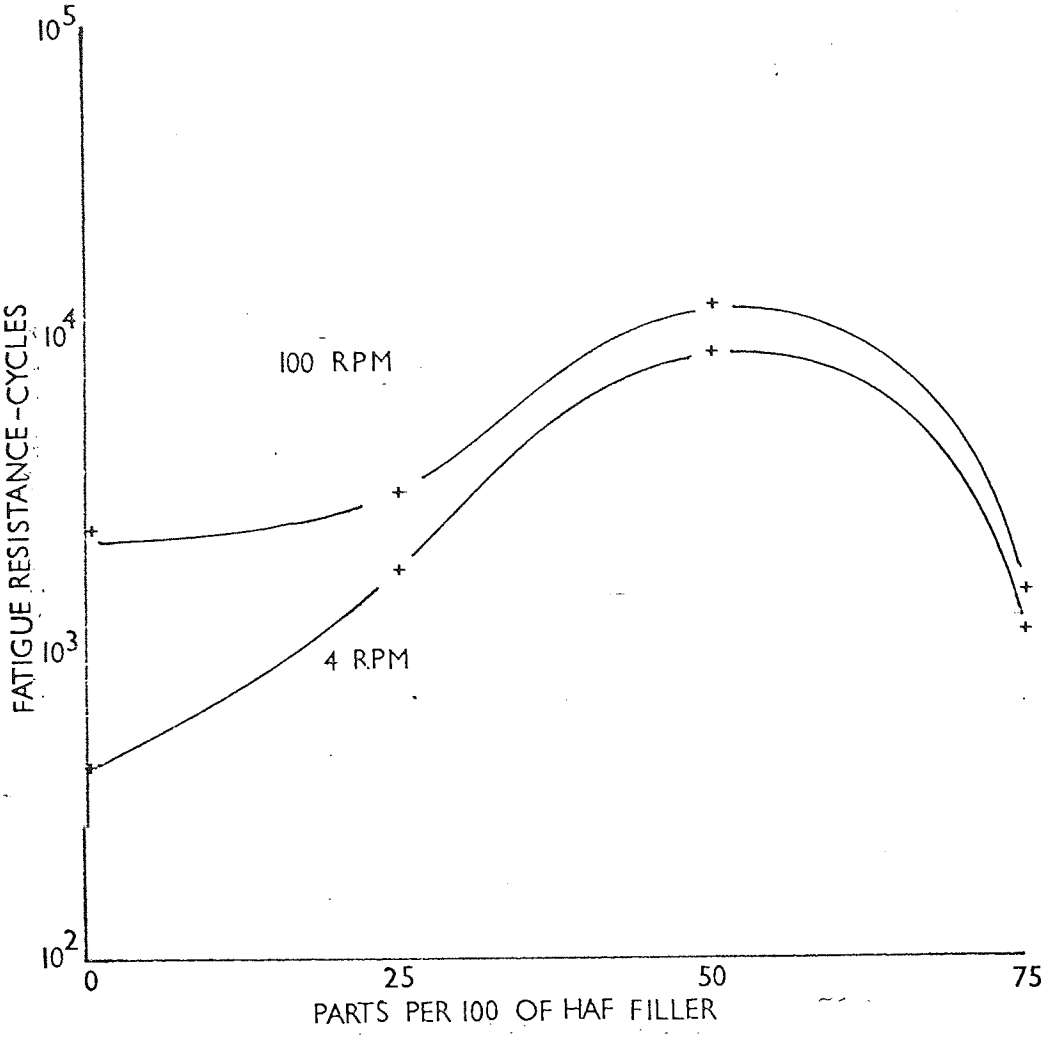

Figure 6.4. The Effect of filler content on the fatigue resistance of styrene-butadiene rubber at one temperature and two frequencies for a fixed deformation cycle.

shape of the N-f curve but shifts it in a direction parallel to the fatigue resistance axis. The measurements shown in Figure 6.2. were obtained at 20°C and 175% nominal strain. If all the results are compared with the strain energy of the 24/76 SBR then shifts calculated on the basis of equation 1.15. are indicated by the broken lines. N-f curves were also obtained for the compounds 2, 7, 8 and 9 which were the 12/88 styrene-butadiene rubber with 0, 25, 50 and 75 parts by weight of "High Abrasion Furnace" carbon black compounded into the rubber. Where comparisons were made at a given temperature and strain cycle, fatigue resistance was seen to become progressively less frequency dependent as the filler content was increased; the compound containing the highest black loading was almost independent of frequency over the experimental range (Figure 6.3.).

In addition, it is seen that under given conditions of frequency, temperature and strain, an increase in filler content increases the fatigue resistance of a polymer up to some critical level of filler after which the fatigue resistance is seen to decrease again (Figure 6.4.). This maximum in the fatigue resistance-filler content curve has also been recorded in other

strength measurements.

At room temperature and a strain cycle of 0 - 175% a similar effect is seen in the strain-crystallising natural rubber. The N-f curve changes only very slightly with frequency.

In the unfilled amorphous rubbers the fatigue resistance N is a function of frequency. This function is apparently independent of the elastomer (styrene content). Fatigue resistance of this type of test-piece has been described by the equation. (see equation 1.15.)

$$N = G/3(2kW)^4 c_o^3 \quad \ldots \quad \ldots \quad 6.1.$$

G the dynamic cut-growth characteristic shows the same order of magnitude of frequency dependence as N. This frequency dependence of G has been attributed to the so called static cut-growth contribution at lower frequencies (see Appendix I) and this probably accounts for the frequency dependence of fatigue resistance. The addition of filler reduces the frequency dependence probably because it reduces the contribution of the static cut-growth. This phenomenon is also observed when crystallisation

is present in the rubber.

Fillers also increase the fatigue resistance up to some critical volume concentration of the filler in the rubber when comparisons are made at constant strain. Adding filler to the rubber is known to increase the stiffness which would increase the W term in 6.1. and tend to decrease the fatigue resistance. This line of argument again leads to the conclusion that equation 6.1. is affected not only because of changes in the strain energy but also because of an effect upon the G term. If 6.1. is rewritten as :-

$$\text{Log } N = \text{Log } G - \text{Log fn}(W) \quad \ldots \quad 6.2.$$

then changes in fatigue resistance because of filler can be thought of as the sum of two contributions. A beneficial contribution to G as the filler is increased offset by the increases in stored energy caused by an increase in filler content.

6.3. The Effect of Temperature on the N-f curve

Fatigue resistance is seen to have a marked dependence on the temperature at which the measurement is carried out.

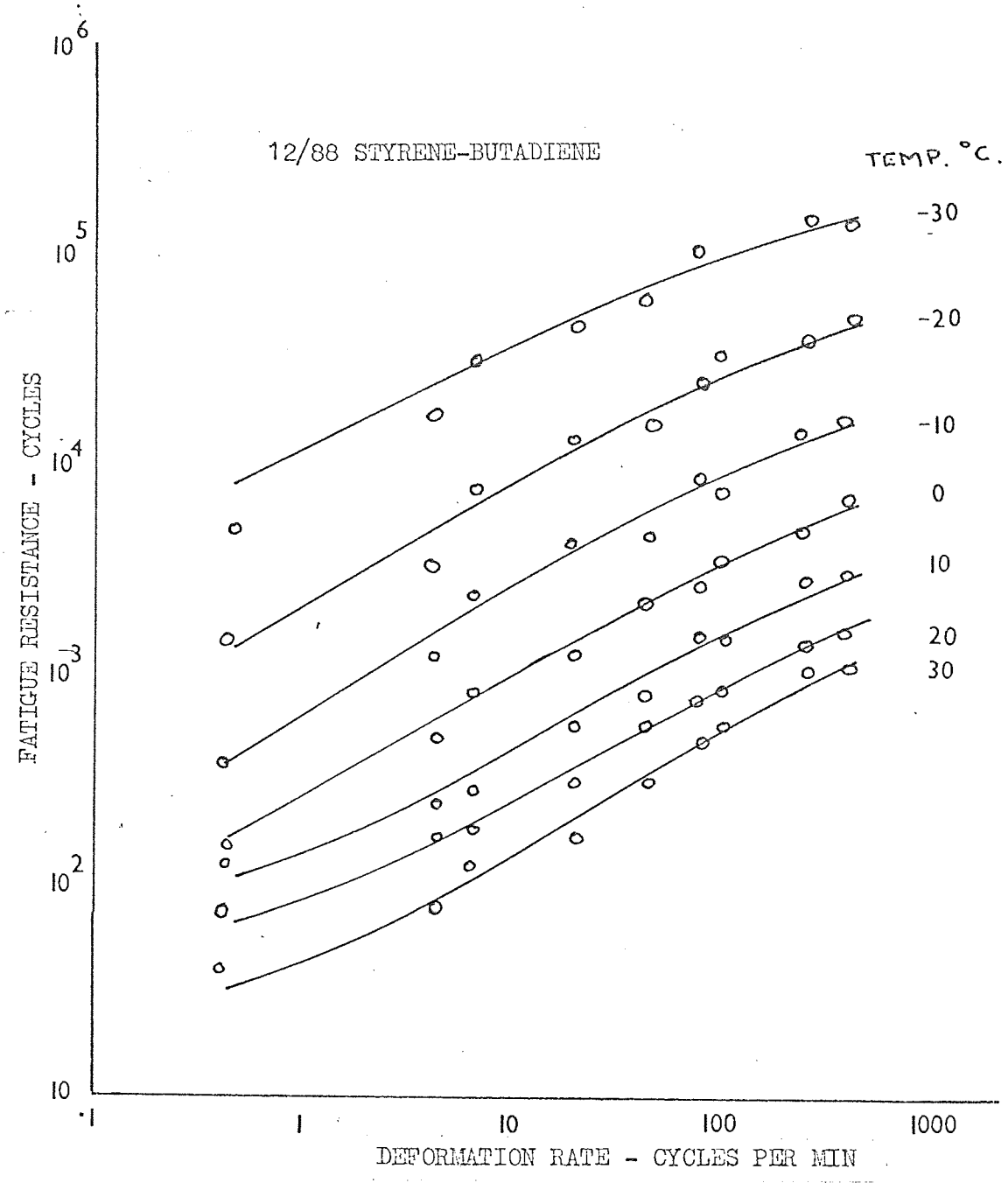

Figure 6.5. The Effect of Temperature on the N-f curve of a butadiene-styrene gum rubber.

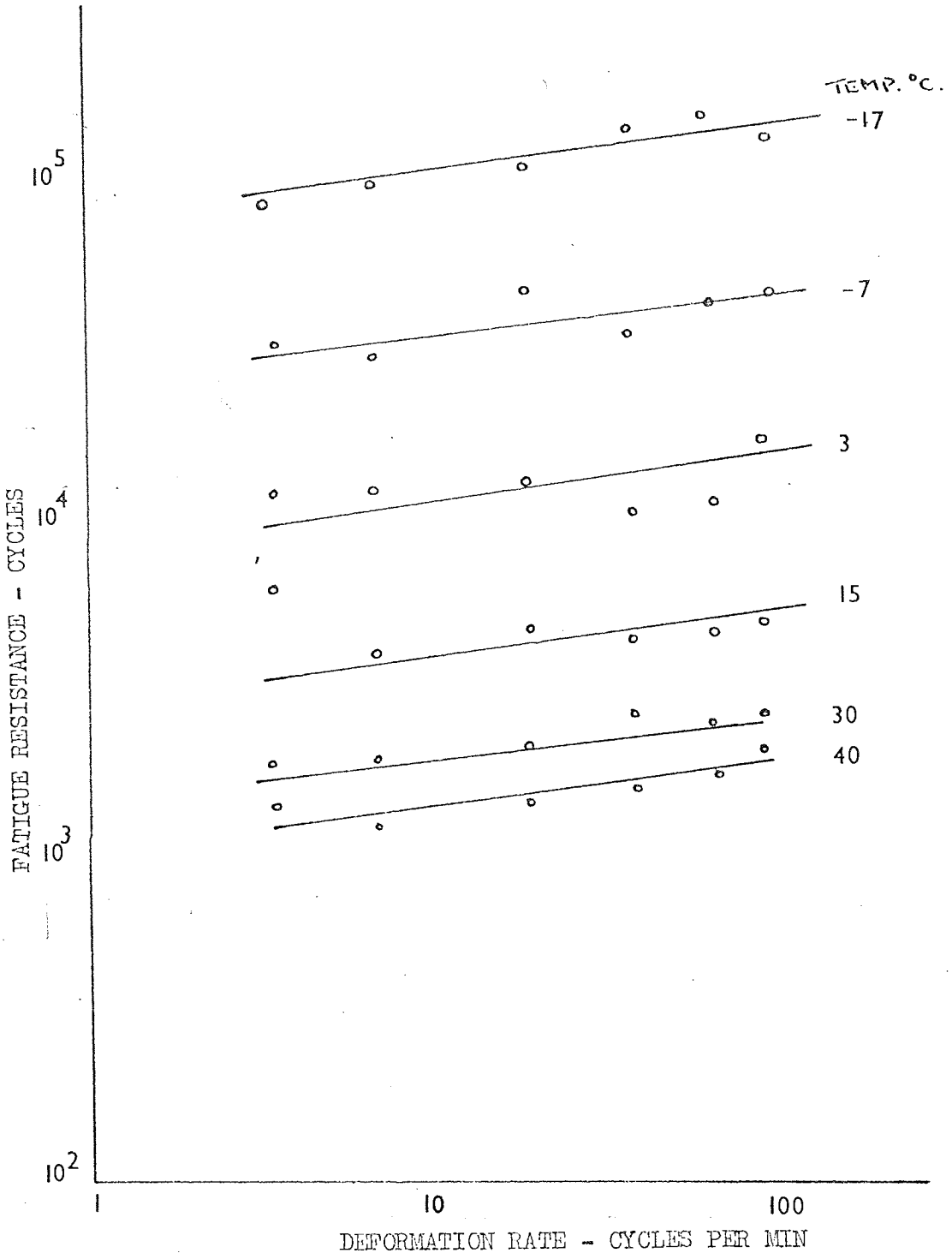

Figure 6.6. The temperature dependence of the N-f curve of a filled (12/88 SBR + 50 parts HAF) styrene-butadiene rubber.

Figure 6.5. shows the effect of temperature on the N-f curve of compound (2), a 12/88 styrene-butadiene rubber. As with changes in styrene-butadiene ratio, the N-f curve is seen to be displaced in the positive direction parallel to the fatigue resistance axis as the temperature is decreased. Thus a family of curves can be built up with neighbouring curves being similar in shape, showing the variation of fatigue resistance with temperature and frequency. In the case of compound 2 a change of 60° C between $+30^{\circ}$C and -30°C produced a change of about 500 times in the fatigue resistance of the rubber. This order of change was confirmed on all the unfilled styrene-butadiene rubbers, N-f plots being obtained for all of these co-polymers in the range -40°C up to $+80^{\circ}$C.

Although the frequency dependence of fatigue resistance is greatly reduced by the addition of fillers the temperature dependence was found to be much the same as in the unfilled co-polymers. Figure 6.6. shows that the N-f curve is shifted in much the same way as in the case of the unfilled elastomer when the test temperature is varied. The rubber is the 12/88 styrene-butadiene co-polymer containing 50 parts of HAF carbon black.

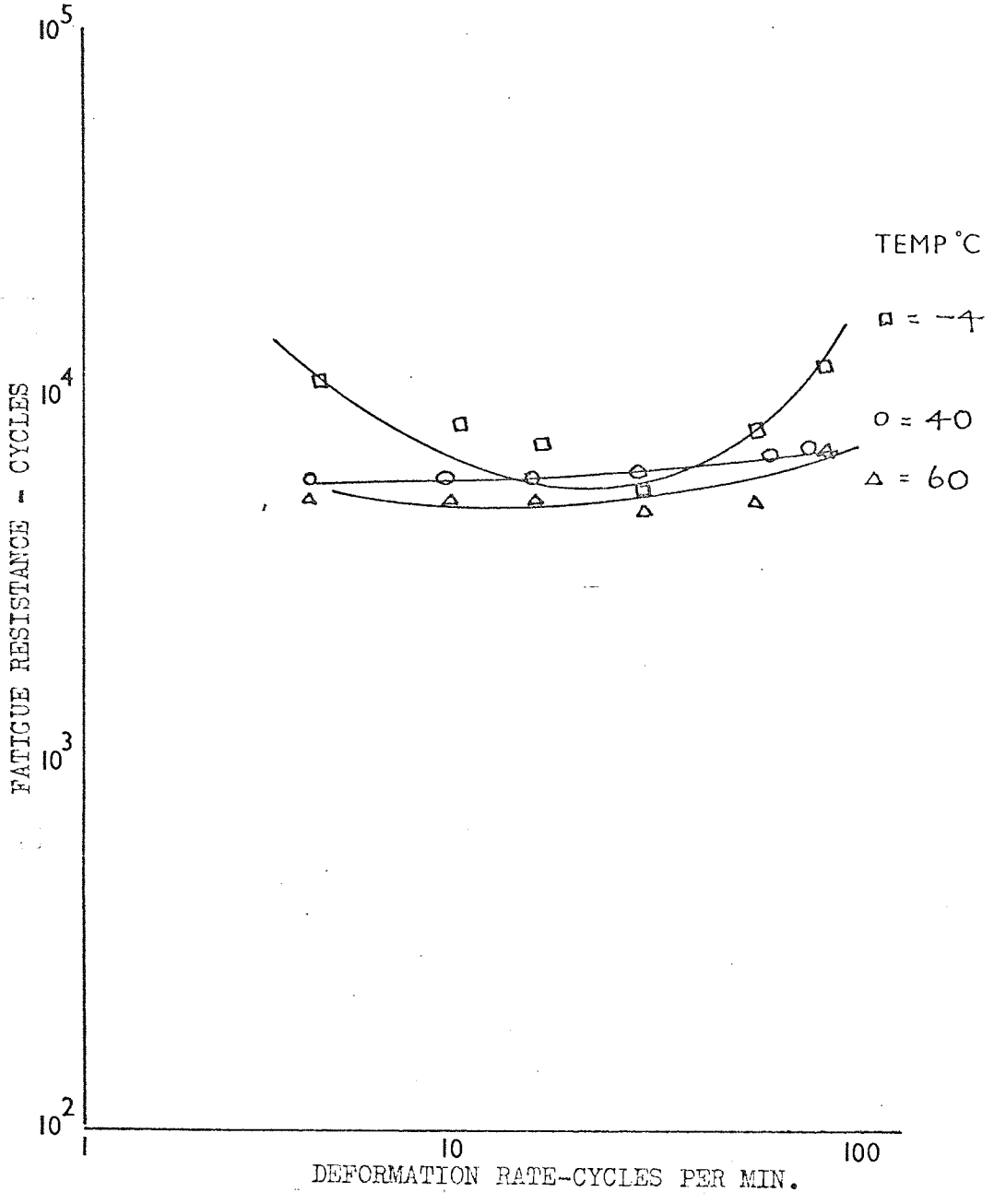

Figure 6.7. The temperature dependence of the N-f curve for unfilled natural rubber.

The dependence of the fatigue resistance of unfilled natural rubber on temperature and frequency was found to be much less than for the amorphous co-polymers and at $-4^{\circ}C$ a minimum in the N-f curve is observed. (Figure 6.7.)

It is interesting to compare these temperature-frequency plots with similar diagrams obtained for the change in tearing energy with temperature and frequency [48]. For unfilled styrene-butadiene co-polymers and for the unfilled strain-crystallising natural rubber the temperature-frequency of tearing energy against frequency and temperature are similar to those for fatigue resistance, the magnitude of the changes caused by these two parameters being less in the case of tearing energy.

Measurements of tearing energy on filled polymers gave a more complicated picture than in the case of fatigue resistance [62]. However, at all temperatures, (for styrene-butadiene rubber with HAF carbon-black filler), there are regions of the tearing energy-rate curve where the tearing energy is apparently independent of rate. In the case of tearing energy this picture is changed by the type of filler used, a factor which should be investigated in the case of fatigue resistance.

6.4. Conclusions

Fatigue resistance measured by the number of cycles to cause a strip of rubber deformed in simple tension to split into two pieces, appears to depend on the temperature and frequency of the measurement. The shape of the N-f curve for amorphous materials is independent of elastomer although increases in the styrene-butadiene ratio in the elastomer gave an increased fatigue resistance. The addition of fillers causes a reduction in the frequency dependence but not in the temperature dependence and there is a maximum value of fatigue resistance at a certain filler content. The presence of crystallisation greatly reduces both the temperature and frequency dependence of fatigue resistance.

Stress-strain measurements indicate that changes in strain energy are in no way sufficient to account for these changes in fatigue resistance in terms of equation 6.1., which is well proven for the effect of strain energy on fatigue resistance. Indications are that changes arise because of variations in the cut-growth characteristic (G), and in equation

6.1. it is important to obtain a more fundamental understanding of the G term.

The reduction in frequency dependence of fatigue resistance with the addition of filler is probably due to the reduction of the static cut-growth contribution. This is consistent with the work of Andrews (see Chapter 3) who proposed a mechanism whereby crack propagation is hindered in the presence of hysteresial energy loss. It is well known that the presence of filler causes greater energy loss in rubber.

It was therefore, thought advisable that a study be made of stress-strain curves in order that a better understanding of the effects of strain energy and energy loss could be developed. This work is described in a later chapter.

The similarity between the temperature and frequency dependence of fatigue resistance and tearing energy in all the rubbers tested, adds weight to the suggestion made at the end of Chapter 4 that this type of measurement is not only a function of the incremental crack-growth properties of the material but also a function of the critical energy (T_c) necessary for catastrophic tearing.

7. THE TEMPERATURE-FREQUENCY TRANSFORM APPLIED TO FATIGUE MEASUREMENTS.

In Chapter 6 the fatigue resistance of a range of styrene-butadiene gum vulcanizates, chosen as exemplifying rubbers which do not crystallise upon extension, was examined over a wide range of temperatures and frequencies of deformation.

In this chapter it is shown that the measured fatigue resistance of all the rubbers examined can be described in a simple unifying way. The fatigue resistance can be completely described by two basic curves, one of which describes its dependence on the frequency of deformation and the other describes the interdependence of frequency and temperature and by a characteristic temperature dependent upon the polymer. The second curve is similar to the so-called W-L-F equation [51] derived from measurements of viscous or visco-elastic properties, and the success of the application of this equation to fatigue resistance data indicates the importance of viscous or visco-elastic processes in determining the fatigue resistance of rubber.

7.1. The Method of Reduced Variables

The response of polymers to deformation has been explained in terms of a model which represents its visco-elastic behaviour. These models take the form of arrangements of springs and dashpots such that the reaction of a polymer to a deformation is related, to the spring constant and the viscosity of the dashpot fluid. A real polymer is represented by the sum of the reactions of an infinite number of these models. The stress required to constrain a body of visco-elastic material at constant deformation gradually diminishes and this corresponds to the gradual releasing of the springs by the motion of the dashpots. The relaxation is represented by the sum of the relaxation of individual elements. On the other hand, a body which is not quite solid and not quite liquid may, whilst flowing under constant stress, store some of the energy input instead of dissipating it all as heat. Thus, when a visco-elastic body is subjected to a simusoidally repeated stress, the strain is neither in phase with the stress (as it would be in a perfectly elastic solid) nor 90° out of phase (as it would be in a perfectly viscous fluid), but somewhere in between, some of the

energy input being stored and recovered in each cycle and some being lost and dissipated as heat as the springs and dashpots move back and forth in a complicated fashion, this behaviour being described mathematically by a retardation spectrum.

The consequence of this hysteresial energy loss in fracture mechanics has been discussed throughout this work. In the last chapter it was indicated that the fatigue resistance may be affected to a large extent by hysteresial energy loss. Where this energy loss arises out of the visco-elastic nature of the rubber then the rules applying to the so-called visco-elastic functions might be expected to apply to the fatigue resistance.

It is in the transition zone between glass-like and rubber-like behaviour that the visco-elastic functions change most spectacularly with temperature and frequency. However, attempts to analyse the way in which a function varies with temperature at a particular frequency leads to very complicated results and it has been necessary to have recourse to the so-called "Method of Reduced Variables" or visco-elastic corresponding states. This provides a valuable simplification in describing the variation of visco-elastic properties with the two principal variables of temperature and time, and the property

can be expressed in terms of a single function, the dependence being determined experimentally.

Ferry and Fitzgerald [77] showed how the use of reduced variables in transforming temperature and frequency scales meant that observed values of a single property such as elastic modulus or di-electric constant could be brought onto a single curve covering a wide range of frequency.

Temperature dependence entered in several ways such as changes in density, thermal expansion and primarily in the hindrance to molecular rotation as described in the kinetic theory of rubber elasticity and which depends directly on temperature. Therefore on a logarithmic plot the effect of increasing the temperature of a property against frequency is to shift the curve upwards by a factor $\rho T / \rho_o T_o$. The relaxation times of a polymer are further affected in several ways by temperature, the most important one being in the effect on the internal friction co-efficient which controls segmental rotation of the molecular chains. These effects are contained in one term usually denoted A_T which represents the ratio of relaxation times at temperature T and some arbitrary temperature T_o.

$$A_T = \tau_{(T)} / \tau (T_o)$$

τ is relaxation time.

Thus an increase in temperature shifts a logarithmic plot of property versus frequency along the time axis as well. In fact, an increase in temperature causes a negative shift on the time scale as the time shift is dominated by the temperature effects on the hindrance to segmental rotation, thus high temperatures will correspond to shorter times.

Hence a curve of visco-elastic function against temperature can be reduced to the position it would have occupied at temperature T_o by adjusting the function first by multiplying $T_o \rho_o / T \rho$ and then by multiplying the time $1/A_T$ that is, multiplying the frequency by A_T. In practice this frequency shift is carried out by moving a curve obtained at the temperature T parallel to the frequency axis to co-incide with the curve obtained at temperature T_o.

Figure 7.1. shows modulus frequency curves obtained at a number of different temperature and the broken line shows how

they can be moved to coincide with the position of the extrapolated curve at one temperature and thus form a composite curve describing the modulus of the material over a wide range of frequencies.

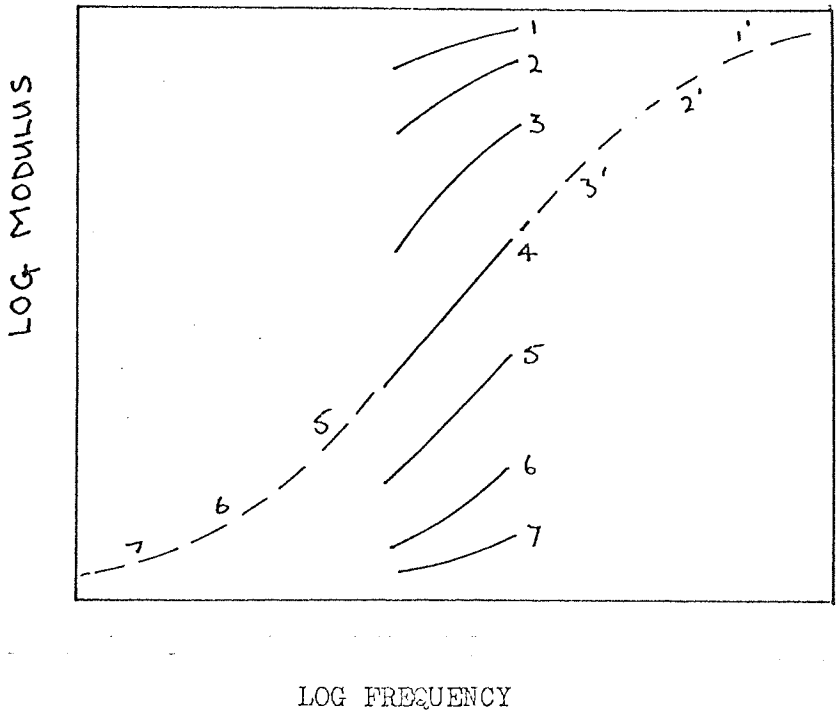

Figure 7.1. Construction of a composite frequency-modulus curve from curves obtained at different temperatures. Curve 4 is the reference curve i.e. temperature T_o

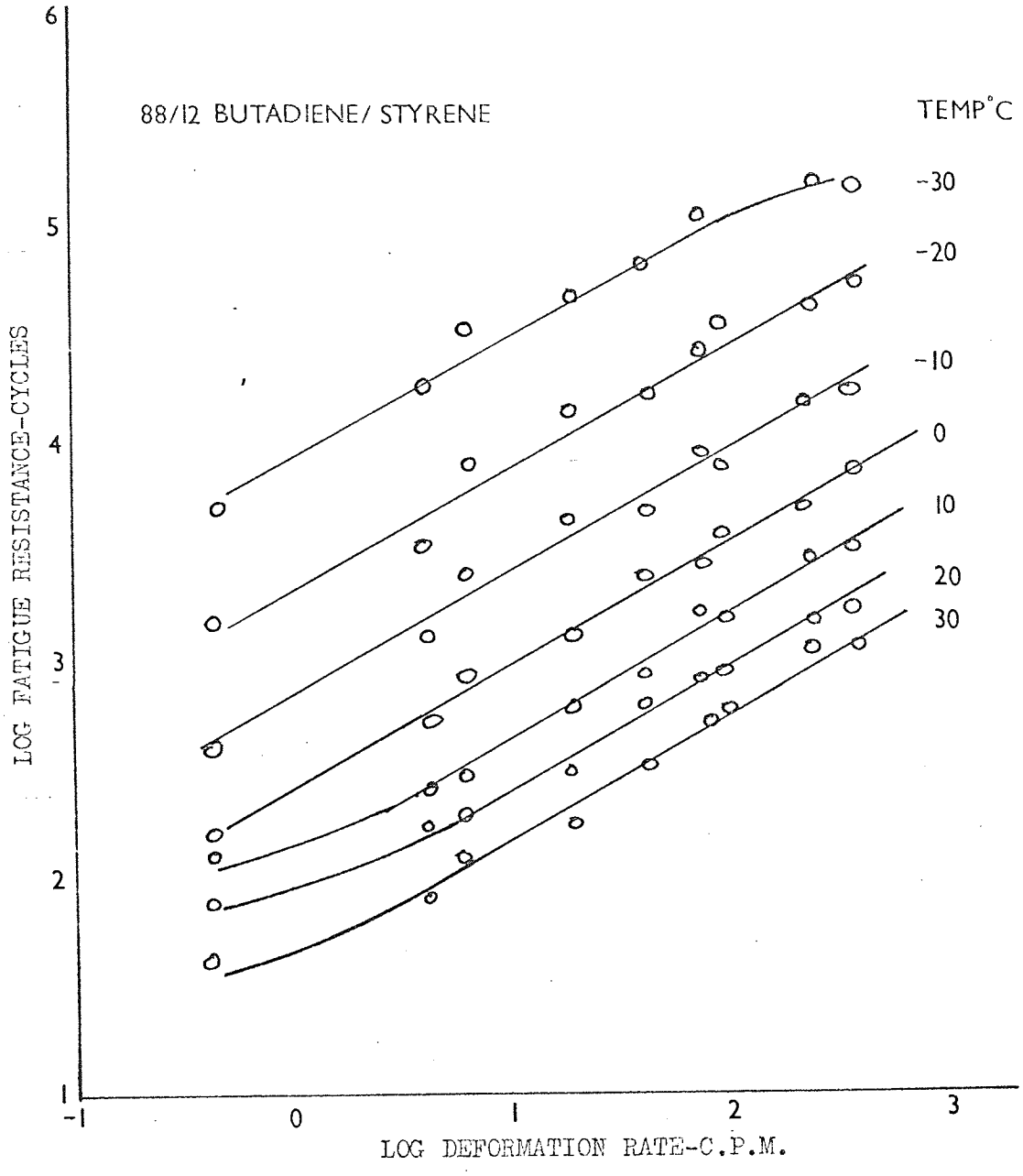

Figure 7.2. Temperature-Rate dependence of the fatigue resistance of a styrene-butadiene gum rubber.

This is of practical importance when the available experimental frequency range is limited, since tests at various temperatures enable the observer to predict the effect of a much wider range of frequencies.

Further if the difference ΔT between the temperature at which a particular curve was obtained and that of the reference curve is plotted against A_T the frequency shift necessary to make these curves coincide then the resulting curve is described by the W-L-F equation, which was discussed in Chapter 3 :-

$$\text{Log } A_T = 8.86\,(T - T_s)/(101.6 + T - T_s) \quad \ldots \quad 7.1.$$

where T_s, the reference temperature is a characteristic temperature of the material under examination. T_s was originally chosen arbitrarily for one polymer ($243^{\circ}K$ for polyisobutylene) being a fixed distance from the glass transition temperature. In general T_s has been quoted at $46 \pm 5^{\circ}C$ [69] and $50 \pm 5^{\circ}C$ [78] above the glass transition temperature.

7.2. The Application of Reduced Variables to Fatigue Resistance

Figure 7.2. shows the fatigue resistance of a 12/88

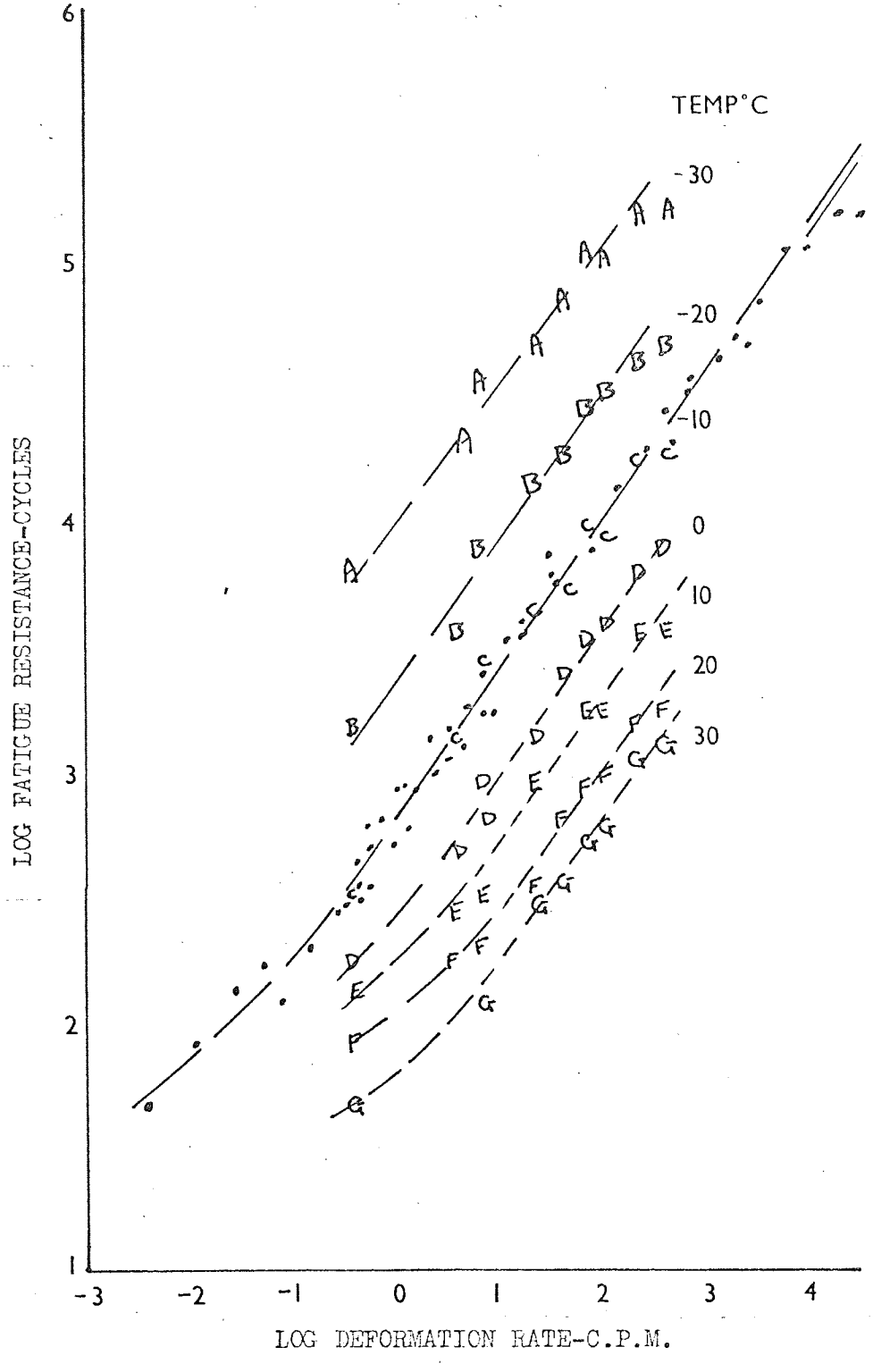

Figure 7.3. Data from Figure 7.2. and the composite curve formed by shifting this data parallel to the rate axis to be co-incident with the N-f curve for -10°C.

styrene-butadiene co-polymer compound number 2 from Appendix III.

Stage 1 Kinetic Theory and Density Changes

The experimental results were obtained over the temperature range 243 - 303°K. They were compared with the reference temperature 263°K. A maximum temperature difference of 40°K would result in changes of the order of 15 per cent in fatigue resistance, when the factor $\rho_o T_o / \rho T$ was applied, that is a maximum difference of 6 per cent on a logarithmic scale. As this is within the scatter of the experimental results correction by the factoe $\rho_o T_o / \rho T$ has been omitted.

Stage 2 Transformation in Time Scale

Figure 7.3. shows the separate curves for fatigue resistance against frequency and temperature, plotted individually in Figure 7.2., shifted parallel to the frequency axis to form a composite curve of fatigue resistance against frequency.

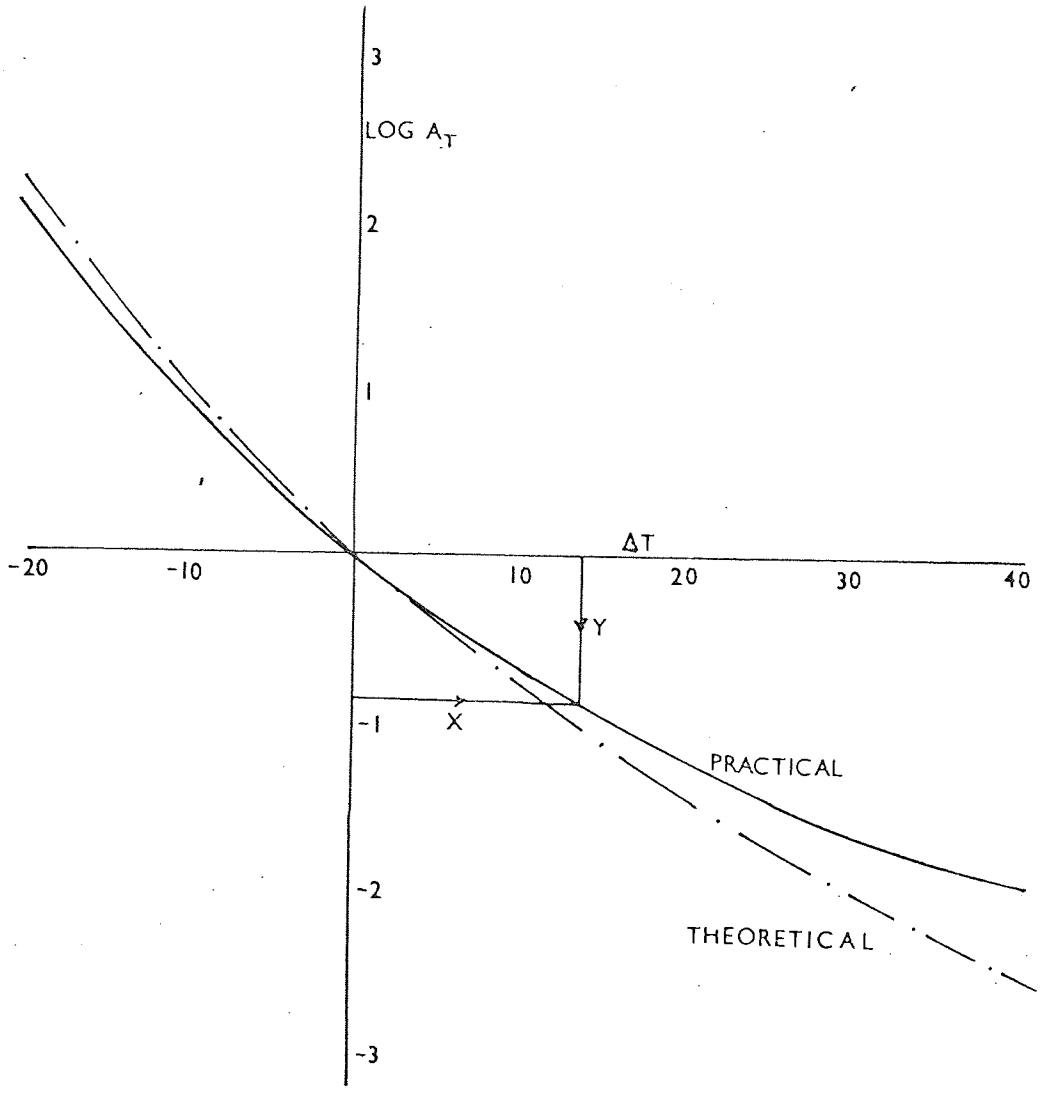

Figure 7.4. The full line shows the 'rate shifts' necessary to transform the fatigue data of Figure 7.2. to a temperature of $-10^{\circ}C$ vs. the temperature differences (ΔT). The broken line is the theoretical W-L-F equation.

The reference temperature chosen for this procedure was the curve at $-10^{\circ}C$ $(263^{\circ}K)$ since this was at about the midpoint of the experimental data. Figure 7.4. is a plot of (ΔT) the temperature difference between the temperatures at which the separate curves were measured and the reference temperature against the "rate shifts" necessary for co-incidence. The dotted line is the W-L-F equation, i.e. Log A_T vs $T-T_s$ from equation 7.1. It is possible to make the theoretical and experimental curves co-incide by moving the experimental curve a distance x along the ΔT - axis and a distance y along the log A_T - axis.

Then:- $$\Delta T = (T - T_s) - x \quad \ldots \quad \ldots \quad 7.2.$$

$$\Delta \log A'_{To} = \log A'_{Ts} - y \quad \ldots \quad 7.3.$$

where x and y depend upon the arbitrary choice of reference temperatures. If $-10^{\circ}C$ happened to be T_s for the 12/88 styrene-butadiene rubber then the two curves would coincide, and x and y would be zero.

Now from 7.2. when $\Delta T = 0$ $(T = T_o)$

$$T_s = T_o - x \quad \ldots \quad \ldots \quad \ldots \quad 7.4.$$

Hence from T_o and x we can calculate the characteristic temperature.

Also if $T = T_o$ then from 8.3. we can write

$$y = -8.86 (T_o - T_s)/(101.6 + T_o - T_s) \quad \ldots \quad 7.5.$$

and T_s may be calculated from y and T_o.

Thus equations 7.4. and 7.5. provide two methods of calculating the reference temperature T_s of the polymer. The two calculations should give the same value for T_s and the closeness of agreement is a measure of the accuracy of fit of the experimental results to the W-L-F equation. This process was carried out for five amorphous unfilled styrene-butadiene rubbers (compound 1 - 5 Appendix III) and the calculated values of T_s are shown in Table 7.1.

TABLE 7.1. CALCULATED VALUES OF T_S

Styrene Ratio in SBR (%)	48	36	24	12	0
T_s-x-shift	30.0	20	0°C	-15	-23°
T_s-y shift	32.5	20	.7°C	-14	-29°
Mean T_s	31.3	20	.4°C	-14.5°C	-26°

The agreement between T_s values calculated from the x and y shifts is good in all cases except for the polybutadiene (0 parts of styrene).

It was felt that this calculation of T_s provided a good check of the validity of the results and it was decided to compare the T_s values with measurements of T_s from other sources.

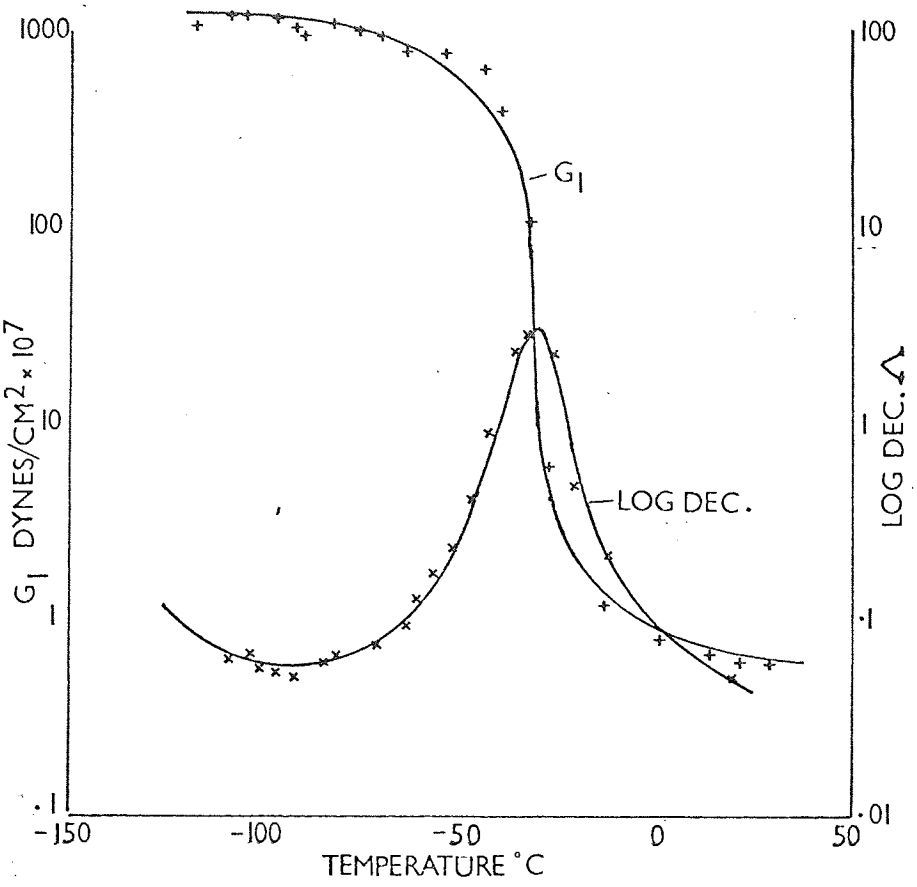

Figure 7.5. The real part of the complex modulus (G_1) and the logarithmic decrement vs. temperature.

7.3. Measurement of T_s

To measure T_s use is made of its fixed relationship with T_g, the glass transition temperature of the polymer. The glass transition temperature was measured in two ways - statically and dynamically, and the results obtained, together with the calculated values of T_s are given in Table 7.2. The two methods of measurement are summarized below.

Static

A volume dilatometer [79] was used to measure the rate of change of volume of three small pellets of rubber, by the change in the height of a column of alcohol in a capillary. An abrupt change in the slope of the graph of volume against temperature indicates the transition temperature.

Dynamic

Graphs of the real part of the complex modulus and of the logarithmic decrement of the rubber when plotted against temperature show an inflection and a maximum respectively. (Figure 7.5.)

The two turning points coincide at approximately the same temperature in the region of the glass-transition temperature. These two quantities can be measured using a torsional pendulum (see Appendix IV). The term glass-transition temperature refers to the value obtained under static conditions. Under dynamic conditions however, the visco-elastic properties of the material cause the onset of glass-like properties to occur at a higher temperature than is observed in static experiments. The dynamic measurements using the torsion pendulum were in the frequency range 1 - 10 cycles per second. It has been suggested that the glass transition temperature lies about $20^{\circ}K$ below the temperature at which maximum damping occurs [83] for a frequency of oscillation of 100 cps.

Other workers have studied the effect of styrene content in styrene-butadiene co-polymers on the static second order transition temperature. Gerke [84] found an empirical relationship between the transition temperature of the two constituent polymers $T_1{}^{\circ}C$, $T_2{}^{\circ}C$ and the resulting co-polymer $Tg^{\circ}C$ as follows :-

$$\log \ (273 + T_1)/(273 + T_g) \ = \ C_2 \log \ (273 + T_1)/(273 + T_2)$$

... ... 7.6.

where C_2 is the volume fraction of the constituent polymer with transition temperature T_2. Wood [85] has derived the relationship :-

$$T_g = T_1 (1 - C_2) + kC_2T_2 \ / \ 1 - C_2 + kC_2 \quad ... \quad 7.7.$$

where k is a constant related to the co-efficient of thermal expansion of the two polymers above and below their transition temperatures. For styrene-butadiene co-polymers k = .50

Table 7.2. is a summary of the measurements of glass-transition temperature as a function of the amount of styrene present in a styrene-butadiene co-polymer. Four of the measurements are based on static dilatometric methods and two on the dynamic methods, torsional pendulum and vibrating reed.

TABLE 7.2.

Method of Measurement	Ref.	Transition Temperature °C — Styrene to Butadiene Ratio				
		0/100	12/88	24/76	36/64	48/12
1) Volume Dilatometer	-	-80	-65	-51	-38	-22
2) Volume Dilatometer	[81]			-47.5	-36.4	-20.5
3) Torsional Pendulum	-	-80	-64	-54	-32	-24
4) Vibrating Reed	[82]	-50	-39	-26	-8	+10
5) Calculated from Gerrard's equation	[85]	-80	-64	-46	-28	-8
6) Calculated from Wood's equation	[86]	-80	-69	-56	-40	-22
7) Ts from Table 7.1. minus 50°C	-	-76	-64.5	-54	-30	-18.7

The measurements 1 and 3 were performed specifically for this investigation and the others were obtained from published data, the reference being given in

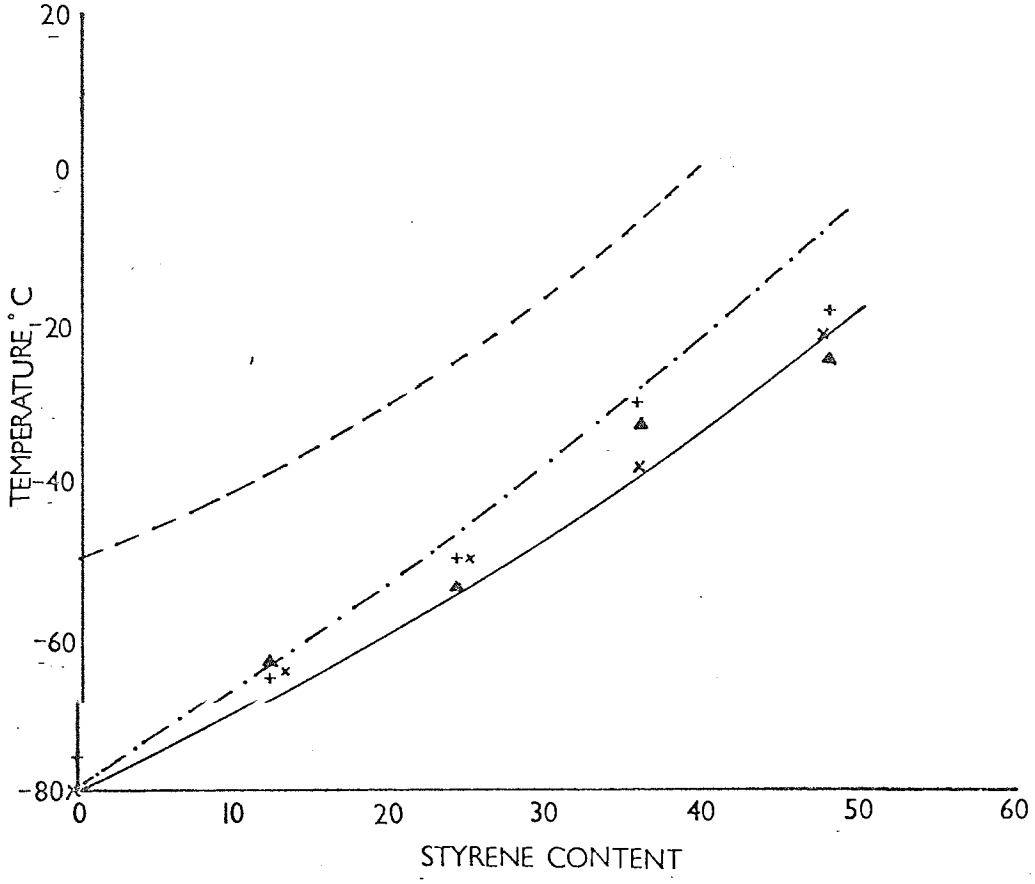

Figure 7.6. Glass transition temperature vs. the percentage of styrene for styrene-butadiene rubber. Results calculated from the temperature-rate transformation of fatigue data (+) and measurements from a dilatometer (x) and a torsional Pendulum (▲) are compared with the published results of Gerke (-·-·-·-) and Wood (————) and also vibrating reed measurements(- - - - -).

Table 7.2. The results are displayed graphically in Figure 7.6. The graphs show that there are wide discrepancies even in static measurements of Gerke and Wood. The experimental work carried out for this investigation and the reported work of D.N. Keyte [81] shows good agreement, the results falling somewhere between those of Gerke and Wood. The torsional pendulum results do not show the expected shift with frequency but are distributed about the line of the static measurements of this investigation with apparently large variation, much of which probably stems from errors in estimating the exact position of the point of inflection of the modulus and the damping maximum. On the other hand the vibrating reed measurements do show the predicted shift of about $30^{\circ}C$.

In Figure 7.6. are also included the results given in Table 7.1., plotted on the graph in the form $T_g = T_s - 50^{\circ}C$. It is seen that they are slightly higher than the statically observed values of this investigation but are well within the range of observed values for these co-polymers. The general level of agreement of the calculated values of the T_s values with observed glass-transition temperature values confirms the validity of the W-L-F transform method of analysis applied to fatigue

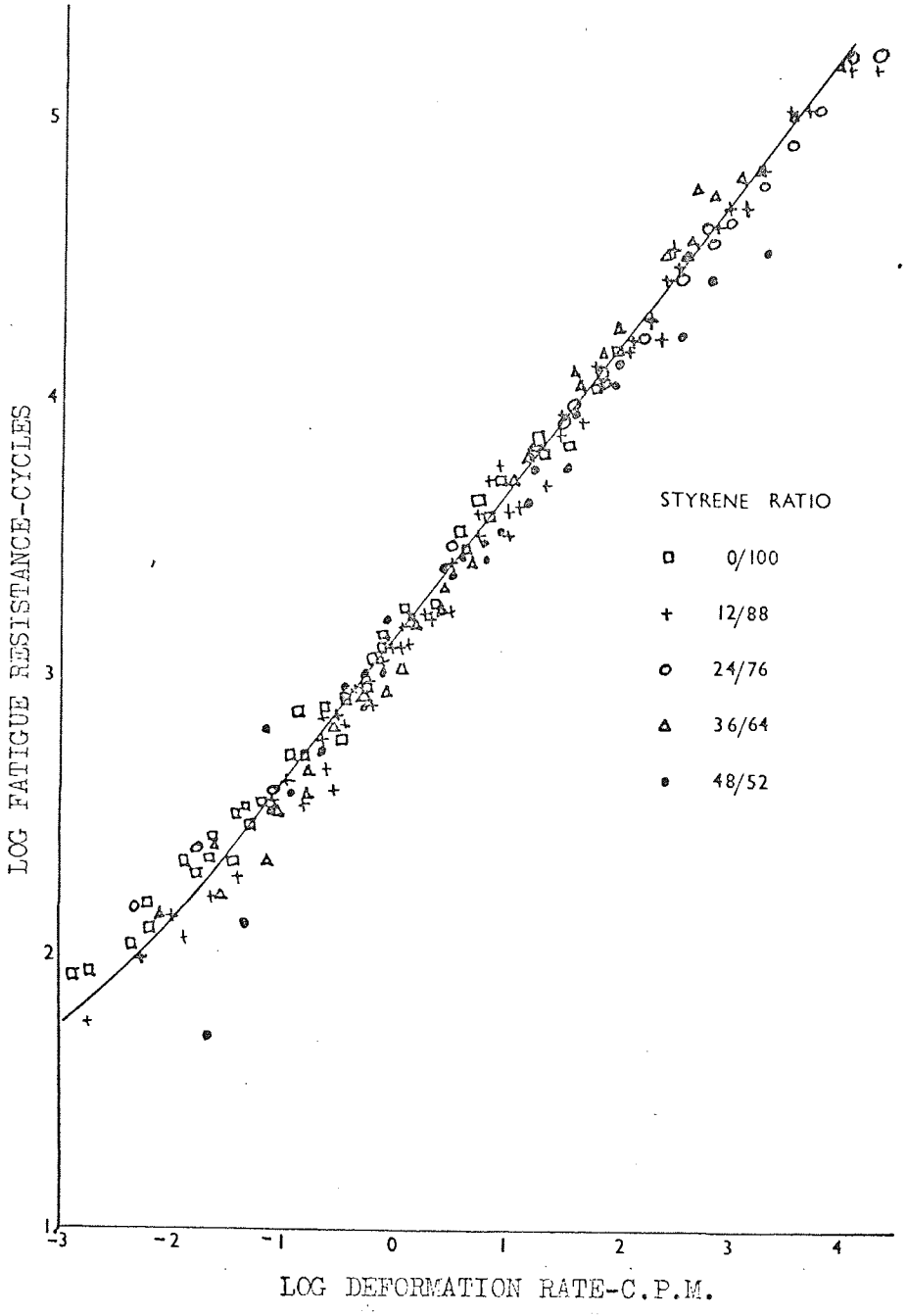

Figure 7.7. Fatigue Resistance Data for five styrene-butadiene gum rubbers. Co-incidence occurs when transformation is referred to T_s a characteristic temperature of the polymer.

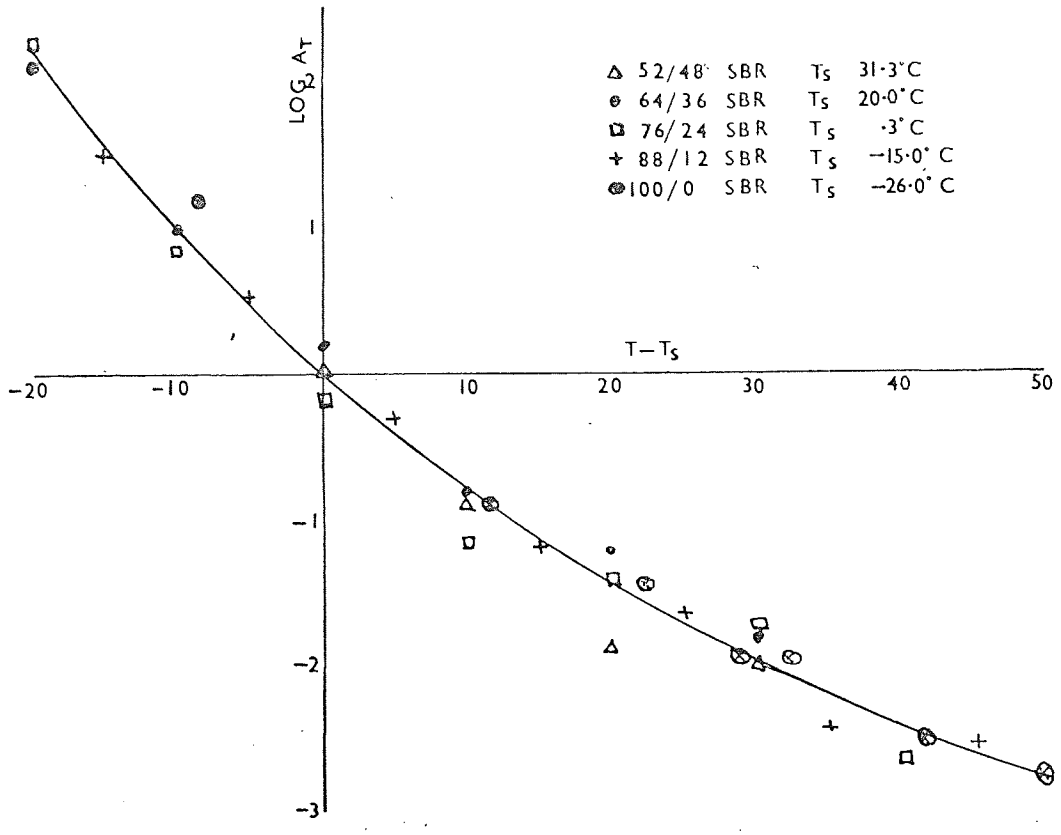

Figure 7.8. (A_T) the 'rate shift' necessary to construct the master curve shown in Figure 7.7. vs. ($T - T_S$) the temperature differences.

resistance measurements on unfilled polymers.

7.4. Master Curves

If a composite curve such as Figure 7.3. is obtained using the T_s of the polymer as a reference temperature then the results for the five styrene-butadiene co-polymers used in this investigation are seen to fall on one curve of frequency vs fatigue resistance. Figure 7.7. The figure shows transformed values of fatigue resistance obtained on all the vulcanizates, compounds 1 - 5 in Table 6.1. The figure was constructed in a similar way to that used for Figure 7.3., and the full line is the same as that in Figure 7.3. The rate-temperature transform necessary to construct Figure 7.7. is shown in Figure 7.8. The change in rate A_T equivalent to a change in temperature was determined solely by the lateral translation of each curve of fatigue resistance against frequency of deformation to the curve at the reference temperature.

It is seen that for all the co-polymers examined the fatigue resistance is completely described by the two basic curves shown in Figures 7.7. and 7.8. It therefore, appears that the

fatigue resistance of the co-polymers is controlled by their chemical composition only inasmuch as it affects the second order transition temperature.

7.5. The Effect of Carbon Black Filler

It was shown in Figure 6.3. how the dependence of fatigue resistance on frequency was progressively reduced as the concentration of filler in the rubber was increased, while the temperature dependence was similar to that of the unfilled polymers. In the range of frequencies at which the measurements were performed neighbouring curves are again similar in shape, but because of the reduced frequency dependence transformation by the usual process would give increased values of the frequency shift A_T associated with a particular temperature interval, thus it is possible that a curve of the W-L-F type may be formed. However, for the filler concentrations used in this investigation the frequency dependence was removed to such a degree that no temperature-frequency was attempted.

The calculation shown in Appendix I together with Figure 2.3. suggests that the major part of the frequency

dependence arises from the static contribution (G_S) to cut-growth. The way in which fillers affect this contribution together with their effect on the visco-elastic dependence of strength are obviously important and it is suggested that the effect of the successive additions of small concentrations of filler on the transformation found for the unfilled rubbers might give valuable information on the role of filler in reinforcement.

7.6. Discussion

Mullins [56] points out that the rate-temperature transform found necessary to describe tearing behaviour is different from that determined by Ferry to describe viscous and visco-elastic behaviour, although it is of a similar shape. He points out that the measured value of the tearing energy is proportional to the product of the strain energy at break and the radius at the tip of the tear, both of these properties being rate and temperature dependent and reflecting the visco-elastic properties of the rubber, and therefore concludes that the dependence of tearing energy on rate and temperature will be more complex than the original Ferry transform. However, the same

argument should apply to tensile strength measurements and to fatigue resistance but in both cases the Ferry equation is seen to hold. This seems to suggest that in the case of tearing the discrepancy arises not from complications in the W-L-F relationship, but in the interpretation of measurements of the glass transition temperature in dynamic experiments. The work of Greensmith and Thomas [48] and Mullins [56] is seen to agree much more closely with the above investigations of tensile rupture and crack-growth if the transform is referred to the temperature of maximum damping measured in that investigation.

8. FATIGUE RESISTANCE AS A FUNCTION OF MECHANICAL DAMPING.

As with many properties of vulcanized rubbers it is difficult to reconcile the simple visco-elastic dependence of the fatigue resistance experienced in gum rubber with the complex situation that arises when inorganic reinforcing fillers are present. In the filled rubbers used in this investigation it was found more useful to relate the fatigue resistance to a property which shows the same sort of dependence on the visco-elastic nature of the rubber and which could be measured on a more convenient time scale rather than to try to analyse results by the methods outlined in the previous chapter. Because of theoretical predictions of the dependence of crack-propagation on energy loss mechanisms, fatigue resistance measurements were correlated with mechanical damping measurements made on the same rubber.

8.1. Fatigue as a Function of Damping in Unfilled Rubbers

The work described in Chapter 7 showed that a mathematical

expression for the fatigue resistance (N) of an amorphous unfilled rubber at a particular temperature (θ) and frequency (f), other things being equal, was

$$\log N = G(\theta, \log f) \quad \ldots \quad \ldots \quad 8.1.$$

where G is a particular function. At a reference temperature θ_s,

$$\log N = G(\log f) \quad \ldots \quad \ldots \quad 8.2.$$

at any other temperature θ

$$\log N = G(\log f + \log A_T) \quad \ldots \quad 8.3.$$

where A_T is given by the W-L-F equation

$$\log A_T = -8.86 (\theta - \theta_s)/101.6 + (\theta - \theta_s)$$

For any property which depends solely on the visco-elastic nature of the rubber, a functional relationship like 8.3.

can be derived, and fatigue resistance may be related to this property by eliminating the term $(\log f + \log A_T)$.

As an example consider the mechanical damping of a polymer in response to a small deformation. In a visco-elastic material force is proportional to both displacement and rate of displacement.

$$F = Kx + d(\dot{x}) \quad \ldots \quad \ldots \quad 8.4.$$

where K is a constant called the dynamic modulus.
and d is a constant called the dynamic viscosity.
For sinusoidal oscillations,

$$x = x_o \exp(i\omega t)$$

$$\text{and } \dot{x} = i\omega x_o \exp(i\omega t)$$

therefore equation 8.4. becomes

$$F = Kx_o \exp(i\omega t) + i\omega d x_o \exp(i\omega t)$$

$$F = (K + i\omega d)\, X \qquad \ldots \qquad \ldots \qquad 8.5.$$

The out-of-phase term ωd implies an energy loss in the system. Thus frequency multiplied by the dynamic viscosity is a measure of the visco-elastic or mechanical damping of the material.

Now the variation of both the dynamic elastic modulus K and dynamic loss modulus ωd with frequency and temperature have been shown to obey the W-L-F transform. For the mechanical damping term ωd this implies that

$$\omega d = fn\,(\log f + \log A_T) \qquad \ldots \qquad 8.6.$$

Hence comparing 8.3. with 8.6. we should obtain a functional relationship between fatigue life N and damping ωd, provided both measurements are compared at the same temperature and frequency.

The mechanical damping can be measured on a torsional pendulum and was in fact calculated from the damping results measured in connection with the glass transition temperature and

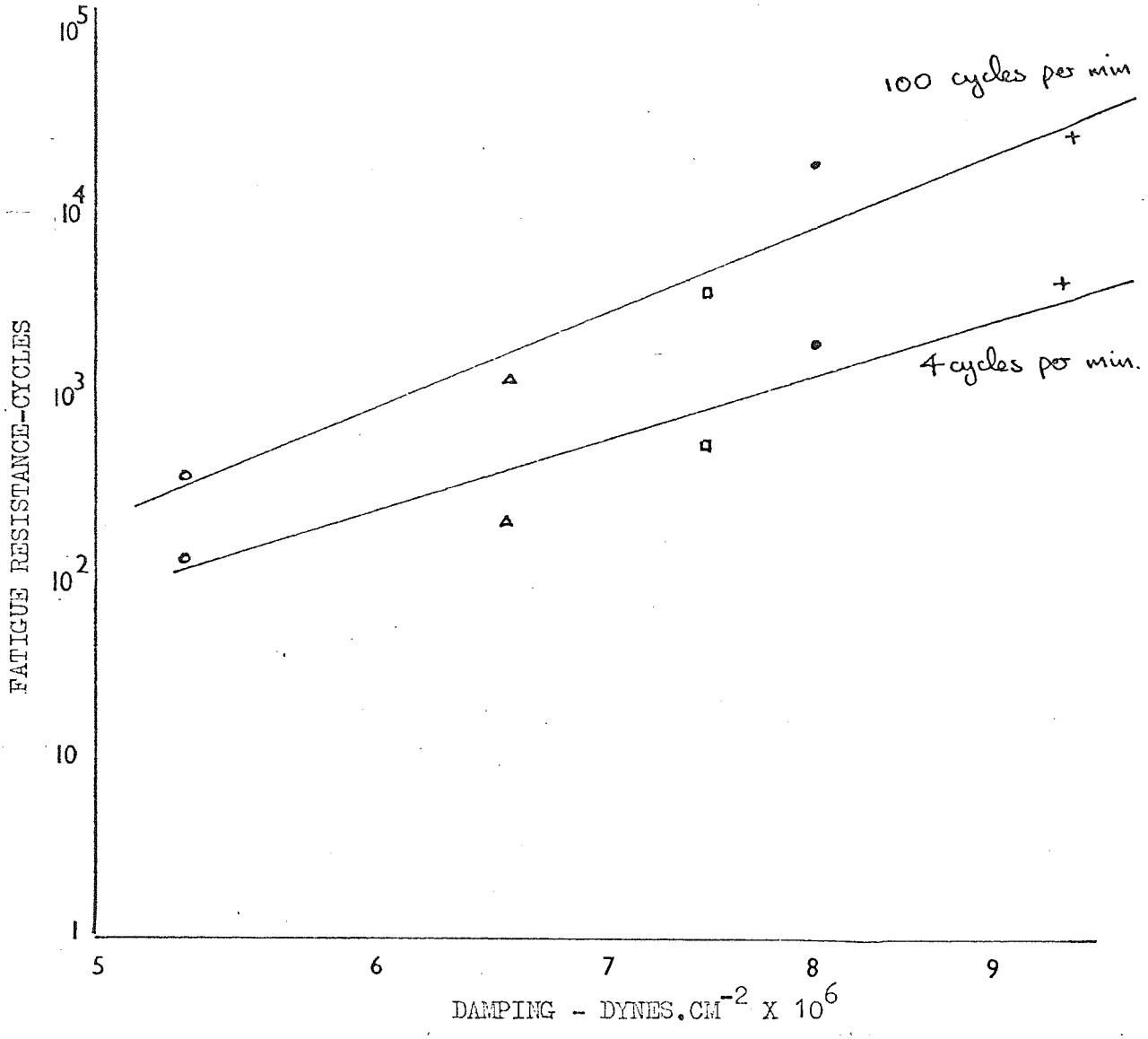

Figure 8.1. Fatigue Resistance vs. Damping for two rates of fatigue testing for the unfilled rubbers (o) - polybutadiene, (Δ) - 12/88 styrene-butadiene, (□) - 24/76 styrene-butadiene (•) - 36/64 styrene-butadiene, (+) - 48/52 styrene-butadiene. Compounds 1 - 5 Appendix III.

described in Chapter 7. The product ωd is calculated from the expression

$$\omega d = \pi(121I/bh^3)(f.(\Lambda f - \Lambda ofo))/(1 - .63h/b)$$

the symbols having the meaning given as in Appendix IV. Measurements of the mechanical damping at a particular temperature were compared with the fatigue resistance values at the same temperature and for one specific rate. Figure 8.1. shows an approximate proportionality between logarithmic fatigue resistance and logarithmic damping. Since the frequency variation on the torsion pendulum is only small, different curves are obtained for comparison with N obtained at different frequencies.

8.2. Fatigue Resistance in Filled Rubbers as a Function of Damping.

As with the unfilled co-polymers the fatigue resistance of the filled rubbers was compared with the damping as measured on torsional pendulum. Figure 8.2. shows results obtained for the compounds 2, 6, 7 and 8 of Appendix III which was the 12/88

styrene-butadiene rubber compounded with 0, 25, 50 and 75 parts of HAF carbon-black, measurements of fatigue resistance being referred to the same temperature, frequency and deformation cycle. When comparisons are made for the same deformation cycle the effect of adding filler is to increase the modulus and therefore the strain energy stored in the test-piece in any cycle.

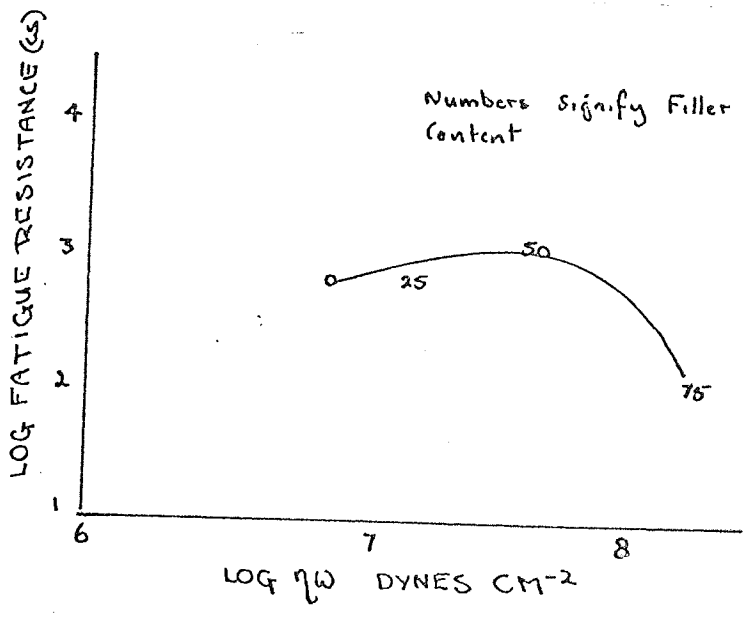

Figure 8.2. Fatigue Resistance vs Damping for 12/88 Styrene-Butadiene Rubber containing 0, 25, 50 and 75 parts of HAF filler.

Assuming the validity of equation 1.15. it is possible to estimate the dependence on damping of fatigue resistance of these filled and unfilled co-polymers when comparisons are made at the same stored energy of deformation. Equation 1.15. may be written

$$N = Gc_o^{(1-n)}/(n-1)\,(2kW)^n \quad \ldots \quad \ldots \quad 8.7.$$

thus if fatigue resistance is known at one value of the stored energy of deformation W, providing the index n is known, the term $Gc_o^{(1-n)}$ can be determined and fatigue resistance calculated for any other value of W. In this way a fatigue resistance for the filled rubbers was calculated for the average stored energy of the unfilled co-polymers under the conditions of measurement at which the results shown in Figure 8.1. were obtained. The index n has the value 4 for unfilled rubbers. The value for the filled rubbers was measured as follows.

8.2.1. Measurement of the index n for Filled Rubbers

The growth dc of a crack of length c in one extension

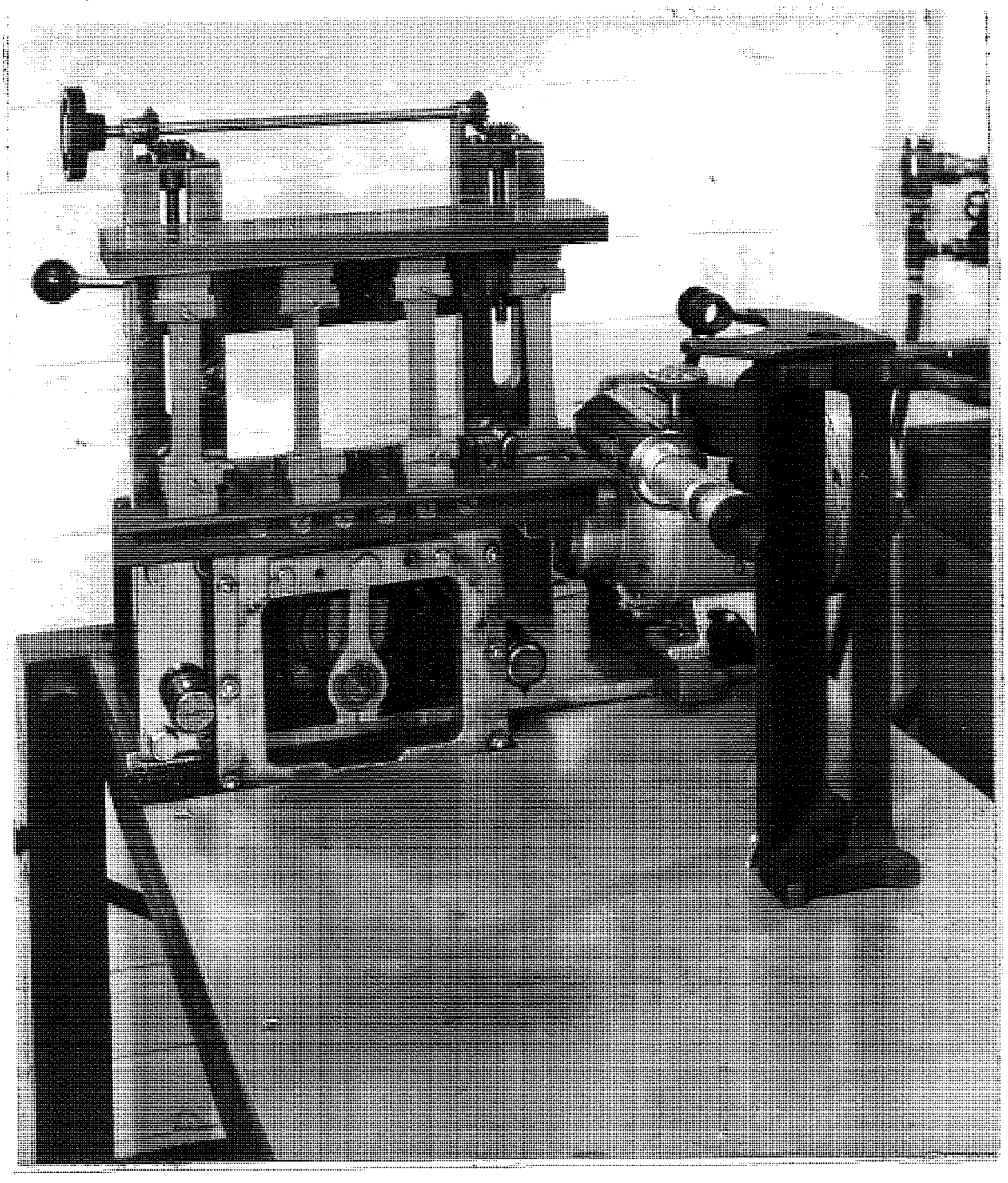

Figure 8.3. Apparatus for determining the index 'n'. Showing four samples in tension and travelling microscope. (Foreground)

of a tensile test-piece is given by equation 1.13., Chapter I viz :-

$$dc/dn = \mathcal{T}^n/G \qquad \ldots \qquad \ldots \qquad 8.8.$$

where $\mathcal{T}$ the tearing energy is given by

$$\mathcal{T} = 2kWc \qquad \ldots \qquad \ldots \qquad 8.9.$$

W is the energy stored during deformation and k is a constant that depends only slightly on strain. Hence the index n is the gradient of a logarithmic plot of dc/dn against $\mathcal{T}$.

The rate of cut-growth in the filled rubbers (compounds 6 - 8, Appendix III), that is, the rate of propagation of a crack through the material, was measured for use in determining the index n. The basic framework of the test-machine is similar to the twelve-station fatigue machine described in Chapter 5 and is shown in Figure 8.3. A sample is repeatedly extended by a motor, gear box and eccentric arrangement. The machine is mounted on a table on which a travelling microscope can be

positioned conveniently to observe the samples. The motor is a $\frac{1}{4}$ H.P. d.c. motor which is controlled by a 'Berco' controller to give a machine frequency range of 10 - 300 revolutions per minute.

The test-piece is a one inch wide strip of rubber which has bars moulded along the clamping edges for secure fastening. A 1mm long cut is made in the edge of the test-piece with a razor blade, whilst it is held in a special clamping device to restrict the depth of cut. The cut-length is measured initially with a travelling microscope. The sample is then placed on the machine and deformed in a cyclic manner the length of the cut being measured after fixed intervals of time. Thus the cut-growth rate dc/dn could be determined for a particular cut-length and maximum extension by finding the incremental growth for a number of cycles. The tearing energy J associated with this maximum extension was calculated from equation 8.9.

The stored energy W was found by integrating the stress-strain curve obtained by extending the sample on an 'Instron' tester up to value of the maximum strain for the test. As the tearing energy J is proportional to c, the rate of cut-growth varies with the distance grown. This enables the cut-growth

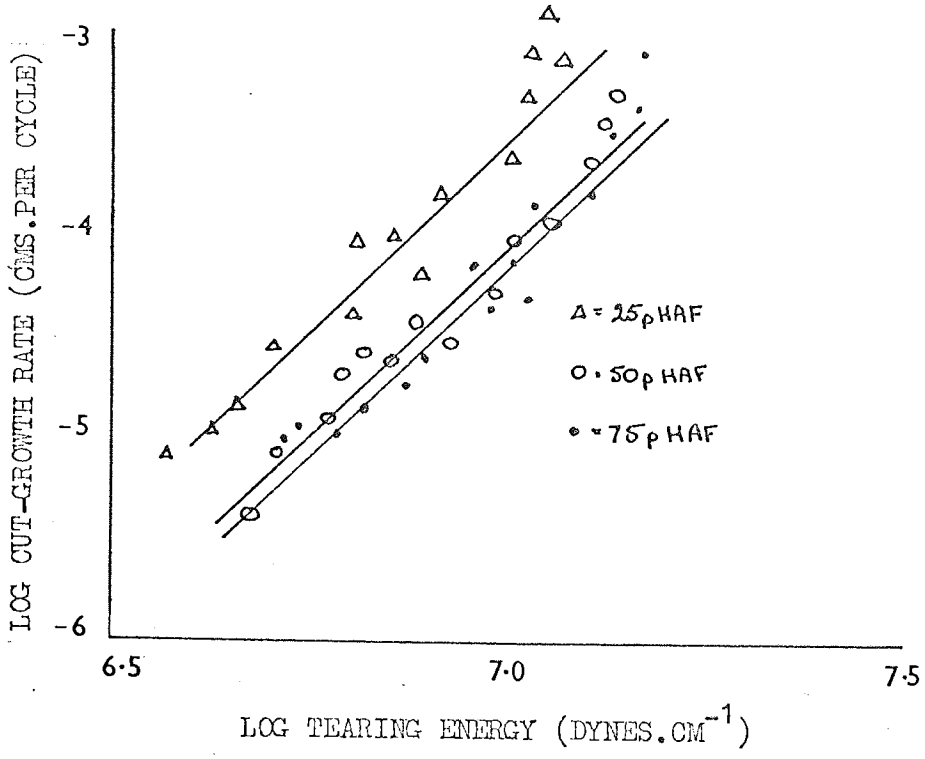

Figure 8.4. Cut-growth rate dc/dn vs. Log tearing energy $\mathcal{T}$. for three filled 12/88 Styrene-Butadiene rubbers.

rates to be obtained over a range of J values from a single test-piece.

Results for the rubbers (compounds 6 - 8) are shown in Figure 8.4. as a plot of log dc/dn against log J. The straight lines all have slopes which are close to 3.5. in value and this number was used for n in the calculation outlined earlier in this section to calculate values of fatigue resistance of the filled rubbers which might be expected at the reduced level of stored energy associated with the unfilled polymers.

The stored energy of the unfilled polymers (1 - 5 Appendix III) was measured on the 'Instron' tensometer under the conditions of strain, temperature and frequency relevent to the results shown in Figure 8.1. The average of these stored energy values was taken and the fatigue resistance values of the filled rubbers (6 - 8 Appendix III) shown in Figure 8.2. were then calculated according to equation 8.7. to be consistent with the average stored energy of the unfilled rubbers. If the results shown in Figure 8.1. and the calculated results of the filled rubbers are now compared with damping values, then as is

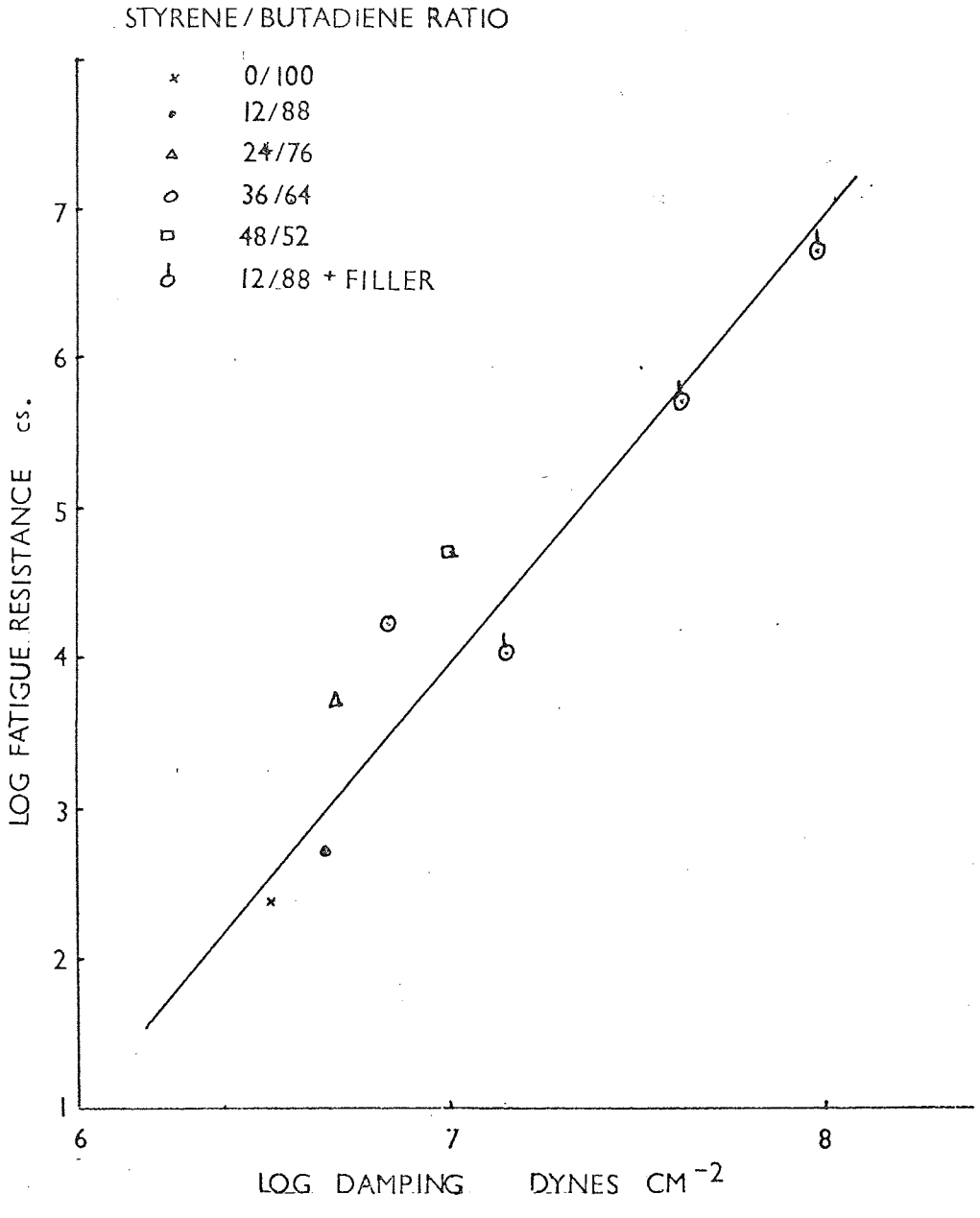

Figure 8.5. Fatigue as a Function of Damping for Filled and Unfilled SBR co-polymers. Fatigue Resistance values being calculated according to equation 8.7.

shown in Figure 8.5. all the results are approximately co-linear.

Therefore consideration of the overall hysteresis in the system unifies the results of the unfilled and the filled rubbers when comparisons are made at the same input energy. The gradient of the straight line shown in Figure 8.5. is 3.5 which is the same as the index n of the filled rubbers.

8.3. Discussion

Figure 8.5. illustrated the importance of comparing the fatigue resistance of different rubbers under equivalent conditions of energy input and shows that under these conditions there is a logarithmic proportionality between fatigue resistance and mechanical damping.

It may be argued that the damping is measured at deformations which have little in common with a typical fatigue measurement and indeed at deformations at which no fatigue failure occurs. For this reason it was decided to extend the mechanical damping measurements to high strains so that fatigue resistance might be compared with the actual hysteresial energy loss experienced in a typical fatigue test.

9. ENERGY LOSS PER CYCLE AND ITS INFLUENCE ON FATIGUE

9.1. Hysteresis and Strength

A number of investigators [86], [87], [88], [89], [90], [91], [92] and [93] have demonstrated the role of hysteresis in determining the mechanical properties of the rubber. More recently its influence on the failure mechanisms of rubber has been the subject of a number of investigations many of which have been described earlier. This investigation has extended this knowledge to cover the case of fatigue resistance. Chapter 7 indicates a dependence of the fatigue resistance on the visco-elastic nature of the rubber, and in Chapter 8 the role of hysteresis was further demonstrated as the damping characteristics of the rubber as measured on a torsional pendulum were shown to be simply related to the fatigue resistance. To confirm these conclusions it was decided to compare fatigue resistance with the energy loss measured directly during a cycle of a typical fatigue test.

9.2. The Stress-Strain Curve

The kinetic theory of rubber elasticity [94] makes it possible to predict the stress-strain response of vulcanised rubbers from a purely mathematical standpoint. The following expression applies to either simple elongation or simple compression.

$$\text{Stress} = \text{Shear Modulus} \left[\lambda - \lambda^{-2} \right]$$

where λ is the ratio of the strained to the unstrained length. This formula may be modified to account for deviations at high levels of deformation, the above expression being valid from about 50% compression to 150% extension. Thus a stress-strain curve would appear as shown in Figure 9.1. and a curve showing extension and retraction cycles for this non-linear deformation is shown in Figure 9.2.

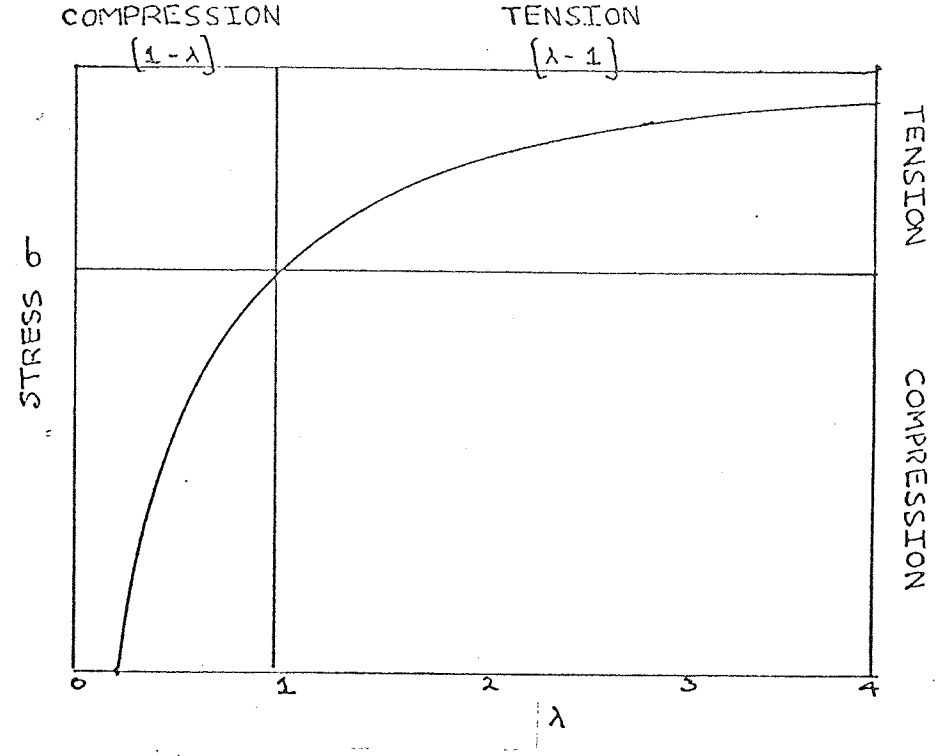

Figure 9.1. Stress-Strain Curve for Rubber.

The area under the upper curve is a measure of the energy used in deforming the rubber and the area under the lower curve is the energy which is stored in the rubber and may be recovered during the retraction cycle. The area between the

two curves is called the hysteresis loop and this area is related to the energy dissipated in deforming the rubber.

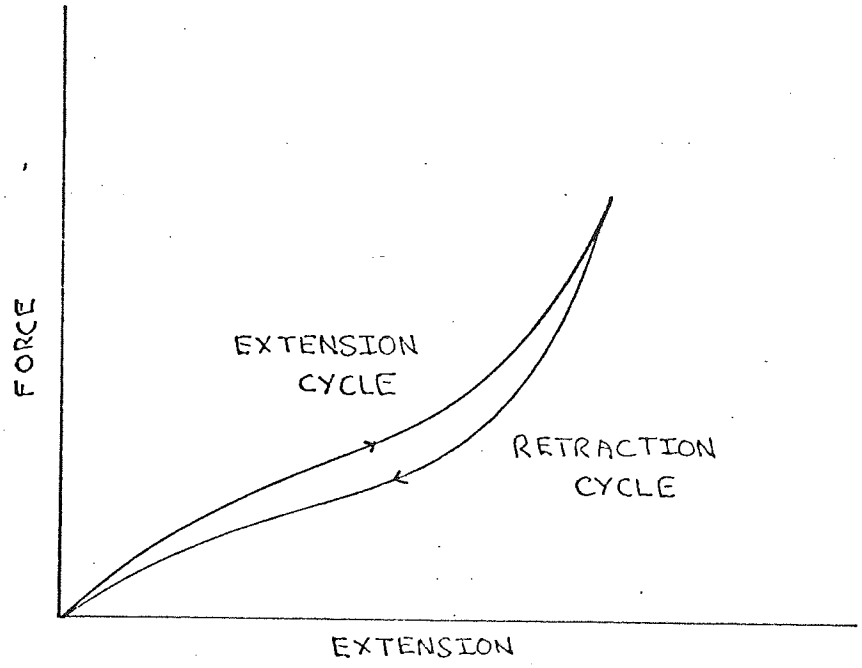

Figure 9.2. Stress-Strain Curve for Extension and Retraction.

There are several mechanisms which give rise to hysteresis. Probably the most important are visco-elasticity, crystallisation and

the redistribution of network chains. A filled rubber is more hysteretic than a gum rubber.

The basis of hysteresis arising from visco-elastic considerations has been described earlier. Strain crystallisation takes place in rubbers like natural rubber and cis-polybutadiene, and this has been described [57] as an energy loss or hysteresial process, which adds to the visco-elastic losses. The crystallisation process is time and strain dependent and the time for the crystals to appear may vary from fractions of a second to weeks depending on the amount of deformation. At high rates of deformation crystallisation will not have time to occur and the behaviour of the rubber will be more visco-elastic in character.

Network redistribution takes place in filled and unfilled rubbers. They exhibit what is known as the "Mullins Effect" or stress-softening [95] . The rubber requires a greater stress to produce a given elongation in the first cycle than in subsequent cycles. The amount of softening reduces until the stress-strain cycle becomes substantially constant after about 10 cycles. Associated with this softening there will be a loss of energy although these first few cycles will not

be significant in a typical fatigue test.

The increased hysteresis in filled rubbers has been explained in terms of a breakdown of the filler structure, and also as the consequence of introducing the inextensible filler particles into the rubber matrix, giving a higher than observed strain in the rubber phase [96]. Thus the hysteresis measurement considered in this investigation will be governed only by visco-elasticity and the effect of fillers.

9.3. The Hysteresis Loop

If, as in the fatigue resistance measurements of this investigation, an approximately sinusoidal strain is applied the resulting stress assuming Hookean conditions to apply is a similar curve displaced in the negative direction along the time scale. The time lag which exists in rubbers between the application of the stress and the achievement of the appropriate strain can be important in conditions where rubbers are subject to cyclic deformations or any repeated deformation. To simplify mathematical interpretation the stress is said to be made up of an elastic component in phase with the strain and a

viscous component 90^{o} out of phase with the strain, 90^{o} because viscous resistance depends on rate of strain and hence is a maximum at maximum rate of increase of strain. The resultant of the two stresses each varying sinusoidally is a sinusoidal stress displaced relative to the strain by an angle δ where $\delta = A_2/A_1$ and A_2 and A_1 are the amplitude of viscous and elastic stress. The angle is called the mechanical loss angle because the existance of this "lag" causes some of the energy input to be lost by conversion into heat.

As explained above because of the difference in phase of the stress and the strain some of the energy put into the rubber during the deformation part of the cycle is not returned during the recovery part of the cycle, and if a graph of stress against strain is plotted it takes the form of a loop called a hysteresis loop, the area of which represents the energy lost. There are many dynamic testing machines which measure this effect.

In rubber the shape of the hysteresis loop is an ellipse providing that the amount of deformation is small enough so that the stress-strain curve is almost linear. At higher strains the stress ceases to be sinusoidal for a sinusoidal strain

and the loop moves towards the shape shown in Figure 9.2.

A method has been developed to record this hysteresis loop during a fatigue test at the rate of extension and temperature of the test to obtain a more direct estimate of the relationship between fatigue life and the hysteresis of the material.

9.4. Measurement of the Hysteresis Loop

The apparatus used for recording the hysteresis loop is an adaptation of the high frequency test machine described in Chapter 5. A sample is extended in a horizontal plane by a motor, gear-box, eccentric arrangement. One end of the sample is attached to a load cell. The other end of the sample is deformed by a moveable carriage on which is mounted the "core" of a displacement transducer which measures the displacement of the moveable end of the sample. The signal from the load-cell is fed through a meter and a low-pass filter onto the y-plates of an oscilloscope, the signal from the displacement transducer is fed through a meter and a low-pass filter onto the x-plates of an oscilloscope. The filters

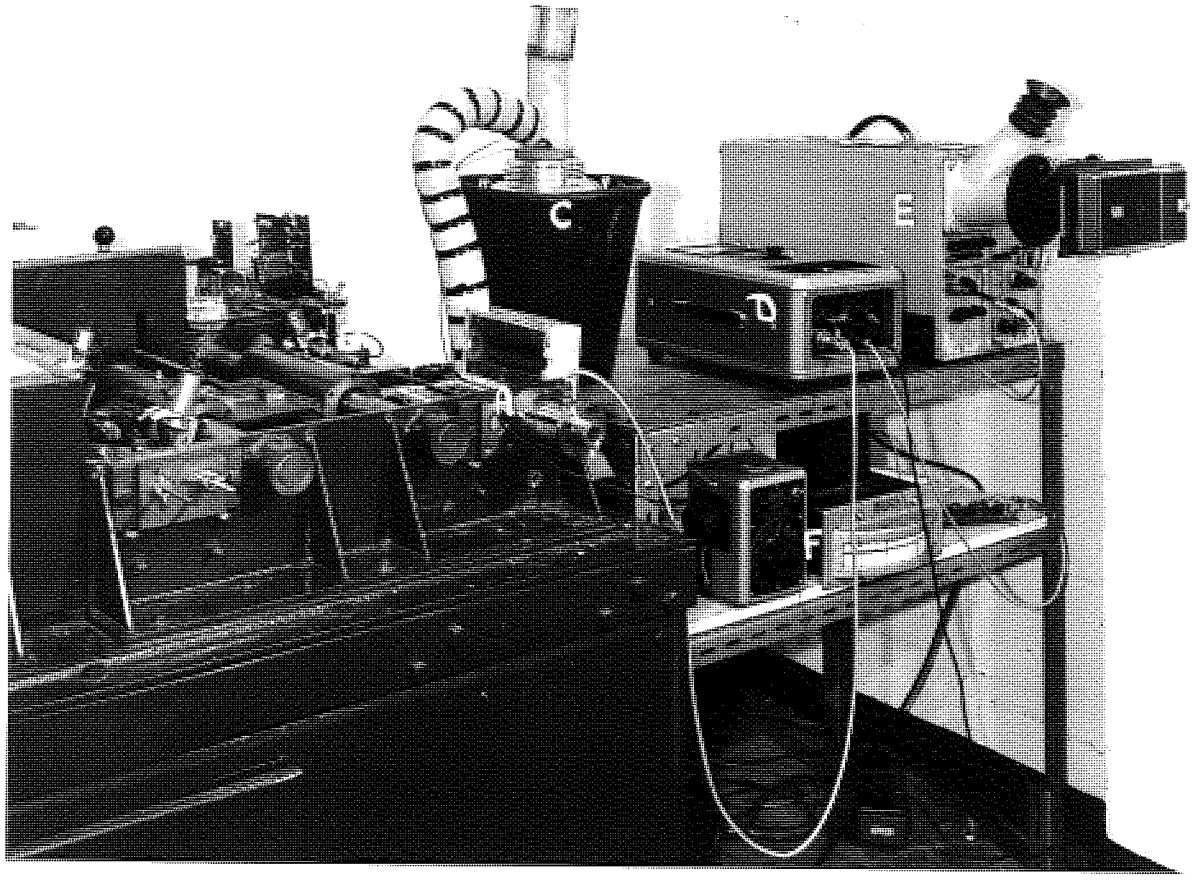

Figure 9.3. *Single station fatigue test and associated apparatus for displaying hysteresis loop.*

A. Temperature cabinet and load cell (Figure 5.8.)

B. Displacement transducer meter.

C. Liquid nitrogen flask.

D. Load cell meter.

E. Oscilloscope.

F. Temperature control and recorder.

remove the natural vibrations of the machinery and electrical interference. Thus an image of the hysteresis loop is displayed on the screen of the oscilloscope.

The sample is a "dumb-bell" shaped tensile test-piece. The shape being the same as is shown in Figure 5.6. on which the fatigue resistance measurements were made though the sample is thicker (2.5 mm) and the length is reduced to 3cm. The sample is enclosed in an asbestos oven. An air stream is directed into the oven. This air stream can be taken across a "heating" element and heated such that the temperature of the oven may be raised to $+120^{o}C$. It is possible to isolate the heating element and blow into the enclosure liquid nitrogen which has been "boiled" out of a "Dewar" of liquid nitrogen by a second heating element. Both heating elements are controlled by a "variac" which is in turn controlled by a thermocouple-pyromaxim arrangement. The thermostat of the pyromaxim controls the temperature of the enclosure to $\pm 1^{o}C$ in the range $-50^{o}C \rightarrow +120^{o}C$. The complete set up is as shown in Figure 9.3.

Calibration of the Load Cell.

Before calibrating the load cell it was necessary to

ensure that none of the "lag" causing the hysteresis loop was in fact delay in the electronics. This was done by replacing the sample with a metal spring. In the Hookean region of the spring there is no delay between the stress and the strain and thus if a sinusoidal deformation is applied to the spring the applied stress will be sinusoidal and in phase with the strain. Instead of a hysteresis loop the stress-strain curve representing a cycle of deformation is a straight line. Thus the electronic circuitry associated with the transducer was checked for any delay.

The load cell was calibrated by hanging loads from it via a pulley. The signal to the y-plates of the oscilloscope was disconnected and the machine was then rotated with varying loads on the load-cell. Each load gave a line parallel to the x-axis on the screen of the oscilloscope. The lines could be photographed by means of a polaroid camera attached to the oscilloscope screen. The photograph is a record of the displacement associated with a particular load. This process is repeated with and without the temperature cabinet in position in order to ascertain the effect of temperature on the calibration of the load cell, however, the distance between the test-piece clamps and the load cell prevented this from being a

problem.

The Loop Area

The area of the loop represents the energy lost on deforming the sample. The "loop" which is displayed on the screen of the oscilloscope is photographed with a polaroid camera. Using an epidiascope the photograph is projected onto a screen magnified four times. The magnification is checked by means of a grid projected from the same plane as the photograph. The projected image of the loop is traced onto the screen. This can be repeated with a calibration pircture in the epidiascope to mark out the axes. The area of the "loop" is then determined by integrating under the curves using Simpson's rule.

9.5. Fatigue Resistance as a Function of Loop Area.

The criterion of fatigue resistance embodied in the equation $\text{Log } N = \text{Log } G - \text{Log } f_n (kWc_o)$ has proved

useful when strain energy is the independent variable. However, the way in which the cut-growth constant G accounts for the changes due to other variables is not well understood. One factor known to greatly influence the strength of visco-elastic materials is hysteresis and the results of this investigation so far confirm the importance of loss mechanisms in defining the resistance to crack propagation in a rubber.

The hysteresis of the material can be altered by changing the temperature or swelling in solvent [97]. The first method was used to examine the compounds 2, 3, 4, 5, and 6 of Appendix III in the temperature range $-50^{\circ}C$ to $+50^{\circ}C$. Most measurements were carried out at one high frequency (300cpm) though the machine was later modified to make measurements at a lower frequency.

All materials tested were subjected to a complete fatigue resistance measurement, the force-deformation curve being recorded at regular intervals throughout the test.

The force-deformation curve becomes substantially constant after the first few cycles. The area of the region between the extension and retraction portions of the force deformation curve was then compared with fatigue resistance

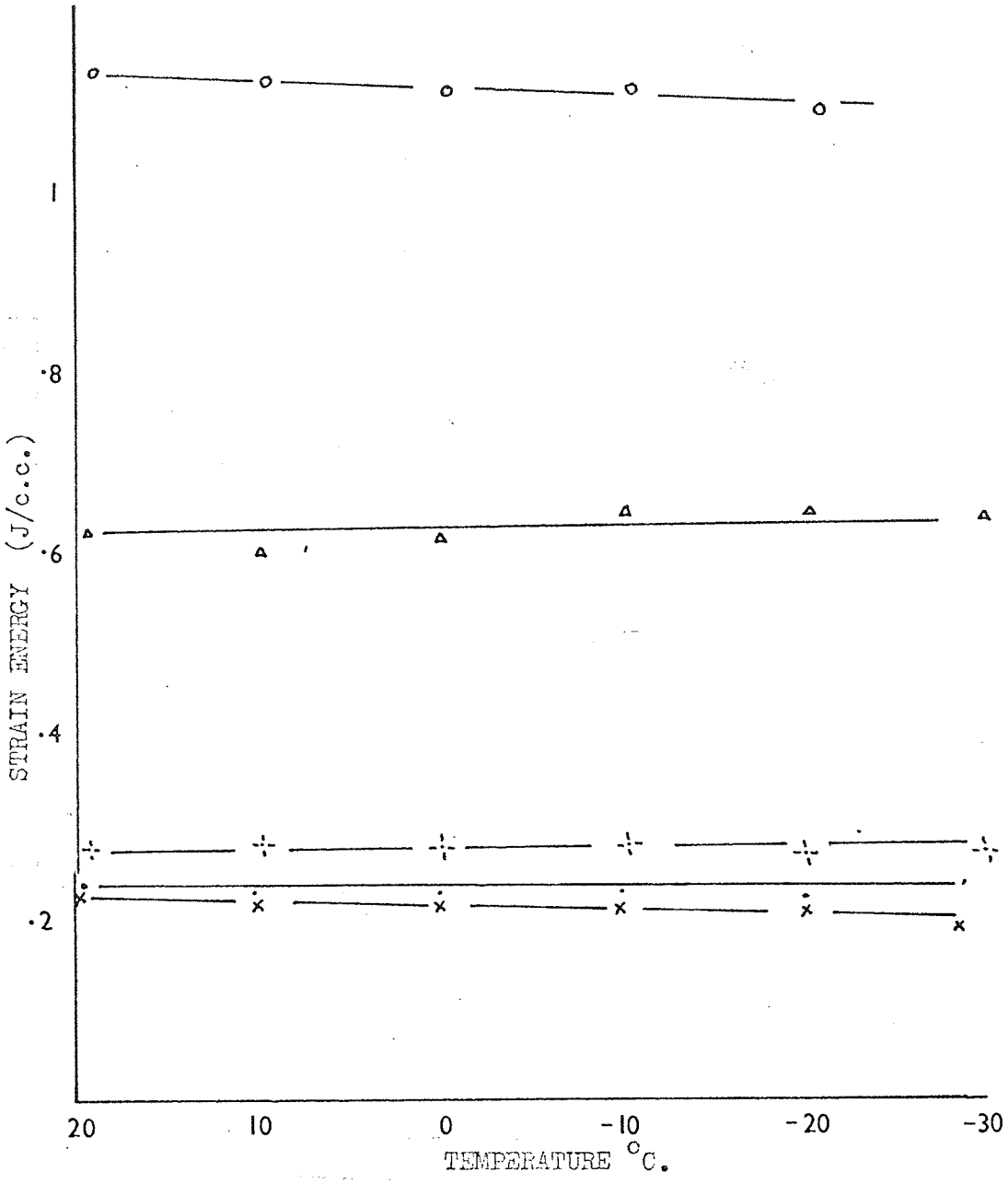

Figure 9.4. The Effect of temperature on strain energy for gum styrene-butadiene rubbers (× , • , -+-) and 12/88 styrene-butadiene with Δ - 25 parts of filler, O - 50 parts of filler.

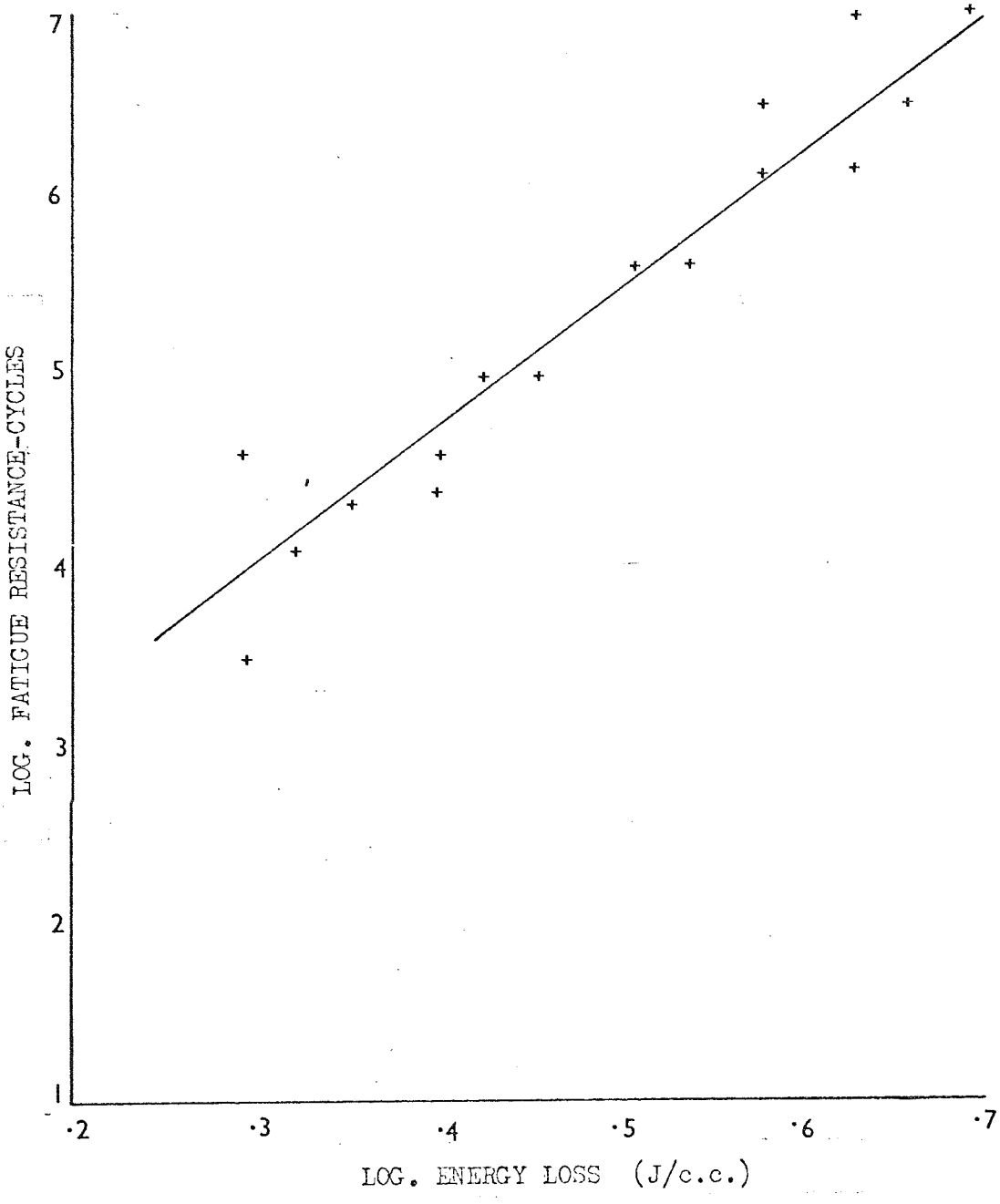

Figure 9.5. Fatigue Resistance vs. Energy Loss per cycle for 3 unfilled styrene-butadiene co-polymers.

measured under the same conditions of maximum deformation, temperature and frequency.

Unfilled Rubbers

It was shown in Chapter 5 that where test-pieces were compared under conditions of the same maximum deformation and frequency but with varying temperatures fatigue resistance was extremely sensitive to the temperature of test. Equations such as 1.15. describe fatigue resistance in terms of strain energy but as Figure 9.4. shows strain energy does not vary greatly with temperature over the experimental temperature range except in the region of the glass transition temperature. On the other hand the area under the retraction part of the curve and the loop area representing the energy stored and the hysteresial energy loss show a marked change over the temperature range, and Figure 9.5. shows fatigue resistance at a particular temperature as a function of the energy loss in a cycle of a typical fatigue test at that temperature. Thus we may write the equation for fatigue resistance at a particular strain or strain energy for the unfilled styrene-butadiene rubbers as

$$N = kH^n \quad \ldots \quad \ldots \quad \ldots \quad 9.1.$$

where N is fatigue resistance.

H is the energy loss per cycle, and k and n are constants.

Figure 9.5. includes the results of measurements on three different co-polymers of styrene-butadiene rubber and therefore the function for these three rubbers appears to be independent of styrene content. The results shown are for the same strain cycle which for the three co-polymers tested is equivalent to a change in maximum strain energy of the order of ten per cent, which according to equation 1.15. could give differences in fatigue resistance of less than 2 times and cause an error of less than three per cent in the results shown in Figure 9.5.

The effect of the strain cycle has not been examined as part of this investigation but as the ratio of loss modulus to the elastic modulus is constant with strain amplitude [98], then by the criterion of equation 1.15. the effect of changing the strain level should be to shift the line to a position parallel to itself altering the value of k in the equation 9.1.

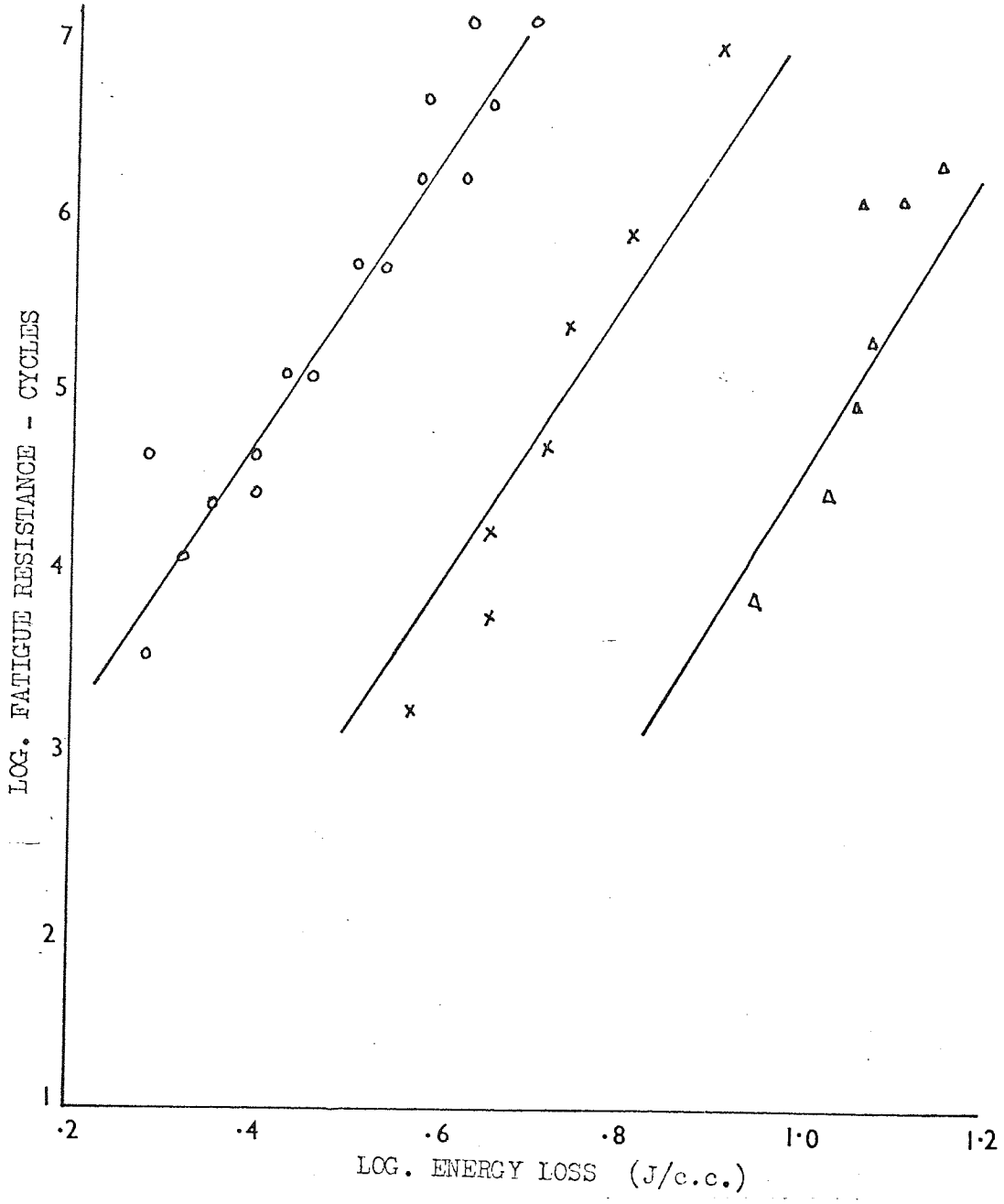

Figure 9.6. Fatigue resistance vs. Energy Loss per cycle. The results of 3 unfilled styrene-butadiene rubbers (o) are compared with 12/88 styrene-butadiene rubber with (x) 25 parts and (Δ) 50 parts of HAF carbon black filler.

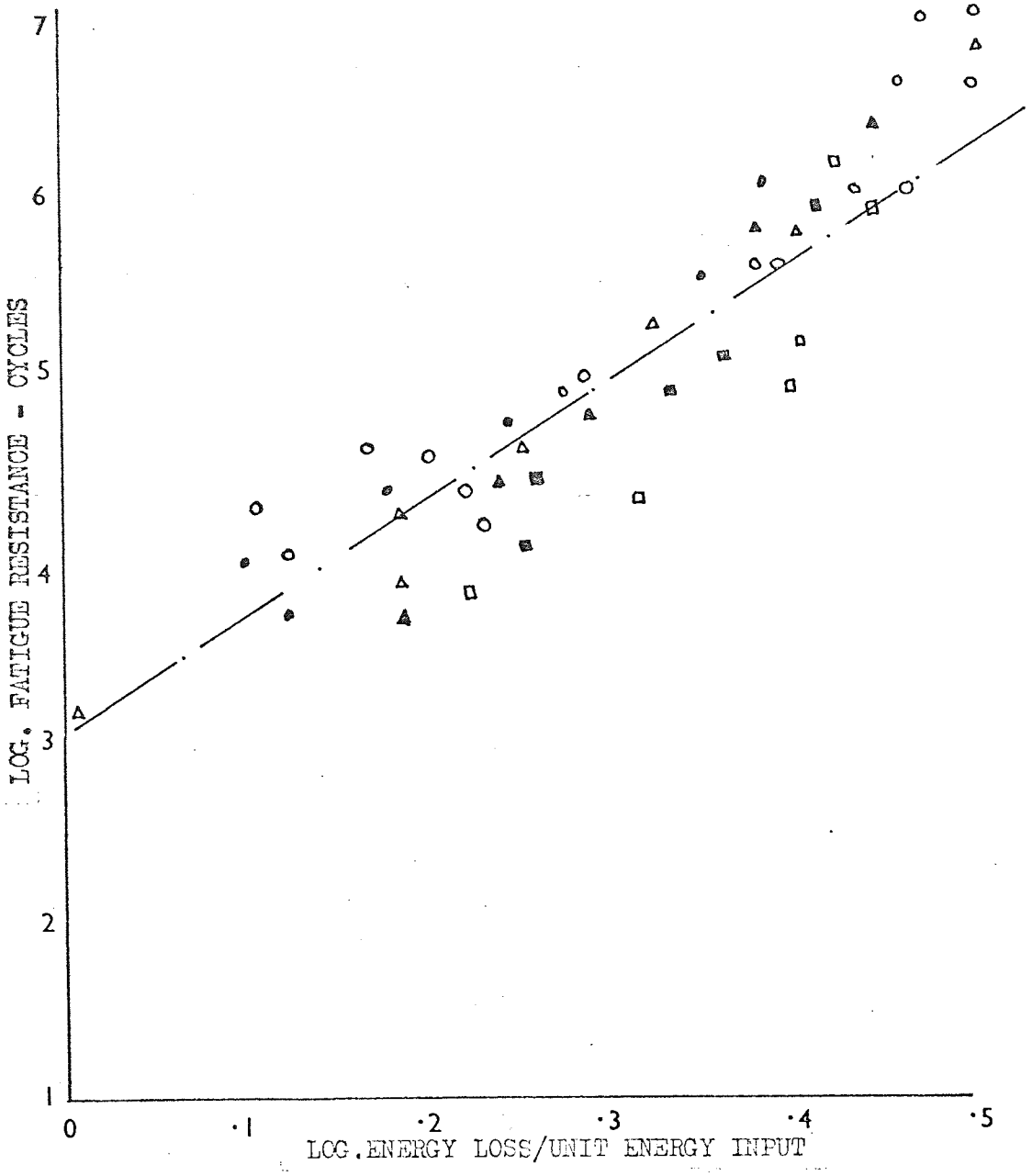

Figure 9.7. Fatigue Resistance vs Energy Loss per unit Energy Input for unfilled SBR co-polymers (circles), 12/88 SBR with 25 parts of HAF filler (triangles) and 12/88 SBR with 50 parts of HAF filler (squares). Open symbols (○ △ □) refer to deformation rate 330 rpm and solid symbols (● ▲ ■) to deformation rate 40 rpm.

Filled Rubbers

When filled rubbers, e.g. compounds 6 and 7 Appendix III are measured at one strain over a range of temperatures, then the fatigue resistance is again seen to be a function of the energy loss per cycle. A log-log plot of fatigue resistance against the energy loss per cycle shows a line displaced along the energy loss axis but with approximately the same gradient. Increasing the filler content further displaces this line. (Figure 9.6.)

The filled rubbers when tested under identical strain cycle conditions have an increased energy of deformation. It is interesting to note that if allowance is made for increased stiffness, plotting the energy loss H per unit energy input I against fatigue resistance then the experimental results shown in Figure 9.6. for both filled and unfilled rubbers fall on a single curve and this is shown in Figure 9.7. In the time available for this investigation it was not possible to examine the exact form of this relation further but for values of log (H/I) up to .4 the relation is approximately linear with values of fatigue resistance falling within plus or minus one half decade

of the best straight line.

Despite this spread of results this is an encouraging result which warrants more examination. Figure 9.7. gives a relationship of the form

$$\log N = \log A + \log (H/I)^k \quad \ldots \quad 9.2.$$

where A and k are constants.

If the strain is altered the line will be shifted parallel to the fatigue resistance axis and therefore the constant A will depend on the strain. This relationship could form a useful basis for comparing fatigue resistance of different compounds at a particular deformation. The second term on the right hand side of equation 9.2. may be simply determined from the elastic and loss moduli which would have to be measured under the experimental conditions and if subsequently a relationship of the form of equation 9.2. proves to be universally applicable to rubbers then it may provide a basis for design in situations like tyre carcasses where the best compound for a fixed strain cycle is required. The equation suggests that the losses in the rubber are maximised

for a particular energy input within the limits of other specifications, e.g. maximum running temperature, which is at variance with present trends in the technology of the subject where "small-particle" fillers and rubbers with higher glass-transition temperatures are used in high hysteresis rubbers giving improved strength.

Equation 9.2. can be compared with equation 1.15. viz :-

$$\text{Log } N = \text{Log } G - \text{Log } ((n - 1)(2kw)^{n} C_{o}^{n - 1})$$

the second term on the right hand side of equation 9.2. and the first term on the right hand side of this equation are independent of strain cycle and it may be possible to equate these two factors. To this end it is intended to determine the function of strain or strain energy relevent to the first term in equation 9.2.

9.6. Energy Loss as a Criterion of Fatigue Resistance

The experimental work described so far, has necessarily been restricted to a limited number of rubbers, nevertheless it

demonstrates the importance of hysteresis in determining crack-propagation in a rubber. Should the relationship between fatigue resistance, energy loss and energy input given by equation 9.2. prove to be applicable to a wider range of materials than those investigated here, it would be a valuable criterion of fatigue resistance, and on the basis of the agreement between the work of Chapter 9 and the damping measurements of Chapter 8 the fatigue resistance might be calculated from values of the elastic and loss moduli obtained, for example, from a torsional pendulum, although comparing Figure 8.1. with Figure 9.5. it is obviously important that comparisons are carried out when the elastic and loss moduli and the fatigue resistance are measured under identical conditions of frequency and temperature.

10. CONCLUSIONS

Flaws and inhomogeneities in vulcanized rubber cause regions of stress concentration in which the rupture stress is exceeded and the formation and propagation of cracks through the material takes place. In this investigation it has been shown that the surface revealed by a fatigue failure usually has two distinct regions, a smooth region which in certain cases may contain regular striations indicating the incremental growth of the crack, and a "rough" region, the formation of which, occupies most of the cyclic lifetime. The "roughness" and extent of this second region are influenced by the presence of fillers and by crystallisation and the extent of the region depends upon the maximum strain energy of the test. The presence of fillers leads to increased hysteresis which can now be seen to play an important part in controlling the cut-growth process leading to fatigue failures. There are obvious differences both in the filled and unfilled situation between the surfaces revealed by the fatigue failure of an amorphous rubber

and that revealed in a rubber where strain crystallisation occurs.

It has been shown that for the same energy of deformation the fatigue resistance of the amorphous rubbers examined could be described by two curves, one of which describes its dependence on the rate of deformation and the other the inter-dependence of rate of deformation and temperature.

In view of the form of this dependence it was concluded that fatigue resistance of these rubbers is controlled by the chemical composition of the rubber only if the chemical composition affects the glass transition temperature of the rubber.

The deformation rate-temperature transform which successfully describes the fatigue data is identical in form to that derived by Ferry on the basis of measurement of viscous or visco-elastic properties, although the exact form depends upon the choice of reference temperature (T_s). The ability of this type of transform to summarize a vast quantity of experimental data indicates the important role of visco-elasticity in the fatigue process. The measurements reported in Chapter 8, which show that fatigue resistance is related to hysteresial damping, add further weight to this conclusion.

In strain crystallising natural rubber within the limits of deformation rate and temperature at which these investigations were conducted there was no evidence of this type of visco-elastic

response. It must be assumed in view of this and also in view differences in failure surface that crystallising rubber derives its crack propagation resistance from a different mechanism and although this has been described as an energy loss mechanism, it may not be adviseable to think of it in these terms.

In filled rubbers there are significant departures from the behaviour expected from a purely visco-elastic mechanism. However, the addition of a filler to a rubber increases both the fatigue resistance and the hysteresis. A possible explanation of the effect of fillers is that they resist crack-propagation in two distinct ways. The first is to increase the relaxation time of the molecular network thereby increasing the hysteresis which controls crack-propagation. The second is by providing a further mechanism of resistance to crack-propagation analagous to that of crystallites in reinforcing natural rubber. This second mechanism is at present a matter of speculation it may be structural in nature or possibly what has been called non-visco-elastic hysteresis causing a frozen stress distribution at the tip of the growing crack.

In a perfectly elastic material the growth of a crack once started would continue to propagate causing complete fracture. In a hysteresial material the stress concentration at a

stationary flaw is greater than at the same flaw which is in a transient or dynamic state. The difference lies in the fact that in the static case every element of the rubber in the region of the flaw is strained to some point on the extension portion of the stress-strain curve whereas in the dynamic case each element experiences a full stress-strain cycle as the tip of the crack approaches and receedes from the region, thus in a hysteresial material when a crack begins to propagate the stress is reduced and propagation is opposed until a critical value of strain at the crack tip is again achieved either by redistribution of the stresses in the molecular network (Static-crack-growth) or because the deformation in the sample is removed and reapplied. (Dynamic-Cut-Growth). It has been possible to fit amorphous unfilled rubbers into this model of hysteresis controling crack propagation, and to some extent amorphous filled rubbers; in the case of crystallising rubbers there appears to be other factors involved which have not yet been explained.

The importance of the total hysteresis in a filled rubber is indicated in the relation between fatigue resistance and damping which is shown to hold in Chapter 8, providing

allowances are made for the increased stiffness of the filled rubber.

The relation of fatigue results to the mechanical damping of the rubber prompted the direct measurement of energy loss in one cycle of a fatigue test. In Chapter 9 a relationship between the fatigue resistance and the energy lost per unit of energy of deformation was suggested and this relationship unified the results for filled and unfilled rubbers when measurements were compared under conditions of equal deformation. If this relationship proves to be widely applicable, it may be a useful design criterion in comparing compounds for use in applications such as vehicle tyres where the best compound for fixed conditions of deformation is required. The relationship suggests that increased fatigue resistance may be obtained by using "lossy" or hysteresial compounds if the associated temperature rise can be limited by design or other considerations.

It is concluded that hysteresis provides an excellent criterion of fracture. This has been demonstrated elsewhere in the case of tensile rupture and has shown in this work to

apply to fatigue. It should also be mentioned that where the abrasion of rubber can be ascribed to a fatigue mechanism the work described in Chapter 9 can be extended to predict the results of abrasion measurements [99]. Thus fracture in general is linked with molecular relaxation times and may ultimately be described in a unifying way in terms of molecular relaxation times, bond breakage and flaw propagation.

APPENDIX I

The Frequency Dependence of Cut-Growth

Consider a strip of rubber in simple tension which is subjected to the strain cycle illustrated below :-

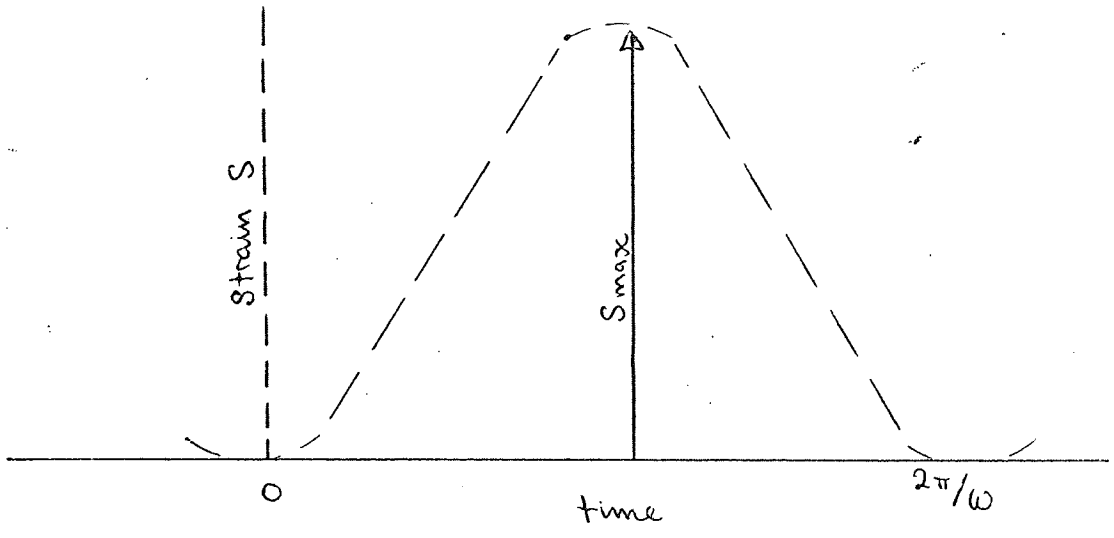

at time t, strain S is given by

$$S = S_{max}(1 - \cos\omega t)/2 \quad \ldots \quad \ldots \quad 2.1.$$

from equation 1.12.

$$dc/dt = \mathcal{J}^4/G_o \quad \ldots \quad \ldots \quad 2.2.$$

where $\mathcal{J} = 2kWc_o$

Lake and Lindley ref. 31. have pointed out that the energy of deformation will obey quite closely a law of the form

$$W = AS^{1.5} \quad \ldots \quad \ldots \quad 2.3.$$

up to quite high deformation.

If we consider a dynamic test to be the summation of the static cut-growth during the fraction of each cycle for which the Tearing Energy can be thought to act

$$\text{then } dc/dn = \int_o^{2\pi/\omega} (\mathcal{J}^4/G_o).\, dt \quad \ldots \quad 2.4.$$

However from equations 2.1., 2.2. and 2.3. $\mathcal{J}$ is a function of time given by

$$\mathcal{J} = 2kc_o A \left[S_{max}(1 - \cos\omega t)/2\right]^{1.5}$$

$$\text{then } dc/dn = \int_o^{2\pi/\omega} \frac{2kc_o A^4 (S_{max}^6)\,(1 - \cos\omega t)^2/2^6}{G_o}\, .dt$$

$$= \frac{\mathcal{J}^4_{max}}{G_o} \quad \frac{1}{2^6} \int_o^{2\pi/\omega} (1 - \cos\omega t)^6 . \quad dt$$

$$1 - \cos\omega t = 2 \sin^2 \omega t/2$$

therefore

$$dc/dn = \frac{\mathcal{J}^4_{max}}{G_o} \int_o^{2\pi/\omega} \sin^{12}(\omega t/2) . \quad dt$$

Substituting

$$\theta = \omega t/2$$

$$dc/dn = {}^2/\omega \quad \frac{\mathcal{J}^4_{max}}{G_o} \int_o^{\pi} \sin^{12}\theta . \quad d\theta$$

All terms in the integral reduce to zero except the final one which is

$${}^{11}/_{12} . {}^9/_{10} . {}^7/_8 . {}^5/_6 . {}^3/_4 . {}^1/_2 . \quad \theta \int_o^{\pi} = .226\ \pi$$

therefore

$$dc/dn = 2\pi/\omega \cdot 0.226 \cdot \mathcal{J}^4_{max}/G_o$$

$$= \frac{0.226}{f} \frac{\mathcal{J}^4}{G_o} \quad \ldots \quad \ldots \quad 2.5.$$

The rate of growth (dc/dn) of a cut under dynamic conditions is given by (Chapter I page 17) $dc/dn = \frac{\mathcal{J}^4}{G}$ ... 2.6.

2.5. and 2.6. are only equal under one condition showing that apart from this special case the static contribution to the rate of cut growth is insignificant at high frequencies and very large at low frequencies and indicates that there is a purely dynamic contribution to the growth of the cut through the rubber.

therefore

$$\frac{dc}{dn} = \frac{\mathcal{J}^4}{G} = \frac{\mathcal{J}^4}{G \text{ dynamic}} + \frac{0.226\mathcal{J}^4}{f\ G \text{ static}}$$

APPENDIX II

COMPOUNDING DETAILS OF RUBBERS USED IN PRELIMINARY INVESTIGATIONS CONCERNED WITH INTERPRETATION OF RESULTS.

Compounding Details	Compound Subscript Numbers							
	0	1	2	3	4	5	6	7
NR pale crepe	100							
NR treadstock		100						
Intol 1500			100					
SBR 12:88				100				
SBR 24:76					100			
SBR 36:64						100		
SBR 48:52							100	
Polybutadiene								100
Sulphur	2.5	2.5	1.75	1.75	1.75	1.75	1.75	1.75
Santocure	.5	.5	1.0	1.0	1.0	1.0	1.0	1.0
S.A.	2.0	2.0	1.0	1.0	1.0	1.0	1.0	1.0
Zinc Oxide	5.0	5.0	3.0	3.0	3.0	3.0	3.0	3.0
Santoflex A.W.			.75	.75	.75	.75	.75	.75
Santoflex I.P.			.75	.75	.75	.75	.75	.75
Process Oil B			5.0	5.0	5.0	5.0	5.0	5.0
Nonox H.F.N.	1.0	1.0						
Min. Oil (^{38}/A)	5.0	5.0						
H.A.F. Black	50.0	50.0						

Figures are given in parts per hundred of polymer.

Cures given were :- NR 15 - 50 @ 30lb.

SBR 15 - 40 @ 50lb.

APPENDIX II.

Intol 1500 is a commercial SBR containing 23% of bound styrene. The other SBR co-polymers were emulsion polymerized at the Dunlop Central Research Division.

APPENDIX III

COMPOUND DETAILS OF RUBBERS USED IN THE MAIN INVESTIGATION OF THE EFFECTS OF TEMPERATURE AND FREQUENCY ON FATIGUE RESISTANCE.

Compound No.	1	2	3	4	5	6	7	8	9
Constituent	Amount of Constituent in parts by weight per hundred parts of polymer								
Polybutadiene	100								
12:88 SBR		100					100	100	100
24:76 SBR			100						
36:64 SBR				100					
48:52 SBR					100				
Natural Rubber						100			
HAF Carbon Black							25	50	75
Sulphur	1.75	1.75	1.75	1.75	1.75	2.5	1.75	1.75	1.75
Santocure	1.0	1.0	1.0	1.0	1.0	0.5	1.0	1.0	1.0
Stearic Acid	1.0	1.0	1.0	1.0	1.0	2.0	1.0	1.0	1.0
Zinc Oxide	3.0	3.0	3.0	3.0	3.0	5.0	3.0	3.0	3.0
Santoflex A.W.	.75	.75	.75	.75	.75		.75	.75	.75
Santoflex I.P.	.75	.75	.75	.75	.75		.75	.75	.75
Process Oil B	5.0	5.0	5.0	5.0	5.0		5.0	5.0	5.0
Nonox H.F.N.						1.0			
Min Oil (^{38}/A)						1.0			
Rise Time (mins)	15	15	15	15	15	15	15	15	15
Vulcanization Time (mins)	50	50	50	50	50	50	50	50	50
Vulcanization Temp. (^{o}C)	148	148	148	148	148	134	148	148	148

APPENDIX IV

THE TORSIONAL PENDULUM USED FOR FINDING GLASS TRANSITION TEMPERATURES

The torsion pendulum consists essentially of a torsion wire which supports at is lower end a mass providing inertia to the system. The mass is connected to a rubber test-piece, which is enclosed in such a way that the ambient temperature can be altered. In the apparatus used in this investigation 80 the sample is twisted at regular intervals by a torque which is applied magnetically to the suspension; the amplitude and period of oscillation are measured and recorded on an ultra-violet chart recorder.

The logarithmic decrement (Λ) and the real part of the complex shear modulus G_1 are derived from measurements taken from the recorded trace of pendulum displacement as a function of time. The trace is a damped sine wave and the measurements made from it are the distance (s) between two peaks on the trace and the trace and the heights (x_o and x_n) of the peaks. The

frequency f is found by counting the number of cycles (n) on a known length of chart which moves at a fixed speed.

Λ and G_1 are calculated from :-

$$\Lambda = 1/n \ln x_o/x_n$$

$$G_1 = (12\pi^2 l I/bh^3) \cdot (f^2 - f_o^2)/(1 - .63h/b)$$

where l,b,h are the dimensions of the test-piece, which is a rectangular prism. I is the moment of inertia of the pendulum; f, f_o are the frequencies of oscillation with and without the sample.

APPENDIX V

LITERATURE REFERENCES

1	Dillon J.H.	Advance in Colloid Science (Interscience)	3	219	(1950)
2	Angioletti A.	Rubber Chem. & Tech.	Oct-Dec	839	(1954)
3	Hodgkinson G.	Dunlop Report C.D.S.1074			(1963)
4	Lloyd D.G.	Monsanto Report			(1966)
5	Beatty J.R.	Rubber Chem. & Tech.	Dec	1341	(1964)
6	Hubball M.	Dunlop Report P.R.2880			(1964)
7	Hubball & Wood	ibid P.R.2620			(1967)
8	Roelig & Fromandi	Rubber Chem. & Tech.	Oct-Dec	1044	(1955)
9	Klitenik & Yamova	Sov. Rubber Tech.	43		(1960)
10	Kragelski, Reznikovski Brodski, Nepomyashi	Sov. Rubber Tech.	24	31	(1965)
11	Kragelski & Nepomyashi	Ivz. Akad. Nauk.S.S.S.R.	5	190	(1963)
12	Bulgin & Walters	Proc. Int. Rubber Conf.		445	(1967)
13	Cooper L.V.	Ind. Eng. Chem. (Anal Ed)	5	350	(1933)
14	Lessig E.T.	ibid	9	582	(1937)
15	Havenhill R.S.	Physics	7	179	(1936)

16	Gough & Parkinson	Trans. I.R.I.	17	168	(1941)
17	Cooper L.V.	Ind. Eng. Chem.(Anal Ed)	2	391	(1930)
18	Cassie, Jones & Naunton	Trans. I.R.I.	12	49	(1936)
19	Cadwell, Merill, Sloman & Yost	Ind. Eng. Chem.(Anal Ed)	12	19	(1940)
20	Torrance & Peterson	India Rubber World	80	62	(1929)
21	Neal & Northam	Ind. Eng. Chem.	23	1449	(1931)
22	Rainer & Gerke	Ind. Eng. Chem. (Anal Ed)	7	368	(1935)
23	Carlton & Reinbold	India Rubber World	108	141	(1943)
24	Breckley J.	Rubber Age	53	331	(1943)
25	Prettymann I.B.	Ind. Eng. Chem.	36	24	(1944)
26	Springer A.	Kautschuk	'19	55	(1943)
27	Springer A.	Rubber Chem & Tech.	18	71	(1945)
28	Bartenev & Zuyev	Strength & Failure of Visco-elastic Materials (Pergammon)			(1964)
29	Rivlin & Thomas	J. Pol. Sci.	10	291	(1953)
30	A.A. Griffith	Phil. Trans. Roy. Soc.	221	183	(1920)
31	Thomas A.G.	J. Pol. Sci.	31	467	(1956)
32	Gent, Lindley & Thomas	J. App. Pol. Sci.	8	455	(1964)

33	Greensmith H.W.	ibid	7	993	(1963)
34	Lake & Lindley	ibid	8	707	(1964)
35	Lindley & Thomas	4th Rubber Tech.Conf.I.R.I.			(1963)
36	Lyons & Prettymann	J. App. Phys.	19	473	(1948)
37	Greensmith, Mullins and Thomas	Chemistry & Physics of Rubberlike Substances (Wiley)			(1963)
38	Busse W.F.	Ind. Eng. Chem.	26	1194	(1934)
39	Gurney & Cheetham	Trans. I.R.I.	35	2	(1959)
40	Dogadkin, Zarazov and Goldberg	Proc. 4th Int. Rubber Conf.		London	(1962)
41	Kaminskii & Lubchanskaya	Rubber Chem & Tech	24	77	(1956)
42	Angioletti A.	Rubber Chem & Tech	29	753	(1956)
43	Hess & Burgess	ibid	36	754	(1965)
44	Smith & Black	ibid	37	338	(1964)
45	Eccher S.	ibid	13	566	(1940)
46	Eccher S.	Goumma	4	1	(1940)
47	Gent A.N.	J. Appl. Pol. Sci.	6	497	(1962)
48	Greensmith & Thomas	J. Pol. Sci.	18	189	(1955)
49	Smith T.L.	ibid	1	3597	(1963)

50	Smith & Frederick	J. App. Phys.	36	2996	(1965)
51	Williams, Landel and Ferry	J. Am. Chem. Soc.	77	3701	(1955)
52	Ferry J.D.	Visco-elastic Properties of Polymer (Wiley)			(1961)
53	Andrews E.H.	Fracture in Polymers (Oliver & Boyd)			(1968)
54	Andrews E.H.	J. Mech. Phys.	11	231	(1961)
55	Smith T.L.	J. Pol. Sci.	32	99	(1958)
56	Mullins L.	Trans. I.R.I.	35	213	(1959)
57	Harwood J.A.C.	J. App. Chem.	17	333	(1967)
58	Cazaud R.	Fatigue in Metals	Chapman & Hall		(1953)
59	Andrews E.H.	J. App. Physics	35	542	(1961)
60	Leewerk & Swarzl	Plastica	8	474	(1955)
61	Bulgin D.	Private Communication			
62	Greensmith H.W.	J. Pol. Sci.	31	175	(1956)
63	Russ J.C.	Jeol News	7M-2	14	(1969)
64	Hunter & McMillan	ASTM Meeting		June	(1967)
65	Halin & Rosenfeld	Mat. Lab. Tech. Report		TR-65-409	(1967)
66	Lemmon & Shalby	Stanford University Report		67-19	(1967)
67	Beacham & Pelloux	ASTM STP-381		210	(1964)

68	Edelson & Baldwin	ASM	55	230	(1962)
69	Payne & Scott	Engineering Design with Rubber		McLaren	(1960)
70	Yabata S.	Nippon Gomu Kyokaishi	36	1081	(1963)
71	Yabata S.	ibid	40	1026	(1967)
72	Yabata S.	ibid	40	1037	(1967)
73	A.N. Gent	Rubber Chem. & Tech	XXXVI	No.3	(1963)
74	S.C.G. Chubb	Private Communication			
75	Lake & Thomas	Kaut. und Gummi	April-May	211	(1967)
76	Lake & Thomas	J. App. Pol. Sci.	9	1233	(1965)
77	Ferry & Fitzgerald	J. Coll. Sci.	8	224	(1953)
78	Williams J.	J. Phys. Chem.	159	95	(1955)
79	Keyte, Parker and Smith	Dunlop Report P.R.2476			(1961)
80	Ball A.P.	Dunlop Report P.R.3026			(1969)
81	Keyte D.N.	Dunlop Report P.R.2562			(1963)
82	Keyte, Parker and Smith	Dunlop Report P.R.2523			(1962)
83	Boyer and Spencer	Advances in Colloid Sci. II			(1947)
84	Gerke R.H.	U.S. Rubber Co. Report			Undated

85	Wood L.A.	J. Pol. Sci.	319		(1958)
86	Payne A.R.	J. App. Pol. Sci.	6	57	(1962)
87	Payne A.R.	Rubber and Plastics Age	42	963	(1961)
88	Payne A.R.	Mat. Res. & Standards		1942	(1961)
89	Bulgin D.	Rubber & Plastics Weekly	143	636	(1962)
90	Andrews E.	Rubber Chem. & Tech	36(2)	325	(1963)
91	Mullins L.	J. Rubber Res.	16	275	(1947)
92	Grosch K.A.	Nature	197	858	(1963)
93	McLaren & Tabor	ibid	197	856	(1963)
94	Treloar G.	The Physics of Rubber Elasticity		Oxford	(1958)
95	Dannenberg E.M.	I.R.I. Trans. Proc.	42	T26	(1966)
96	Mullins & Tobin	J. App. Pol. Sci.	9	2993	(1965)
97	Grosch, Harwood and Payne	Oxford Conf. On Yield and Fracture			(1966)
98	Bulgin D.	Private Communication			
99	Bulgin D.	Inst. Pol. Tech. Conf. Loughborough		May	(1970)

LIST OF SYMBOLS.

A = Area.

A_T = The ratio of frequency at temperature T to the frequency at some reference temperature.

B = Height of a Potential Barrier.

C_o, C = Crack length dimension.

d = Dynamic Viscosity.

E = Total Strain Energy of Test-Piece.

F = Activation Energy.

G = Cut-Growth Characteristic (Rough Cut-Growth Constant).

G_o = Static-cut-growth Constant.

G_S = Smooth-cut-growth Constant.

G_D = Dynamic-cut-growth Constant.

h = Internal Friction Loss.

H = Energy Loss per cycle of deformation.

I = Energy Input per cycle of deformation.

n = Gradient of Logarithmic Plot of Cut-growth rate against Tearing Energy.

N = Fatigue Resistance.

P = Probability.

R = Gas Constant.

S = Strain.

S.D. = Standard Deviation.

t_o, t = Time.

T_o, T = Temperature.

T_c = Critical Tearing Energy.

T_g = Glass Transition Temperature.

T_s = A Characteristic Reference Temperature of a Particular Rubber.

u = Velocity.

U, U_o = Tensile Strength.

v = Velocity.

V_{fo}, V_f = Free Volume.

W = Strain energy/ unit volume.

x, y = Displacement co-ordinates.

α_f = Co-efficient of Thermal Expansion.

δ = Phase angle.

λ = Extension ratio.

Λ = Logarithmic decrement.

ω = Angular frequency.

$\mathcal{T}$ = Tearing Energy.

θ = Temperature.

The symbols a, C_1, C_2, k, m, $\propto$ have been used as arbitrary constants and the abreviations

SBR = Styrene-butadiene rubber.

NR = Natural Rubber.

T.E.M. = Transmission Electron Microscope.

S.E.M. = Stereoscan Electron Miscroscope.

have also been used.